

A device that prepares the subtalar joint for fusion during tibiotalocalcaneal arthrodesis

Campbell, Catherine MacKenzie

De Biasio, Michael

Wang, Kevin

Zhu, Yutong

For Dr. Spencer Montgomery, Dr. Amit Atrey, Dr. Amir Khoshbin

And Professor Chris Bouwmeester, Karly Franz

Wednesday, December 9, 2020

Executive Summary

Tibiototalcalcaneal (TTC) arthrodesis using an intramedullary nail is a surgical procedure performed to fuse the tibia, talus, and calcaneus bones of the ankle. TTC arthrodesis is often required as a salvage procedure following severe trauma to the ankle joints. A typical TTC nailing surgical procedure involves two parts: (1) preparation of both the ankle joint and subtalar joint, and (2) ankle fixation through inserting an intramedullary nail. However, subtalar joint preparation is often not performed in a trauma setting, resulting in lower rates of arthrodesis (fusion), which is correlated with poorer outcomes, higher risk of complications, and ultimate revision surgery.

This report describes a solution to the preparation of the subtalar joint in a trauma setting during TTC arthrodesis through rigorous design methods in order to improve bone fusion rates. Key requirements include cartilage destruction and removal across the joint, as well as subchondral bone exposure and bone graft deposition. These serve as indicators for improved subtalar joint union. Other design requirements include minimizing cost, minimizing surgical time and changes to the technique, maximizing ease of use, and restricting the device to visualization through only x-ray. These are meant to ensure the design is easy to use and can be adopted by surgeons.

Our proposed design is composed of two modular components: A hinged cutting tool and a stiff hollow, guiding tube. The guide tool provides easy access to the subtalar joint to reduce x-ray exposure and allows for use of suction tubing and injection of synthetic bone graft. Our detailed workflow involves tandem use of the guide tube and cutting tool, with an overall workflow complete in 6-7 minutes. To verify our design meets the requirements, we performed validation and verification tests, such as low-fidelity prototyping, force calculations and simulations, timing calculations, and an assessment of the blade scraping path. These tests also helped inform our detailed design, although additional tests on cadaver models will be needed to fully verify our design against the requirements. The estimated cost for our tool is approximately \$43.00 CAD, which includes material and manufacturing costs. Further, a risk analysis was performed using FMEA and fault tree analysis. Identified risks include those associated with the tool's mechanism of action, unintended damage, user error, and tool biocompatibility/sterility. In the future, it is important to make higher-fidelity prototypes and assess surgeon feedback through a detailed tool survey. Finally, future considerations for the design include ergonomic aspects of the handle design and the marketability of our design as a reusable or disposable tool.

Acknowledgements

This project has been a challenging and rewarding experience for our team. We are thankful for the help, support, guidance, and encouragement from many people who have contributed to and assisted with our project. In particular, we would like to thank:

- Dr. Spencer Montgomery, our primary client contact, for always keeping in constant communication with our team, for responding to all of our questions in a timely and concise fashion, and for his expertise and guidance in the design process.
- Dr. Amit Atrey and Dr. Amir Khoshbin, our other clients, for their assistance in the conception and development of our project.
- Professor Chris Bouwmeester, for coordinating the BME489 Capstone Design Course, for providing us with an opportunity to undertake an engineering design project, and for his guidance and feedback in the design process.
- Mrs. Karly Franz, our teaching assistant, who guided us throughout the project, provided us with useful advice, and supported us in making key design decisions.
- Mr. Gary Hoang, the teaching lab and design studio technician, for supporting us in the 3D printing of required components and for providing suggestions of resources we can use to test our design.
- Dr. Jeremy LaMothe and Dr. Mansur Halai, two orthopedic surgeons, for providing their expertise and insight in the design problem and our proposed solution.
- Our fellow Engineering Science Biomedical Systems Option classmates, for inquiring about our design and making this project a memorable one.

Meet the Team

For any questions about the report, please do not hesitate to contact any of the team members.

Their contact information is listed below.

- Catherine MacKenzie Campbell: cm.campbell@mail.utoronto.ca
- Michael De Biasio: michael.debiasio@mail.utoronto.ca
- Kevin Wang: kevinkw.wang@mail.utoronto.ca
- Irina Zhu: yutong.zhu@mail.utoronto.ca

Table of Contents

1. Introduction	1
A. Background	1
B. Needs Statement and Objective	7
C. Project Requirements	7
2. Final Design	12
A. Overview	12
B. Guide Tube	13
C. Tool and Blade Design	15
D. Detailed Workflow	18
E. Materials Selection	21
3. Assessment of Final Design	22
A. Verification Overview	22
B. Low-Fidelity Prototype	25
C. Force to Scrape Cartilage	26
D. Force Calculations on Tool	27
E. Blade Simulation Testing	28
F. Surface Area and Timing Calculations	30
G. Blade Scraping Path and Scrape Region	32
H. Cost Analysis	37
I. Assessment of Requirements	39
J. Risk Analysis	42
4. Summary and Conclusions	48
A. Summary	48
B. Next Steps and Future Considerations	49

5. Appendices	51
A. Bibliography	51
B. Work Plan	57
C. Financial Plan	60
D. Report Attribution Table	62
E. Transcripts from Surgeon and Client Interviews	64
E1: Client Interview - Reference Material	64
E2: Dr. LaMothe Interview - Reference Material	65
E3: Dr. Halai Interview - Reference Material	66
F. Needs Statement Convergence	68
G. QFD Analysis	69
H. Supplemental Figures for Adult Foot Measurements	71
I. Surgeon Confidence Survey	72
J. Supplemental Information for Cartilage Scraping Force Calculations	76
K. Supplemental Information for Tool Force Calculations	78
L. Force Simulation Results	80
M. Full Surface Area and Timing Calculations	84
N. Cost Analysis Supplemental Information	85
O. Risk Analysis Supplemental Info	87
P. FMEA Risk Analysis	88
Q. Blade Angle Determination	90

1. Introduction

The goal of this report is to outline the importance of subtalar joint preparation in an orthopedic surgical technique called tibiototalcalcaneal (TTC) arthrodesis and provide a comprehensive summary of our proposed design that addresses a minimally-invasive way to prepare the subtalar joint. We start by giving background on the project, discussing the project goals and needs statement, and outlining engineering requirements for a suitable design (**Section 1**). Then, we comprehensively detail our final design, both in terms of a systems-level overview of the device workflow as well as a modular description of the device's components (**Section 2**). Next, we document the assessment of our final design against the requirements, including tests to verify the validity of our approach and a risk assessment (**Section 3**). Finally, we conclude by providing a summary of and reflection on our design, looking ahead to future work and potential implications of our design within the landscape of orthopedic surgical procedures (**Section 4**).

A. Background

Tibiototalcalcaneal (TTC) arthrodesis is a surgical procedure performed to fuse the tibia, talus, and calcaneus bones of the ankle. In this procedure, both the ankle (tibiotalar) and subtalar (talocalcaneal) joints are fused (**Figure 1**). These joints are essential in our everyday movement, bearing a force of ~5 times body weight during normal gait [1]. As such, TTC arthrodesis is often required following severe trauma to the ankle joint, such as in pilon fractures (a tibia fracture involving its articulating surface at the ankle joint). Other indications to perform the surgery include degenerative arthritis, unstable ankle fractures in geriatric patients and patients with neuropathy, avascular necrosis of the talus, and failed previous attempts at ankle fusion [2]. In these challenging cases, TTC arthrodesis provides a valuable alternative to amputation, offering a salvage procedure in patients with severe ankle deformities [3][4]. The goal of TTC arthrodesis is the relief of pain and deformities, achieved through the development of a functional, solid fusion between the ankle and subtalar joints [2]. This is typically assessed 6 months post-surgery via X-ray imaging of the joint. It is a valuable procedure that dates back to the late 1900s and is still frequently performed today [2][3].

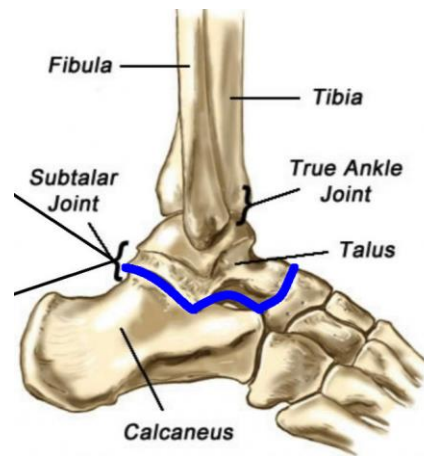


Figure 1: Ankle Anatomy. (Source: [Ankle, Foot & Orthotic Center, AU](#))

Surgical Technique

In order to perform TTC arthrodesis, various methods have been utilized. These include the use of cancellous bone screws, intramedullary nails, staples, plates, pins and external fixators [4]. Among these, the use of an intramedullary nail that crosses both the ankle and subtalar joints to connect the tibia, talus and calcaneus (**Figure 2**) has emerged as the most common technique among surgeons [3][5]. Here, the inserted nail renders the hindfoot stiff by mechanically inhibiting motion at the ankle and subtalar joints [6]. The increased popularity of intramedullary nails is due to the satisfactory compression and joint stability achieved through its use, which is thought to improve arthrodesis (i.e., bone fusion) [3]. Further, studies have demonstrated that intramedullary nails have superior bending and torsional properties, as well as improved micromotion stability, as compared to other constructs [3][4].

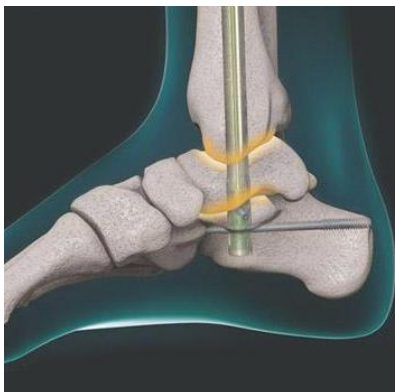


Figure 2: TTC Arthrodesis with Intramedullary Nail. (Source: [MedShape DynaNail®](#))

In a typical TTC arthrodesis with an intramedullary nail [1][7], the surgical procedure consists of two parts: (1) preparation of the joints and (2) fixation of the ankle. In the first part, the ankle and subtalar joints are prepared by removing cartilage tissue from the bone surfaces. Here, the goal is to remove the cartilage layer down to the bleeding, subchondral cancellous bone, preserving the natural shape of the articulating surfaces if possible. The disruption of the subchondral bone is important to promote bone growth into the joint space to allow for fusion, where divots are often made in the subchondral bone in a procedure termed “golfballing” (**Appendix E3**). In order to perform this preparation, a ~10cm incision is made in the side of the foot, exposing the ankle and subtalar joints (**Figure 3a**). Then, using various tools such as osteotomes/chisels, curettes, and/or burrs, the surgeon prepares the joint to the best of their ability. In the case of misalignment, an osteotomy (surgical cutting of bone) is often required. The removed bone can then be used for an autologous bone graft later on in the surgical procedure.

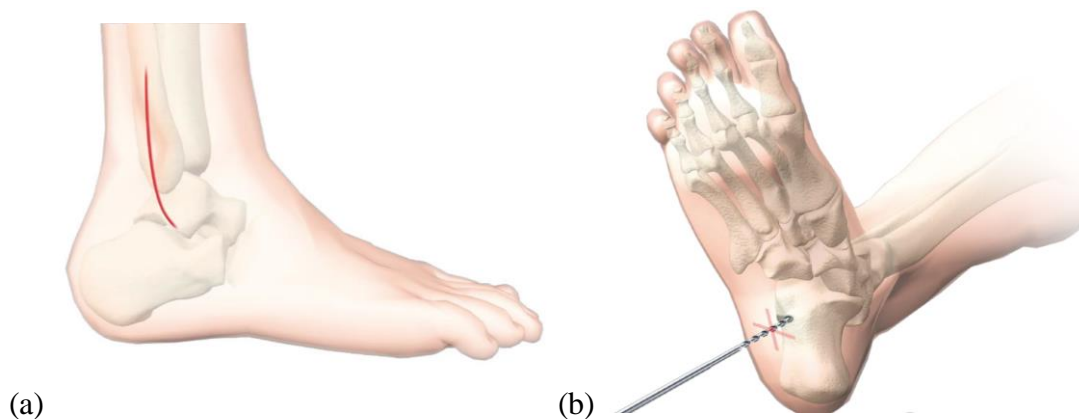


Figure 3: Illustrations of the surgical procedure. (a) Depiction of 10cm incision traditionally made for joint preparation. (b) Entry point for a plantar incision in the foot. (Source: [Stryker](#)).

In the second part, the ankle is fixed through the insertion of an intramedullary nail, followed by compression screws to lock the nail in place. To do this, a 3cm plantar incision is made in the sole of the foot (**Figure 3b**). Then, a guide wire is inserted through the calcaneus, talus, and into the tibial medullary canal, using X-ray imaging for guidance. Progressive reaming (widening of the hole) is performed using reamers passed over the guidewire in 0.5mm increments. If an osteotomy was performed, or a synthetic bone graft is available, the bone graft may be inserted into the ankle and subtalar joint spaces to facilitate fusion. Then, after determining the appropriate nail length, a nail-mounted compression device is used to insert the medullary nail, achieving compression across the ankle and subtalar joints. The nail diameters range from 11-14mm, depending on the individual patient (**Appendix E3**). Finally, using the compression

device as a guide, screws are inserted into the tibia, talus, and calcaneus to lock the medullary nail in place (**Figure 4**), completing the surgery.

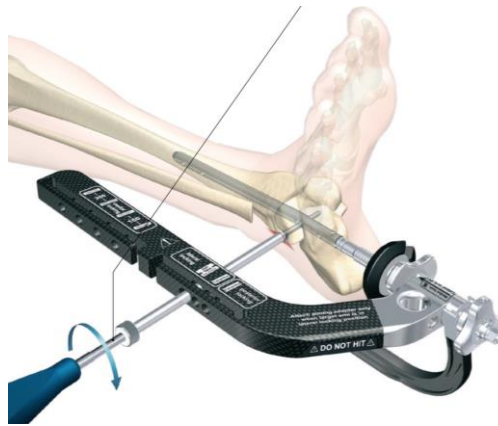


Figure 4: Nail-mounted compression device being used to insert a nail into the talus. Depicts guides along the nail-mounted compression device for inserting compression screws into the tibia, talus, and calcaneus. (Source: [Stryker](#)).

Modifications to the Surgical Technique in a Trauma Setting

While joint preparation has been performed in a trauma setting (i.e., pilon fractures) via ankle incisions (as described above in part 1 of the surgical procedure), issues with healing and the potential risk for infection have led clinicians to stop this approach when performing TTC arthrodesis (**Appendix E2**). The lack of open joint preparation is often accepted because there is already sufficient damage to the ankle joint, so activating the subchondral bone to promote fusion is often not considered necessary. In fact, studies have reported that ankle joint union can occur up to 90% of the time without joint preparation [8][9] in a trauma setting. However, in these situations, while the trauma accounts for the preparation of the ankle joint, the subtalar joint is left unprepared, leaving a significant amount of remaining cartilage that poses a barrier to the goal of union.

That said, if we could prepare the subtalar joint non-invasively, the benefits for union are clear. More specifically, in a study from earlier this year by Yoshimoto et al. [5], the effect of subtalar joint preparation on outcomes from TTC arthrodesis with an intramedullary nail were investigated. Here, they analyzed 53 joints that had undergone this procedure from 1997-2016, where some surgeons had prepared the subtalar joint while the others had not. They found that patients with prepared subtalar joints had a subtalar union rate of 92%, while patients with no preparation had a subtalar union rate of 45%. Further, joints without subtalar preparation were significantly associated with non-union at the subtalar joint ($p = 0.0012$). This subtalar non-union is painful and often requires revision surgery (for example, in this study

[5], revision surgery was performed in 22% of cases of subtalar non-union, while all cases of subtalar union did not require revision surgery).

Overview of the Project and Market Space

Thus, the goal of our project is to make a device to prepare the subtalar joint for fusion through a plantar incision in the foot (**Figure 3b**), aiming for a minimally-invasive approach. To achieve fusion at the joint, the articular cartilage must be removed and the underlying subchondral bone must be disrupted to facilitate new bone formation. Such a tool would help improve reliability for fusion during procedures using an intramedullary nail for TTC arthrodesis. By providing a minimally-invasive way to prepare the joint, surgeons can gain greater confidence that they will achieve desired fusion at the subtalar joint. A tool that can achieve this would be something they would be willing to readily adopt (**Appendices E1-E3**). Moreover, conversations with our client have indicated that if our tool is reliably adopted in the trauma setting, it could be utilized in other settings (not just trauma), increasing the potential market impact through its use in the various settings where TTC nailing is performed.

The current market space for cartilage removal tools includes burrs, curettes, and osteotomes (**Figure 5**), which are used to remove cartilage through an open incision in the side of the ankle. Some of these surgical tools cost roughly US\$30-40 per tool [10][11][12], but others, such as osteotomes, can be upwards of US\$100 [13]. Various companies populate the surgical instrumentation space, including World Precision Instruments (WPI), Brasseler Medical, and Surtex Instruments. However, none of these businesses offer a tool that can remove cartilage through a single plantar incision in the foot, which our device aims to address. Thus, despite being targeted for use in a trauma setting, our device could easily be adopted into joint preparation procedures for all settings that require TTC arthrodesis via an intramedullary nail.

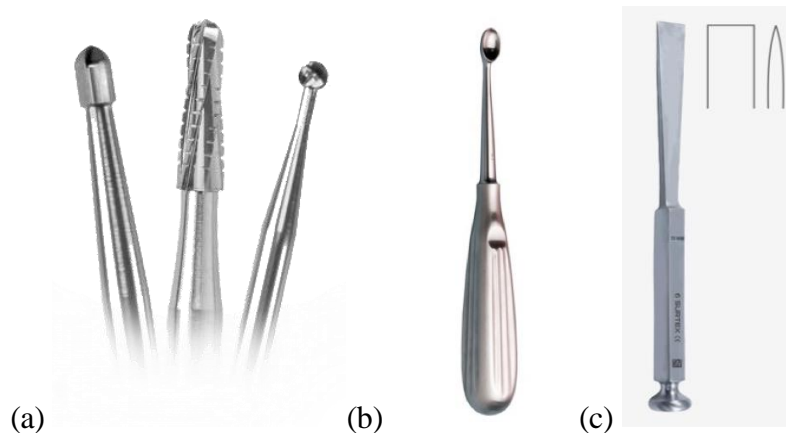


Figure 5: Common surgical tools used to prepare the joint, including surgical burrs (a), curettes (b), and osteotomes/chisels (c). (Sources: [Brasseler Medical](#), [WPI](#), [Surtex Instruments](#))

More Context on Subtalar Joint Anatomy and Preparation

As mentioned above, the subtalar joint lies between the talus and calcaneus [14], with ~3mm of space between these two bones (**Appendix E1**). The joint has a sigmoidal shape, with this shape illustrated by the green shading in **Figure 6a** and a scale bar showing the relative size of the joint is on the order of a few centimeters. The sigmoidal, domed shape of the articulating surfaces can be seen nicely in a cross-section of the talus (**Figure 6b**), where the articulating surface with the calcaneus is on the bottom. In this cross-section, you can clearly see the division between the ~1mm of cartilage [15] and the spongy bone beneath. As described above, the goal of subtalar joint preparation is to remove this ~1mm layer of cartilage and then dig into the underlying subchondral bone. Surgeons try to penetrate at least 1-2mm into the subchondral bone during joint preparation procedures in order to sufficiently activate the subchondral bone for union (**Appendix E3**).

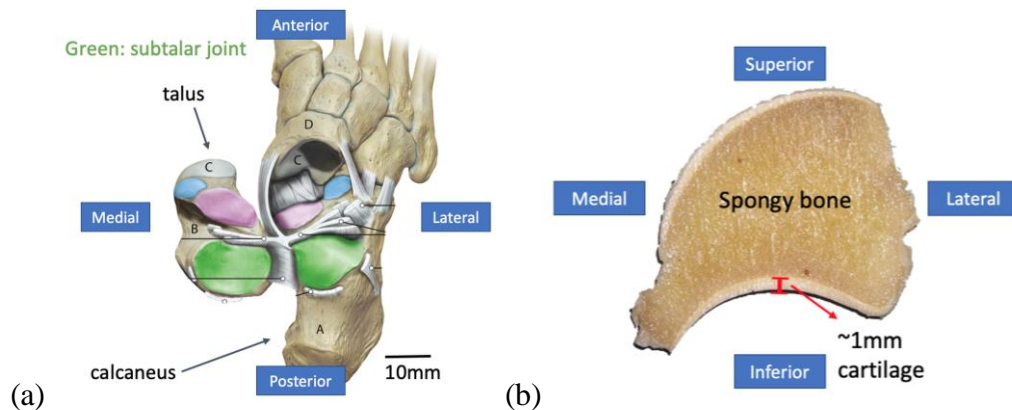


Figure 6: Subtalar Joint Anatomy. (a) View from above of the subtalar joint (green), with the joint's sigmoidal shape illustrated by the green shading and the anatomical directions indicated in blue boxes.

(b) Cross section of the talus bone, with spongy bone and cartilage labelled along with anatomic directions in blue boxes. The articulating surface with the calcaneus is inferior (on the bottom).

(Sources: [Scientific Reports 2020](#) and [Osteoarthritis and Cartilage 2012](#))

B. Needs Statement and Objective

Our project aims to address the following needs statement: **A way to prepare the subtalar joint through a plantar incision in patients undergoing TTC nailing in a trauma setting that improves bone fusion rates.** We converged on this needs statement through an iterative process with our project team and client (**Appendix F**). The rationale behind defining this needs statement were contextualized in detail in the above Background (**Section 1A**). A key selection criteria was framing within a trauma setting. This was important to contextualize that the joint preparation is typically not performed, and thus there is no incision made along the side of the ankle. Therefore, we must prepare the subtalar joint through a plantar incision, due to potential infections and complications from additional incisions.

The primary objective of the project is focused on two aspects: outcome and usability. In terms of outcome, the ultimate goal of this design is to achieve higher rates of subtalar union in patients. Since measuring patient subtalar union is not within the scope of this course, as it is based on a 6-month radiographic follow-up, we have instead developed proxy outcomes that can reasonably predict subtalar union (see Project Requirements, **Section 1C**), based on discussions with our client and an understanding of the importance of joint preparation for subtalar union as documented in the literature [5]. In terms of usability, the design should fit within the current surgical workflow of TTC nailing, as detailed in the Background (**Section 1A**).

C. Project Requirements

To address the project needs statement and objectives, the team has developed a set of project requirements. These are listed as objectives, metrics, criteria, and constraints in **Table 1** below. Due to the large number of requirements, they are divided into space, outcome, cost, and usability categories. The analysis is mainly based on direct communication with our client Dr. Montgomery and other experts in the field to whom he has connected us (Dr. LaMothe and Dr. Halai) (**Appendix E**), with Appendices E1, E2, and E3 containing testimony from orthopedic surgeons Dr. Montgomery, Dr. LaMothe, and Dr. Halai. In addition, the team has also reviewed relevant literature to support the validity of the requirements. The reasoning behind the requirements, along with associated criteria and constraints, are also outlined in **Table 1** below. Lastly, the team has utilized quality functions deployment (QFD) analysis tools to help structure design planning and ensure client needs are met through the requirements (**Appendix G**).

Table 1: Requirements, metrics, criteria, and constraints for the project

#	Requirement; Metric	Constraints	Criteria	Supporting Justification
Space				
1	The design must access the ~3mm joint space through an 11-mm reamed hole diameter; Measured by size of tool designed to remove cartilage.	Must be able to access the joint space through an 11mm reamed hole.	n/a	The joint space (distance between talus and calcaneus) is ~3mm (Appendix E1). Nail diameter ranges from 11-14mm (Appendix E3), with lengths or sizes ranging from 150-300mm [16]. Reaming must be performed until the medullary canal is 0.5-1mm greater than the nail diameter [16]. Thus, our tool must fit within the minimum size of an 11mm reamed hole.
2	The design must be long enough to traverse up through the reamed hole in the calcaneus to access the subtalar joint; Measured by the length of the design such that it can easily reach the subtalar joint surfaces.	Tool must be at least 10cm in length to accommodate varying foot anatomy.	Adjusting length to improve usability and/or device handling is preferred.	Given that the height of the posterior facet in the calcaneus ranges from 23.8mm to 35.1mm [17], which spans at least 70% of the joint height, we thus want our tool to be able to extend into bone by at least $35.1\text{mm}/70\% = 50\text{mm}$ [17]. Accounting for the soft tissue at the sole of the foot, the tool must extend 10cm into the foot space, which gives ample space based on approximate measurements on a typical adult foot (Figure H1, Appendix H).
Outcome				
3	The design should achieve cartilage destruction; Measured by percent (%) of cartilage destruction across the joint, determined via the joint surface area (SA) the tool is used on compared to the total joint SA.	Must be more than 25% destruction across the joint.	Up to 50% cartilage destruction across the joint is preferred.	Since union is considered as 25-49% of total surface area with bridged bone fusion sites (as measured via X-ray) [18] (Appendix E1 & E2), we make the reasonable assumption that we must remove that % of cartilage to facilitate fusion, assuming you remove the full 1mm depth of cartilage with the tool.
4	The design should achieve removal of broken, loose cartilage; Measured by percentage (%) of removed broken cartilage, determined via the volume of cartilage suctioned out of the joint as compared to loose cartilage remaining in the joint space.	Should remove at least 50% of loose destroyed cartilage.	Maximal (up to 100%) removal of loose destroyed cartilage is preferred.	Damage to the articular cartilage can cause an inflammatory response, stiffness, and limits in range of motion [19]. Also, decreases in the elastic modulus of subchondral bone is associated with cartilage damage [20]. Client recommended some removal, however, it is still not a major issue if you leave some broken cartilage behind (Appendix E1).

5	<p>The design should achieve subchondral bone disruption; Measured by the percent of total exposed surface area (SA with cartilage already removed) that is disrupted by the tool (i.e., number of scrapes by a blade with the presence of bone/bone marrow in the suction tube).</p>	<p>Should disrupt 50% of exposed subchondral bone.</p>	<p>The ability to have maximal subchondral disruption (up to 100%) is preferred.</p>	<p>The surgeon’s ability to “feel” the scraping of bone is sensed via a force difference between cartilage and bone scraping (Appendix E1). Scraping cartilage and bone require very different forces, with bone considered softer (lower density) [21] (Appendix E3). Also, there are visible signs of subchondral bone in suctioned debris, including visible marrow and fat (Appendix E3). Drilling small holes, or “golf balls”, into subchondral bone helps stimulate early joint fusion by providing vascular access channels to the newly forming bone [22] (Appendix E3). A similar disruption of subchondral bone will help promote union. Numbers are based on surgeon estimates of how much the posterior SA should be scrapped in order to promote fusion (Appendix E3).</p>
6	<p>The design must be able to penetrate into cartilage/subchondral bone on either side of the joint by at least 3.5mm; Measured by the force a tool can withstand when penetrating into and subsequently removing cartilage.</p>	<p>Must be able to penetrate to depths of at least 3.5mm on either side of the joint.</p>	<p>n/a</p>	<p>Previous characterization of the thickness of cartilage on the subchondral joint has shown it is on average 1mm, although can reach up to ~1.5mm in thickness [15]. We want to activate subchondral bone beyond this, so penetrating an additional 1-2mm (i.e., max 3.5mm total) would be able to go to a sufficient depth to activate subchondral bone (Appendix E3).</p>
7	<p>The design’s penetration into the cartilage/subchondral bone should be controllable; Measured by precision of the control of penetration depth in mm.</p>	<p>Must have control in at least 1mm increments over penetration depth.</p>	<p>Penetration depth being as controllable as possible (i.e., smallest mm increments) is preferred.</p>	<p>Since cartilage thickness can vary from patient-to-patient [15], giving the surgeon the ability to control penetration into the cartilage/subchondral bone (penetration depth) is key to ensuring the tool can be adaptable to all patients. Since cartilage thickness is ~1mm [15], controlling the tool with this precision is a must. Here, controllable refers to the ability to control the penetration depth)in the smallest increment resolution.</p>
8	<p>The design should be able to act (promote fusion) in the anterior-posterior direction (A-P, front-to-back); Measured by the range of angles the tool can accommodate in degrees.</p>	<p>Must be able to work in a range of angles, specifically $48^{\circ} \pm 15^{\circ}$ and $132^{\circ} \pm 15^{\circ}$.</p>	<p>Ability to move in an angle range from 0° to 180° is preferred.</p>	<p>The anterior-posterior (A/P) direction is the only joint direction that will be prepared by surgeons to achieve the 25-50% cartilage destruction, since it is safer, easier to assess via X-ray, and can still give desirable union outcomes (Appendix E1, E3). In the A/P direction, the average inclination angle is 42° [23] (Figure H2, Appendix H), which is known to vary considerably (with a reasonable estimate of variance $\pm 15^{\circ}$) [23]. Since the reamed hole</p>

				is through the bone's center, the tool must work both up ($42^\circ + 90^\circ = 132^\circ$) and down (complimentary angle, $90^\circ - 42^\circ = 48^\circ$) the slope.
9	The design should facilitate deposition of synthetic bone graft (or autologous) into the joint space; Measured by X-ray.	Must be compatible with existing bone graft syringes.	Minimizing difficulty of using pre-existing bone graft syringes is preferred.	Bone graft may be placed at the fusion site to facilitate union. This is recommended due to other factors (i.e., bony defects, talus osteonecrosis) that could complicate union [24]. Typical syringes are ~6mm [25][26], which will fit through the reamed hole. While most syringes are solid, inflexible objects, a flexible plastic (i.e., PVC, polyvinyl-chloride) tube can be used to inject the bone graft into the desired region via the reamed hole after joint preparation.
Cost				
10	Minimize cost of the device; Measured as the dollar amount for production of tool, relative to current tools used during the surgery.	Must avoid making the device raw cost more than \$100 CAD (assuming it sells at double this cost, or \$200 CAD).	Fitting within the price profile of the current individual tools (~\$150 CAD, assumed cost \$75 CAD) used in the surgery is preferred.	Currently, the surgical procedure involves the use of various tools such as chisels and burrs to prepare the subtalar joint. From Brasseler Canada [12], a typical surgical burr head costs ~\$42.60 CAD (reusable), while a disposable burr head has a unit price of ~\$6.35 CAD (but also requires sterilization costs, estimated to be ~\$4.16 CAD per instrument [27]). Further, the cost of surgical osteotomes/chisels is ~\$150 CAD [13]. As such, we can approximate joint preparation tools costs roughly \$200 CAD. Assuming 100% markup, we can assume all tools used cost ~\$100 CAD to produce. Since our tool would allow for non-invasive preparation and improved efficacy, we assume that having a tool at this price, higher than typical prices for individual tools account for improved efficacy, is manageable.
Usability				
11	Minimize surgical time; Measured in minutes.	Must add less than 10 minutes to the surgical procedure time.	Adding less than 5 minutes to the surgical procedure time is preferred.	Based on interviews with our client (Appendix E1) and other surgeons (Appendix E2), not exceeding 10 minutes is key to ensure the device will be adopted by clinicians. In addition, minimizing time relates to the device being "not finicky" (Appendix E2). Taking longer to use, whether in added set up time or added steps to remove cartilage, contributes to being perceived as finicky.

12	Minimize changes to technique, such that the device is intuitive to use; Measured by the number of steps to use the tool.	Must not add time consuming steps to the joint preparation workflow.	Having less steps than the current joint preparation workflow is preferred.	Based on interviews with clinicians (Appendix E1 & E2), the device “must be intuitive”. For this, the surgeon must not need to learn any drastically unfamiliar procedures or techniques. This is based on the number of steps in the workflow to use the tool, not wanting to have more steps than the current joint preparation workflow that surgeons are accustomed to ¹ . Intuitiveness is also based on a post-usage survey given to surgeons, where they rate how confident they would feel to use the tool. In this survey, surgeons will also comment on aspects of the tool design and its ease of use. This rating obtained in a survey based on previously developed approaches taken in the literature and a 5-point Likert scale [28][29][30]. This survey would be provided to surgeons after use of the tool on a cadaver, and can be found in Appendix I .
13	Maximize the intuitiveness and ease of use of the design; Measured by the response of surgeons/participants in a follow-up Likert-scale survey assessing surgeon ease of use with our design.	Must score at or above Neutral for overall intuitiveness, safety, and usability measures.	Having higher scores on Likert scale for all measures is preferred.	
14	Tool should be able to be used without direct visualization of the joint space; Measured by the visualization method required for the tool.	Must use current X-ray images for visualizing the joint preparation.	Being reliable enough to replace existing open arthrodesis is preferred.	When exposing the joint surface, it is essential to avoid injury to the neurovascular bundle. If the full joint surface cannot be visualized, a medical incision may be needed to reduce potential nerve damage [24]. According to the interview with our client (Dr. Montgomery), additional visualization tools such as cameras should not be used, as it will be time prohibitive (Appendix E1).

¹ Current surgical workflow includes: (1) ankle incision; (2) expose subtalar joint; (3) use chisel to dislodge cartilage; (4) suction off/manually remove cartilage; (5) repeat steps 3-4 as necessary; (6) activate subchondral bone via golf-balling (making small 1-2mm divots) with a burr; (7) prepare synthetic/autologous bone graft; (8) inject bone graft; (9) close ankle incision; (10) begin reaming hole for intra-medullary nail.

2. Final Design

A. Overview

Our proposed design is composed of two modular components: a hinged cutting tool and a stiff hollow, guiding tube. Traditionally, after a hole is reamed in the foot, a nail is immediately inserted. This can lead to non-union of the ankle, due to insufficient removal of cartilage and subchondral bone.

Our proposed procedure changes this workflow as follows. Following the steps in **Figure 7**, once the hole is reamed (1), our guide tube is inserted into the hole guided by a flexible Kirschner Wire (2). It is locked in place via manual pressure, and its position is adjusted using x-ray so as to lead directly into the joint space (3). The cutting tool is then inserted into the guide tube, after which it will exit and enter the joint space (4). The surgeon will expand the tool, which presses it against the top and bottom of the joint (5). Then, the surgeon merely has to pull the cutting tool down to cut cartilage (6). The cutting tool is then removed from the guide tube (8) and the cut cartilage can be removed using suction (9). These steps are then repeated to remove the subchondral bone in order to promote bone union (10). Finally, as an optional step, a bone graft can be injected through a flexible tube that is also guided using the guide tube (11).

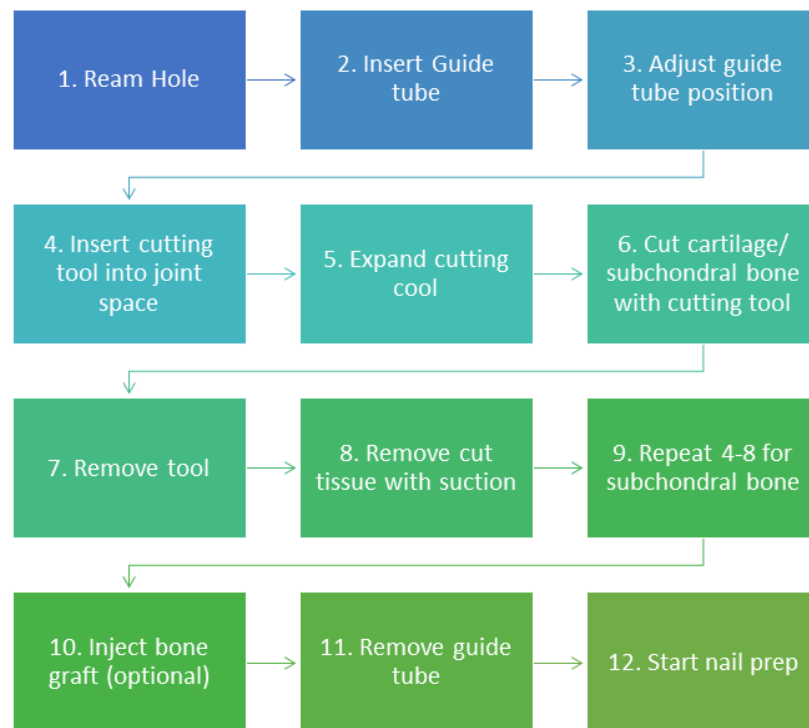


Figure 7: Workflow for Tool to Cut Cartilage for Preparation of Subtalar Joint for TTC Arthrodesis

Section 2B-2D below will describe the components of our design and its workflow in detail. Then, this section concludes with a discussion of the materials used in the design in **Section 2E**.

B. Guide Tube

Our first component is the guide tube, which guides the cutting tool into the joint space. As shown in **Figure 8**, the guide tube consists of a hollow bolt (1), nut (3), and circular disk (2).

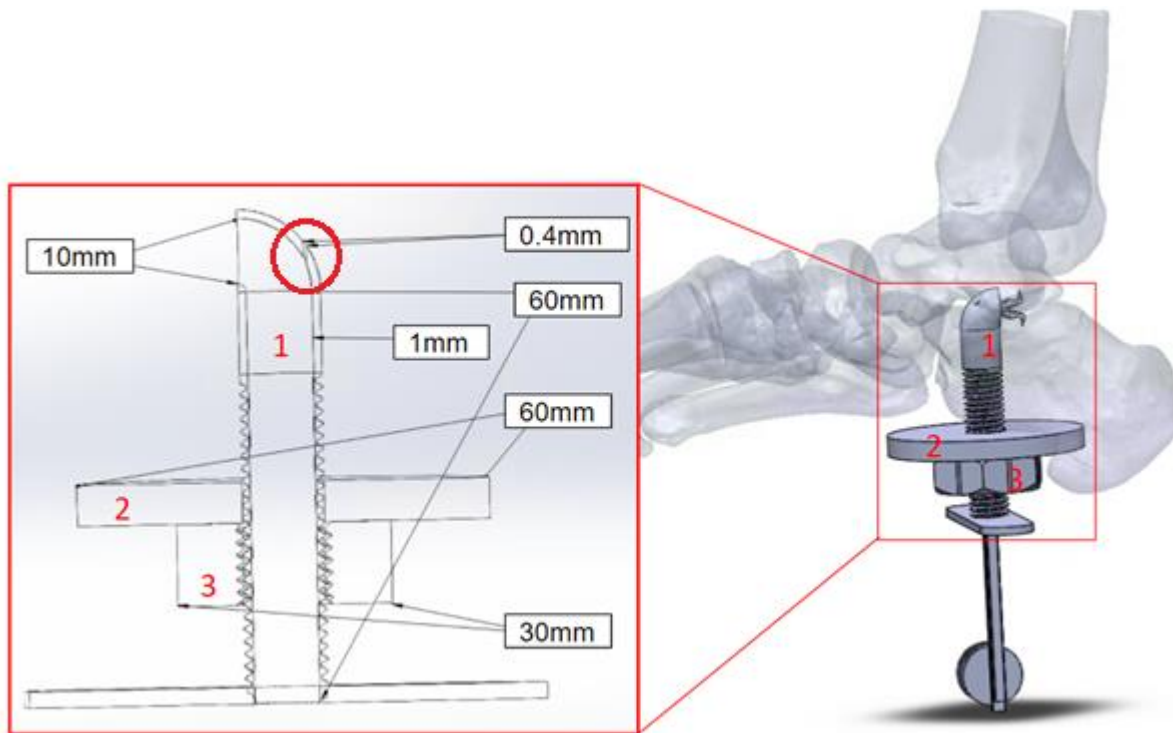


Figure 8: Scaled CAD model of guide tube, cutting tool, and foot. This figure displays the primed cutting position of the cutting tool and guide tube in the foot. A cross section of the guide tube is shown on the left, where 1 corresponds to the hollow bolt, 2 to the circular disk, and 3 to the nut. The red circle indicates a hole to accommodate for Kirschner wires used in the reaming of the ankle (discussed further in **Section 2D**).

Figure 8 above gives a scale view of the entire system and the ankle. For further visualization, the exploded view of the guide tube is shown in **Figure 9**.

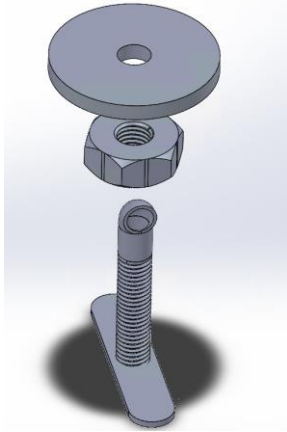


Figure 9: Exploded View of Guide Tube

Guide Tube Functionality

Once the guide tube is inserted with the disk pressed against the heel, it can be adjusted up and down by turning the nut so that the tip of the exit of the bolt aligns with the joint space. The bar at the bottom of the bolt helps lock it in place during adjustments. The optimal finger placement for this locking mechanism is shown by **Figure 10**, where the left hand locks the guide tube in place with their thumb, index, and middle fingers. The right hand is then free to rotate the nut with the thumb and the index or middle finger.

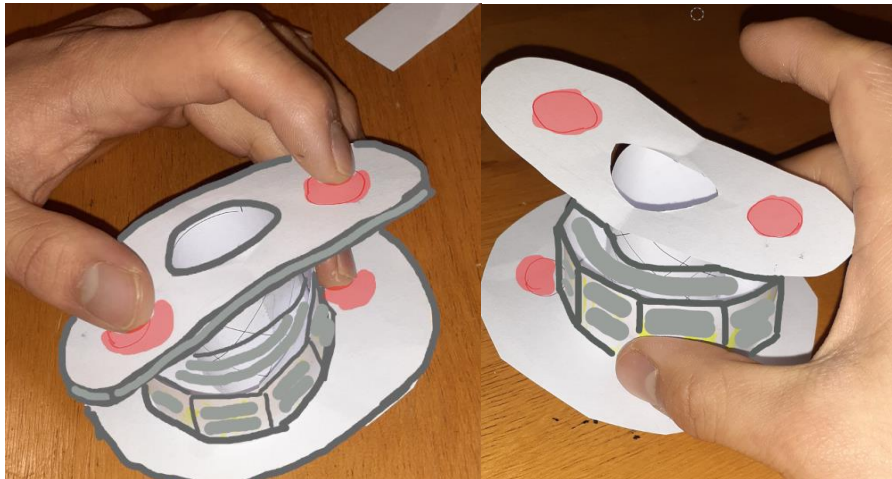


Figure 10: Right and Left Hand Placement for Guide Tube Handling. Pictured is a cartoon representation of the Guide Tube. The highlighted red dots indicate positioning for the right hand. The brown surface underneath the cartoon tool represents the foot the tool will be pressed against.

Guide Tool Purpose

The guide tube is used to help reduce surgery time and surgeon x-ray exposure. This is because once the guide tube is aligned to the joint space via x-ray, the surgeon inserts the cutting tool into the guide tube and it will exit exactly into the joint space. They can then pull the tool in and out of the joint space without requiring additional imaging or time to find the joint space again for re-insertion of the cutting tool. This also is meant to help give the surgeon confidence in their positioning. Further, the guide tube also facilitates easy access of the joint space for suction tubing and bone graft injection. By fitting the bone graft syringe with flexible tubing, that tubing can be guided into the joint space by the guide tube, and bone graft can be deposited to further promote bone union.

C. Tool and Blade Design

Cutting Tool Design

Our cutting tool comprises two rods, each with a knuckle-hinged blade attached. The two blades are pinned together, such that the blades can be opened and closed like scissors. The sharp ends of the blades face in opposite directions so that force can be applied to both the top and bottom of the joint space (i.e. the underside of the talus and the top of the calcaneus) (**Figure 11**).

A thumbscrew through one of the rods actuates an internal rack and pinion mechanism similar to that of Vernier Calipers. Turning the thumb screw moves the rod up or down, changing the bend angle at the hinges, and opening the scissor blades. The thumbscrew/rack and pinion assembly operates with a “right to tighten, left to loosen” convention, meaning that turning the screw clockwise opens the scissors and applies force, while turning counter clockwise closes the blades and removes force. Since the rods are only pinned together at the blade end, there is a small band of metal or plastic above the thumb screw to hold the rods in contact with each other (not pictured).

The dimensions of the tool components are constrained by the subtalar anatomy as well as the reamed hole through which the preparation is performed. Each rod has a 3x3mm cross sectional area with filleted outer edges. Thus, the two rods together are 6x3mm. To be comfortable in the hands of surgeons, the thumbscrew should have a diameter of roughly 1-3cm to meet the DIN464 standard (these thumbscrews can have diameters ranging from 5.5mm to 36mm) [31][32].

Lastly, within our workflow, the cutting tool is designed to be held and actuated by the surgeon’s dominant hand.

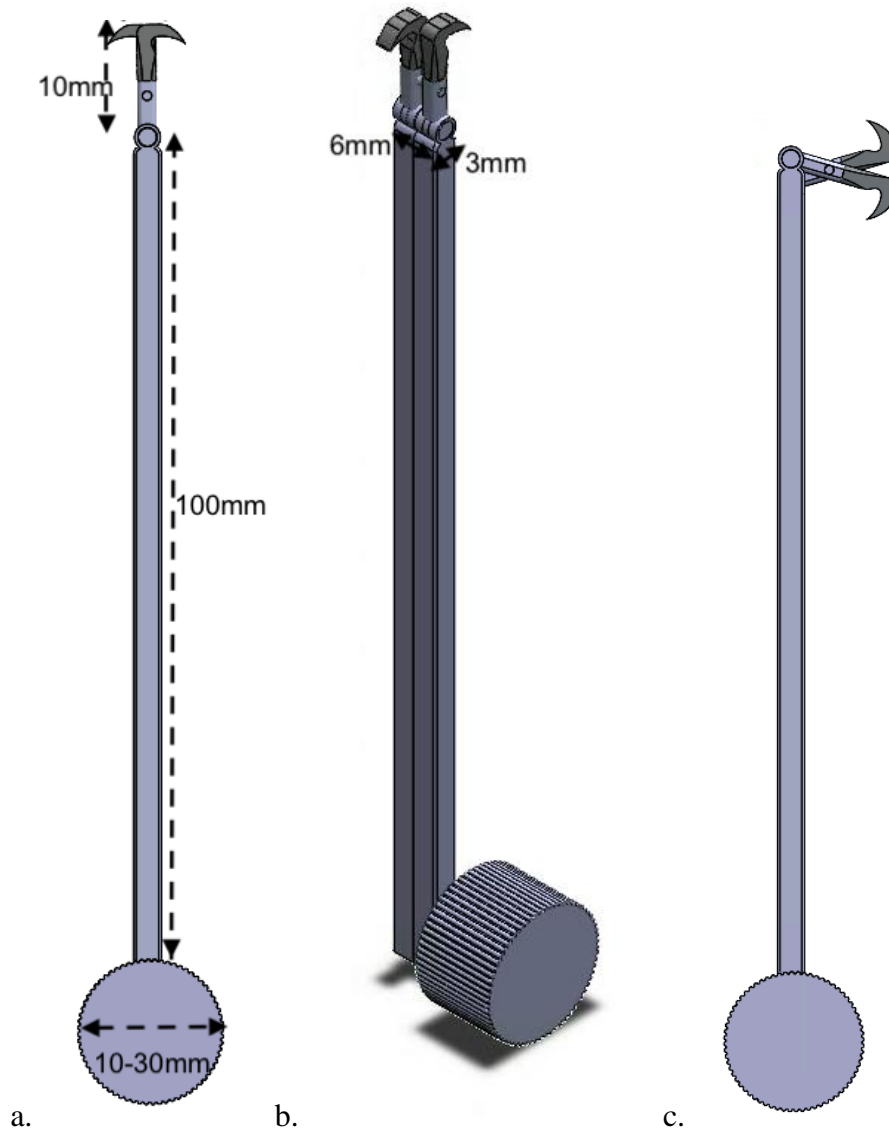


Figure 11: Views of a CAD model of the designed tool, alongside the appropriate dimensions of the tool. **(a)** front view, “closed”; **(b)** isometric view, “closed”; **(c)** front view “open”.

Blade Design

The blade has a hooked shape that tapers to a sharp cutting end (**Figure 12**). The angle of the hook should be 45° so that the cutting angle (or “rake angle”) is 90° when opened to the greatest degree within the joint space (i.e., the blades are in the “open” configuration, as shown in **Figure 12d**, with the two blade tips as far apart as possible). A 90° rake angle will ensure the smallest cutting force is required to remove cartilage (see **Section 3C** for more information regarding the rake angle definition and the force to cut cartilage). The selection of a 45° angle on the blade was based on estimates of the tool in the open configuration within the joint space (see **Appendix Q** for more information).

Just like the tool body, the size of the blade is constrained by the geometry of the reamed hole and guide tube, such that the blades should ideally fit through the guide tube in both an open and closed configuration. When the scissor blade is in the closed configuration, it should be able to be inserted into the joint space without much resistance, so the distance from the blade tip on one rod of the scissor mechanism to the blade tip on the other rod of the scissor mechanism when in the “closed position” (i.e., the position shown in **Figures 12a, 12b, & 12c**) should be as close as possible to 3mm. However, incorporating the 45° curve into the blade design requires more material to be added and makes the total width of the closed blades larger than the desired 3mm. According to surgeon testimony, inserting a larger blade into the joint space should not be a significant concern, as the foot is not weightbearing during the procedure, and the ankle can be put into gentle traction to reduce insertion resistance (**Appendix E1**). The curved shape of the blade should also help to spread the joint space open and prevent the tool from getting stuck in the cartilage during insertion. Further physical testing would be required to definitively confirm whether the current blade size is appropriate or whether a smaller blade must be re-designed and tested.

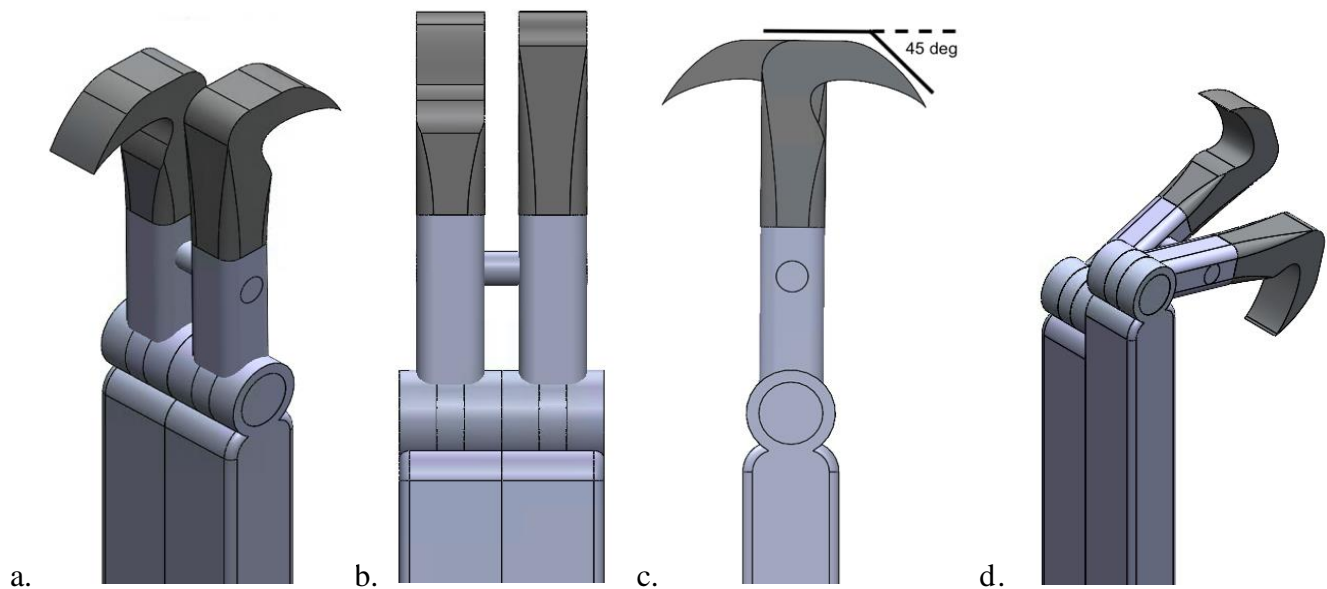
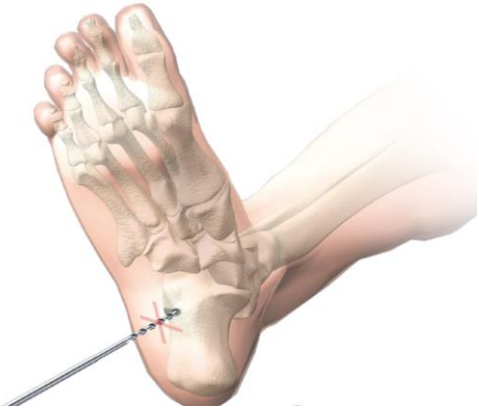
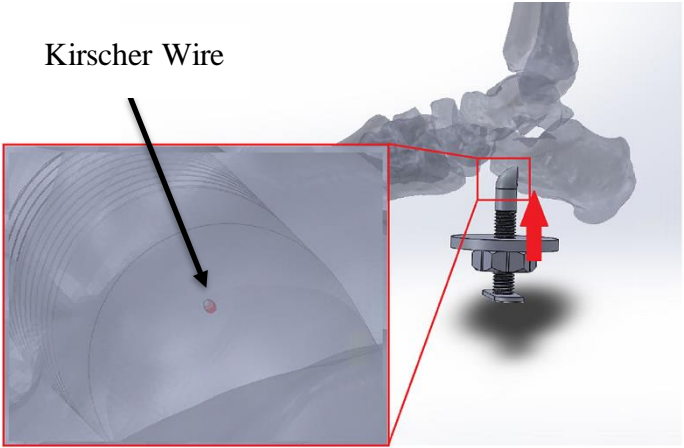


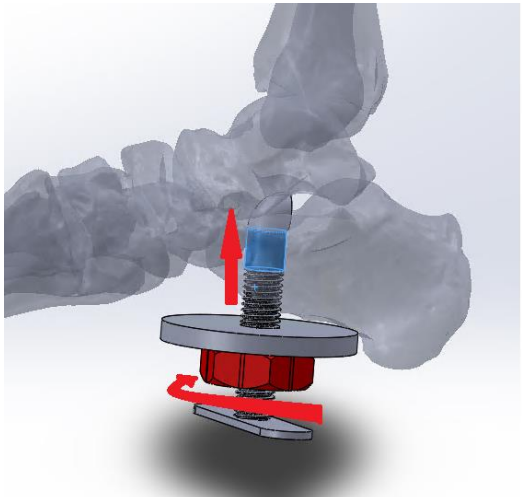
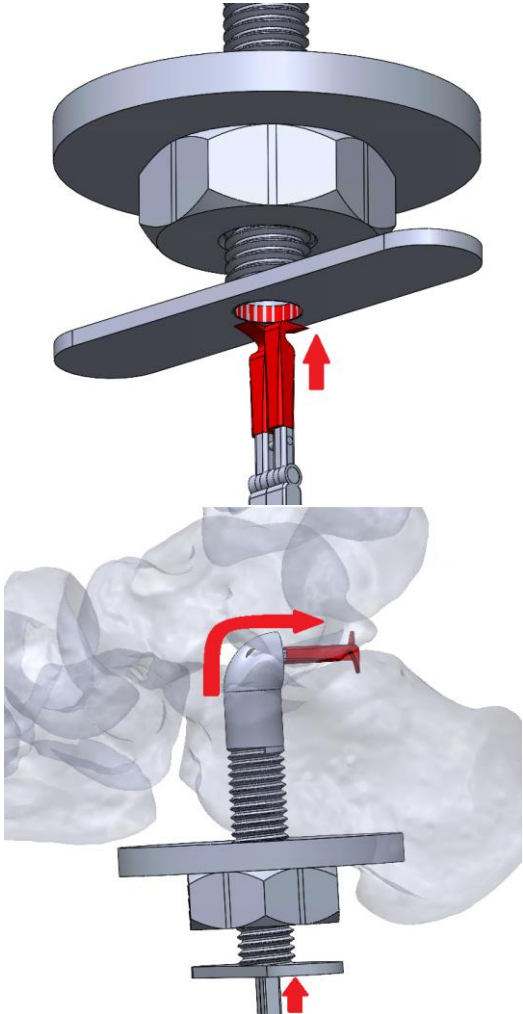
Figure 12: Various views of the blade design of our tool: **(a)** isometric view “closed”; **(b)** side view “closed”; **(c)** front view “closed”; **(d)** isometric view “open”. The blade is made of a different material than the rest of the tool, which is why it is depicted in a different colour. See **Section 2E** for more information on the blade’s materials.

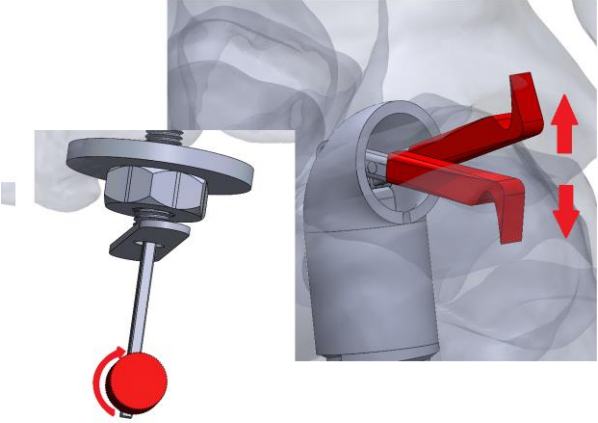
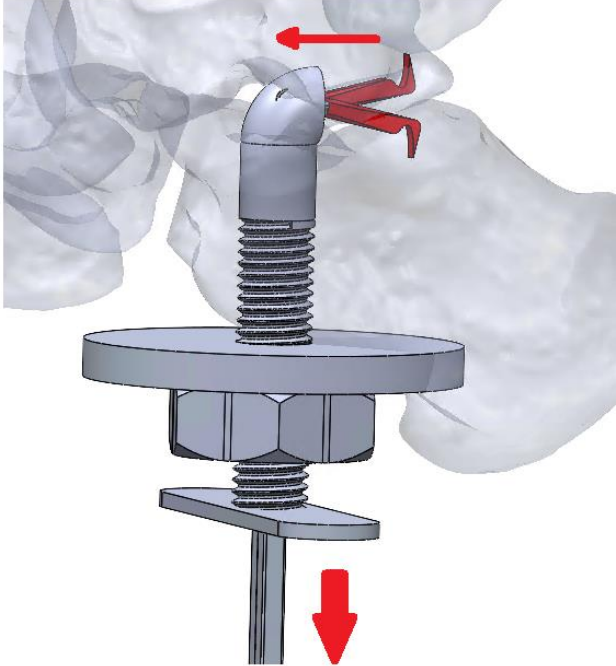
D. Detailed Workflow

This section of the report aims to provide a comprehensive overview of the workflow required to use our tool. Referring back to the workflow in **Figure 7**, each step will be described in detail in **Table 2** below, with schematics provided to aid in comprehension.

Table 2: Detailed workflow for usage of the guide tube and cutting tool to remove cartilage, disrupt subchondral bone, and inject bone graft. Steps correspond to those indicated in **Figure 7**.

Step	Directions	Image
<p>1</p>	<p>Ream Hole</p> <p>A 3cm plantar incision is made in the sole of the foot. Then, a guide wire is inserted through the calcaneus, talus, and into the tibial medullary canal, using x-ray imaging for guidance. Progressive reaming (widening of the hole) is performed using reamers passed over the guidewire in 0.5mm increments.</p>	
<p>2</p>	<p>Insert Guide tube into Reamed Hole</p> <p>The guide tube is inserted into the foot with the exit facing the posterior end of the foot. The guide tube is guided by the Kirscher Wire (not pictured) inserted into the red hole on the top of the guide tube.</p>	 <p>Kirscher Wire</p> <p>Top view of Guide Tube</p>

<p>3</p>	<p>Adjust Guide Tube Position</p> <p>Adjust the guide tube position by turning the nut. Each 360° degree rotation of the nut will cause a 5mm movement of the guide tube. The location of the guide tube exit can be visualized for confirmation and adjustment using x-ray.</p>	
<p>4</p>	<p>Insert the Cutting Tool</p> <p>Insert the cutting tool into the guide tube from the bottom hole. As the cutting tool reaches the curved top of the guide tube, the cutting tool's hinges will allow it to get pushed into the joint space.</p>	

<p>5</p>	<p>Expand Cutting Tool</p> <p>The blades of the cutting tool can be separated and expanded into the top and bottom of the joint space by turning the thumb screw in the handle of the cutting tool. A 90° rotation of the thumb screw will separate the blades by 0.5mm. Thus, while the final judgement will be based on the skills of the surgeon, on average, a 180° rotation of the thumb screw will be sufficient for cartilage removal. An additional 180° rotation will be sufficient for subchondral bone removal.</p>	
<p>6</p>	<p>Cut Cartilage</p> <p>Cartilage is cut by our tool by the surgeon pulling the tool down. The curvature of the guide tube in combination with the hinges of the cutting tool allow the downwards motion to be translated to the appropriate planes for cartilage cutting. Approximately 20 cuts are needed for sufficient cartilage removal (see Section 3F). Further analysis of the blade path can be found in Section 3G.</p>	
<p>7</p>	<p>Remove Cutting Tool</p> <p>The cutting tool can be removed once sufficient cartilage has been cut. The surgeon pulls the cutting tool downwards to remove it from the guide tube.</p>	
<p>8</p>	<p>Remove Cartilage</p> <p>Cartilage can be removed via two avenues. Since some of the removed cartilage is deposited into the guide tube by the cutting tool, when the surgeon removes the guide tube entirely, it will also inherently help remove cartilage from the foot. However, for sufficient removal, it is recommended</p>	

	that the surgeon uses a suction device to suck the cartilage out of the guide tube/subchondral joint space, using the guide tube to guide the suction tubing into the joint space.
9	<p>Repeat Steps 4-8 for the Subchondral Bone</p> <p>For this repetition, the surgeon may resort to a different method to prepare the bone. For example, the currently method to prepare subchondral bone is called “golf-balling”, which the surgeon may want to do with our tool rather than scraping. Here, they would use the cutting tool to make 1-2mm divots in the bone (Appendix E2).</p>
10	<p>(Optional) Inject Bone Graft</p> <p>The surgeon can choose to deposit synthetic bone graft into the joint space of the prepared subtalar joint. This can be achieved through the use of flexible tubing attached to a syringe filled with bone graft. Similar to the cutting tool and suction, this flexible tubing can be directed by the guide tube into the subtalar joint space, where bone graft can be deposited to further promote bone union.</p>
11	<p>Remove the Guide Tube</p> <p>The guide tube is removed by the surgeon and our tools workflow is complete.</p>
12	<p>Start Nail Preparation</p> <p>This step marks the return to the traditional workflow.</p>

E. Materials Selection

For materials, our tool is made of martensitic stainless steel (400-series stainless steel, SAE420 or SAE440) [33], with the blade made of tungsten carbide [34]. The selection of martensitic stainless steel was based on its preferential properties of hardness and durability [35][36][37]. These properties make it the typical material for surgical tools that cut and scrape such as scissors, chisels, and osteotomes, since the hardness better suits instruments that must maintain a precise cutting edge and/or tolerate stress during use [35][36][37][38]. Therefore, its selection for our application was logical. Furthermore, we decided to make the blade out of tungsten carbide in order to harden and sharpen this edge even further, since tungsten carbide is an exceedingly strong, durable metal [35][38]. This is again commonly seen in surgical applications, with the sharp edge of surgical scissors often reinforced with tungsten carbide in order to improve the scissors’ cutting capabilities [35][38].

3. Assessment of Final Design

In this section, we provide a comprehensive review of all of the tests done thus far in order to assess our final design. First, we start by providing an overview of our requirements alongside the planned tests in order to verify/validate those requirements. Then, we discuss in detail the various tests we have performed thus far to test our design, including low-fidelity prototyping, determining the force to scrape cartilage, calculating forces on the tool, performing blade simulations, performing surface area and timing calculations, assessing the blade scraping path, and performing cost analysis. We end with a summary of the tests we have concluded thus far as they stand against our requirements, indicating requirements that need to be further validated/tested in the future.

A. Verification Overview

Table 3 below lists the various requirements for the design, and the tests that correspond to meeting that requirement. Requirement numbers in **Table 3** correspond to those in **Table 1 (Section 1C)**. Tests are labelled in numerical order not corresponding to the requirement number. This is because some tests are utilized to assess multiple requirements with different measurements. Thus, some tests in **Table 3** are repeated, with these repeated tests labelled alphabetically (i.e., T5A, T5B, etc.). Here, the description for the first test “A” (T5A) gives both the overall test and how that specific requirement is being assessed. Then, the subsequent “B,C” tests (i.e., T5B, T5C) only provide a description of how that specific requirement is being assessed using the overall test described in the test “A” description.

Table 3: Tests related to requirements (**Table 1**). *Note:* test # does not correspond to requirement #.

#	Requirement	Verification/Validation Test
1	The design must access the ~3mm joint space through an 11 mm reamed hole.	T0: Dimensions of the final design or prototype.
2	The design must be able to traverse up through the reamed hole to access the subtalar joint.	T0.

3	The design should achieve cartilage destruction (25-50%).	<p>T1: Low-fidelity prototyping to demonstrate tool functionality to appropriately scrape the surfaces of the joint for cartilage/bone removal.</p> <p>T2A: Surface area (SA) calculations, which analyze the percent of cartilage/bone destruction across the joint based on joint SA the tool is used on compared to total joint SA. For this requirement, an average cartilage thickness of 1-2mm is assumed.</p> <p>T3A: Force calculations to determine the forces required to achieve cartilage destruction across the joint. For this requirement, the forces are based on scraping into a 2mm cartilage thickness.</p> <p>T4A: Blade simulations to ensure our tool will be able to withstand appropriate forces. For this requirement, the forces are those to remove cartilage.</p> <p>T5A: Use high-fidelity tool prototype on a sample cadaver foot based on tool usage per the detailed workflow described in Section 2D. For this requirement, assess % cartilage destruction by using tool and performing post-hoc assessment of cartilage destruction (determine how much of the joint surface shows disruption via analyzing a picture of the dissected, exposed joint space).</p>
4	The design should achieve removal of broken, loose cartilage (50-100% of broken cartilage).	<p>T6A: Design allows for easy insertion of flexible tubing into the joint space (Y/N). For this requirement, the flexible tubing is suction tubing to remove broken, loose cartilage.</p> <p>T5B: For this requirement, assess % removal of broken cartilage by comparing volume of cartilage retrieved through suction during the tool workflow versus volume of loose cartilage that can be found still remaining in the joint space. This test can then inform recommendations to surgeons in real surgical practice.</p>
5	The design should achieve subchondral bone disruption (50-100% of exposed bone).	<p>T1.</p> <p>T2B: For this requirement, assume that it is desirable to penetrate ~1.5mm into subchondral bone for sufficient activation (Appendix E2).</p> <p>T3B: For this requirement, spongy bone has required lower forces since it is softer [21] (Appendix E2), so forces determined for cartilage (test T3A) can be assumed to be less than or equal to those for spongy bone, especially since the bone and cartilage are both penetrated to a similar depth.</p> <p>T4B: For this requirement, the same simulation force as test T4A can be used for the same reasoning as in the aforementioned test T3B.</p> <p>T5C: For this requirement, assess % bone disruption within the surface area exposed by the tool (analyze a picture of the dissected, exposed joint space).</p>
6	The design must be able to penetrate into cartilage/subchondral bone	<p>T3C: Consider forces required to penetrate and scrape a 2mm thickness, since 3.5mm thickness scraping will be achieved through 2 successive stages of scrapes that penetrate at a ~1.75mm depth (bone preparation will occur over surfaces previously scraped to remove cartilage).</p>

	on either side of the joint by at least 3.5mm.	T5D: For this requirement, assess how deep the tool penetrates into both sides of the joint by looking at the “divot” on the prepared region in the dissected, exposed joint surface.
7	The design’s penetration into the cartilage/subchondral bone should be controllable.	T7: Depth of tool penetration is controllable (Y/N). T8: If T7 is a yes, with the final prototype, measure the displacement of the blade with every “step” in the mechanism for controlling depth. For example, in the case of our final design, investigate at the resolution of the Vernier caliper mechanism.
8	The design should be able to act (promote fusion) in the A/P direction (angles $48^{\circ} \pm 15^{\circ}$ and $132^{\circ} \pm 15^{\circ}$).	T9: Assess the range of angles that the final design can accommodate in degrees. Determined on the CAD model of the tool as well as the produced prototypes.
9	The design should facilitate deposition of synthetic bone graft into the joint space.	T6B: For this requirement, the flexible tubing is tubing appended to the bone graft syringe to facilitate for graft deposition. T5E: For this requirement, following bone graft insertion in a cadaver model, obtain x-ray images and/or dissect the joint to assess how well bone graft was deposited into the desired joint space region.
10	Minimize cost of the device (< \$100 CAD).	T10: Calculate the cost of the tool based on materials and manufacturing considerations for the design.
11	Minimize surgical time (< 10 minutes).	T11: Estimate the total time required for the procedure based on the expected times to perform each step in the workflow from Section 2 . T12: Time it takes for the surgeon to complete the full subtalar joint preparation procedure on a foot cadaver sample with a high-fidelity prototype of our tool.
12	Minimize changes to technique (avoid time-consuming steps).	T13: Add up the number of steps in the detailed workflow, and compare to the typical joint preparation workflow; for each step, compare the typical time to complete these steps.
13	Maximize the intuitiveness and ease of use of the design.	T14: Compile surgeon responses to our surgeon confidence and ease of use survey (Appendix I) after using a high-fidelity prototype of our tool on a foot cadaver sample.
14	Tool should be used without direct joint space visualization.	T15: Assess whether the tool can be visualized within the joint space, as determined based on the material selection and whether it is visible under x-ray imaging modalities.

In the subsequent sections, we will describe the various tests we have performed thus-far, before summarizing the requirements we have been able to test and those that have been left as next steps and future work moving forward.

B. Low-Fidelity Prototype

To understand whether our proposed mechanism of performing cartilage destruction was sensible, we aimed to create a low-fidelity of our prototype at a much larger scale as a simple proof-of-concept (**Test T1**). Given the constraints of limited time and resources, this was the highest fidelity prototype we were able to generate. A picture of this tool can be seen in **Figure 13a**, alongside a still image of the tool in a pseudo-joint space made out of 2 bars of soap (**Figure 13b**). The tool was constructed by appending ornament hooks onto scissors, with the scissors then added onto the Vernier callipers with tape. Most notably, it can be seen in **Figure 13b** that the tool was able to scrape the soap and generate shards of “cartilage,” a promising result.

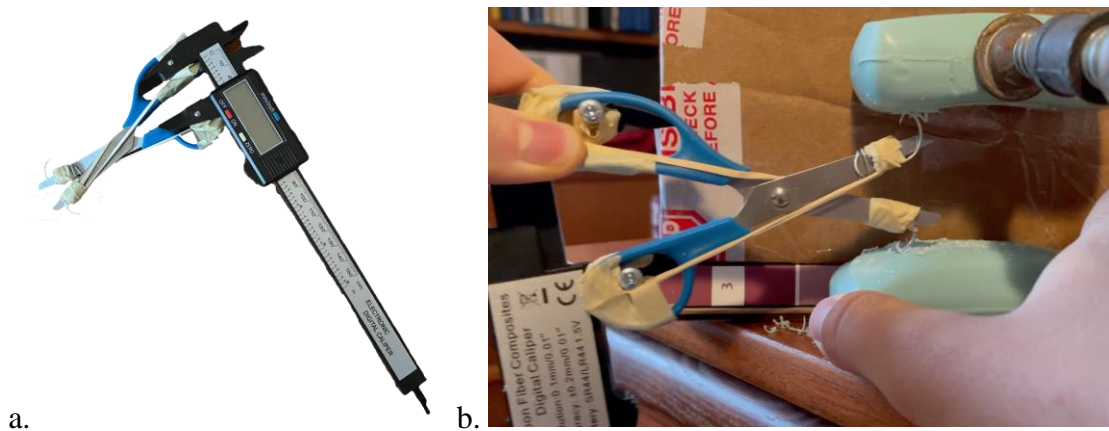


Figure 13: Low-fidelity prototype of our tool. **(a)** A picture of the low-fidelity prototype. **(b)** A picture of the low-fidelity prototype in our pseudo-joint space, with two bars of soap representing the articulating surfaces of the talus and calcaneus. Shards of soap due to scraping are visible.

A key feature missing in this prototype was the presence of a flexible hinge, which could not be implemented in this low-fidelity setting with limited household manufacturing resources. While we tried to create a hinge-like mechanism by drilling screws into the Vernier calipers, the screws did not provide the adequate friction at the hinge in order for them to be tested as a proof-of-concept. Moving forward, having a prototype that can include this hinge mechanism will be important for testing and validation

purposes. Such a tool should be able to be 3D printed and assembled relatively easily, especially if printed at a larger scale.

C. Force to Scrape Cartilage

In order to determine the force required to scrape cartilage (**Test T3**), data was extrapolated from a study that isolated the variables in the cutting of acetabular bovine cartilage [39]. In this study, individual variables were isolated to determine their effect on the force required to cut cartilage, where force was measured using a controlled experimental setup shown in **Figure 14a**. From this study, we determined that cutting depth, initial cutting position, and rake angle of the blade are the three variables that most significantly affect the force required to cut cartilage. The rake angle is the angle that the tool makes with the normal vector to the surface (**Figure 14b**) [40]. By interpolating the information provided through graphs in the paper, a Python script was created that outputs the force required to make one cut of depth X mm, initial position Y mm, and a rake angle of Z degrees, where X , Y , and Z are variables to be specified by the user. From this script, we determined that the maximum force our blade is expected to encounter is **27.6N**, with a 2mm deep cut, which is more than the average expected depth of cartilage. Please see **Appendix J** for the description of the code with sample outputs.

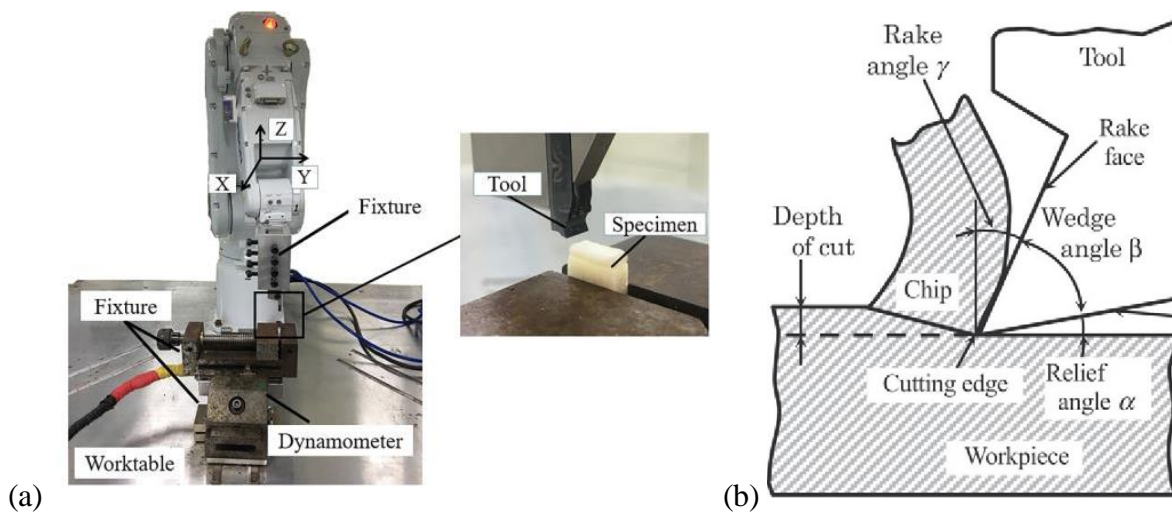


Figure 14: Determining the force to scrape cartilage. **(a)** Experimental setup to measure cartilage cutting force, borrowed from [39]. **(b)** Schematic representation of the definition of the rake angle, borrowed from [40].

D. Force Calculations on Tool

We performed sophisticated calculations of various forces on the tool to assess the tool's ability to cut cartilage, based on the forces determined in **Section 3C** above (**Test T3**). We have mainly focused on three major forces that contribute during the tool operation: handling force, friction force on the hinges, and force on the pin, which are shown in **Figure 15** below.

The handle force and force on the pin were calculated using the relationship developed in a study that modelled the forces of cutting with scissors by *Mahvash et al.* [41]. In terms of the friction on the hinges, it is identified through balancing the torque from the gravity on the scissors at its centre of mass and the torque produced by the friction on the hinges.

Our team has developed a MATLAB program that was used to test values for different variables such as pin position, opening angles of the scissor mechanism, etc. (**Appendix K**). As a result of the tests, we optimized the pin position of our tool to be 3mm, as is shown in **Figure 15**.

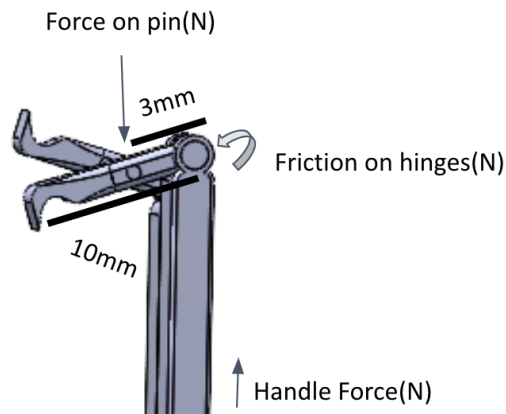


Figure 15: Force Diagram of the tool

The resultant handle force under the 27.6N cutting force is calculated to be 9.17N (**Table 4**). Referring to a survey reported by *Nilsen et al.* regarding grip force and pinch grip in an average adult population [42], the average grip force of an adult is approximately 300N. Therefore, it is assumed that a surgeon can easily apply this handle force when operating our tool for at least 10 minutes. The friction on the hinges was discovered to have a significantly small value on the order of pico-Newtons (**Table 4**), which informs our hinge design to ensure that it will not swing and is instead guided into the joint space. Finally, for the force on the pin, the scissors will only break if there is horizontal pulling force (shear) on the pin, which is not present during the operation of our tool. As such, the force at the pin of 3.93N (**Table 4**) will not be a failure point in our design.

Table 4: Calculated Force Result with 3 mm pin position

Friction on Hinges	6.18 x 10⁻⁹ N
Handle Force	9.17 N
Force on Pin	3.93 N

* details for testing with varying parameters can be found in **Appendix K**

E. Blade Simulation Testing

We performed stress/strain testing in SolidWorks [43] on the proposed blade design to determine stress concentrations, an approximate factor of material safety, and the amount of deformation of the blade (**Test T4**). Static loads of 15N and 50N were applied to the inner face of the blade, while the far end geometry was held fixed (see **Figure 16** for diagram). Tests were run with blade lengths of 5mm and 10mm to determine the effect of length on the aforementioned outcomes. Material properties for tungsten carbide were used to assess the design (elastic modulus = 600-686GPa; Poisson's ratio = 0.2-0.22; density = 15250-15880 kg/m³; yield strength = 335-530 MPa) [34].



Figure 16: Force was applied normally to the red surface. The geometry outlined in green dotted lines was held fixed.

Concentrations of stress were found to be at the bend in the angled blade (see **Figure 17a** for representative example result). Highest material deflection was found at the tip of the blade, as expected (see **Figure 17b** for representative example result). All simulation result images can be found in **Appendix L**.

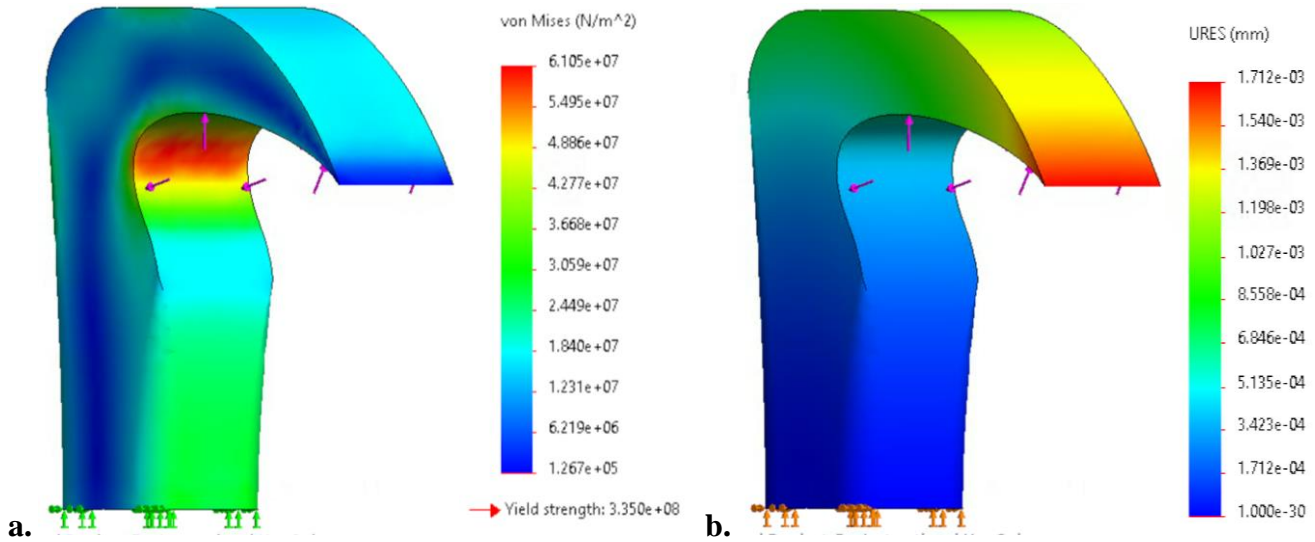


Figure 17: Blade simulation sample results. **(a)** Colour map for stresses experienced by the blade. **(b)** Colour map for deflection experienced by the blade. For all simulation results, see **Appendix L**.

For applied forces of 15N and 50N, where 50N is two times higher than the maximum force to cut cartilage from **Section 3C**, and blade lengths of 5mm and 10mm, the maximum stress, strain, and deflection on the blade were determined (**Table 5**). The maximum stress, $2.0 \times 10^8 \text{ N/m}^2$, was generated by the 50N force and was consistent on both the 5mm and 10mm blade. Compared to tungsten carbide's variable yield strength of $3.35\text{-}5.30 \times 10^8 \text{ N/m}^2$, we have a factor of safety of 1.7-2.7, meaning that we expect stresses to remain in the elastic (as opposed to plastic) regime. However, we do not expect this 50N force to be reached during normal use of the tool. The stress generated by the 15N force, which is a more reasonable force to encounter during the procedure, is under the yield strength by a factor of 5.5-8.9 and is also nearly constant between the 5mm and 10mm blade designs.

The material deflection at the blade tip varied with both blade length and force applied from 1.7-9.1 μm . As mentioned above, these deflections should be elastic and therefore transient. Future tests should include fatigue testing to determine if the repeated loading cycles associated with scraping will permanently damage the blade.

Table 5: Blade stress, strain and deflection under simulated cutting forces of 15N and 50N.

Force Applied (N)	15		50	
Blade length (mm)	5	10	5	10
Max Stress (N/m ²)	6.1×10^7	6.0×10^7	2.0×10^8	2.0×10^8
Max Strain	6.9×10^{-5}	6.9×10^{-5}	2.3×10^{-4}	2.3×10^{-4}
Max Deflection (μm)	1.7	2.7	2.7	9.1

F. Surface Area and Timing Calculations

As previously described, between 25-50% of the total joint surface area should be cleared of cartilage to promote joint fusion. To determine the usability of our tool, we estimated the number of times the surgeon would need to pull the tool across the subtalar joint to achieve this level of cartilage removal (**Test T2**). We measured the size of the articulating surface on each joint from a 3D printed life-size ankle model, using a bounding box approach to simplify the complex sigmoidal shape of the bones. The talar surface was found to have an approximate area of 600 mm² and the calcaneus an area of 726 mm². The depth of cartilage was assumed to be uniformly 1.5 mm, based on the findings of *Akiyama et al.* [15], which indicate the cartilage depth is between 1-1.5 mm in most of the joint. See **Figure 18** below for representations of the talus and calcaneus from [15] with colour scales representing the depth of cartilage across the joint, and our team's measurement information overlaid. Based on the dimensions of our tool, we assumed a scrape size of 2 mm (W) x 10 mm (L) x 1 mm (D), although the depth should be further verified through physical testing of a metal blade on human cartilage (i.e., **Test T5**). The cross-sectional area of the smallest reamed hole used is 35 mm², which we considered to be included in the % surface area cleared.

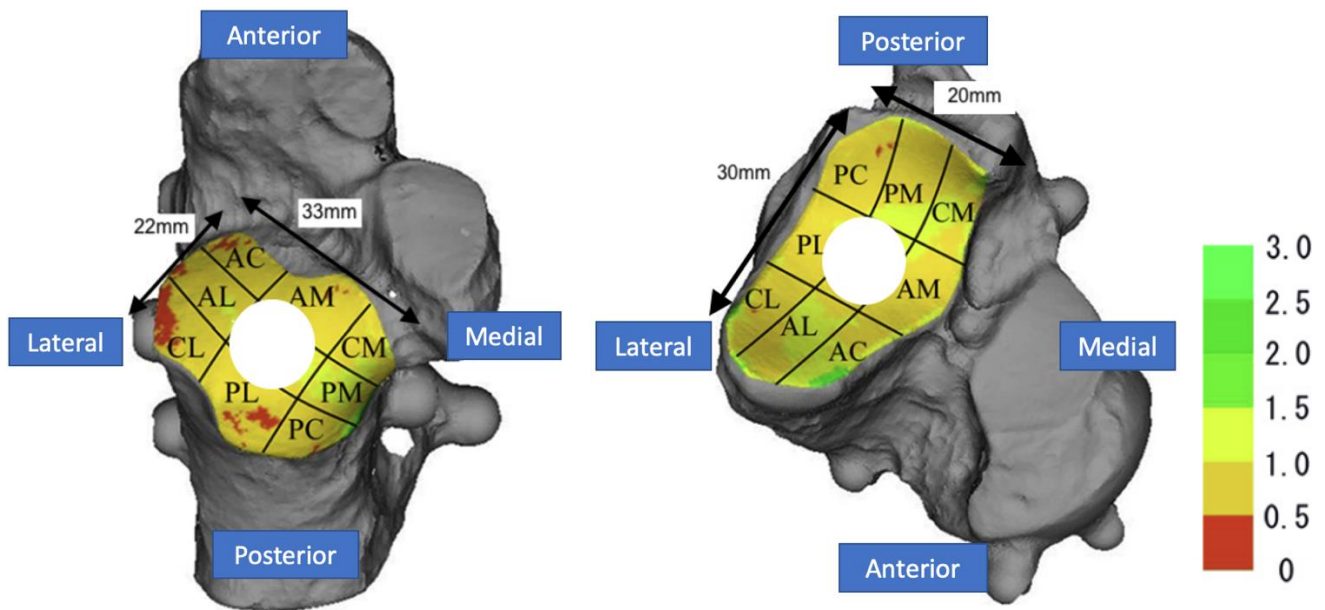


Figure 18: Cartilage thickness along the subtalar joint. Calcaneus (left) and talus (right). Color scale bar is in mm of cartilage thickness. White circle indicates the approximate size and position of the hole reamed through the TTC bones. Borrowed from [15].

The results of the calculations are summarized in **Table 6** and **Table 7** below, with the full calculations available in **Appendix M**. The minimum number of scrapes to remove 25% of the cartilage on the calcaneus is 11, which would remove just over 25% on the talus.

Table 6: Number of scrapes on the talus necessary to remove sufficient cartilage by surface area.

Talus surface area scraped (% of total)	Number of scrapes (2 mm x 10 mm x 1 mm)
25	8.6
50	19.9

Table 7: Number of scrapes on the calcaneus necessary to remove sufficient cartilage by surface area.

Calcaneus surface area scraped (% of total)	Number of scrapes (2 mm x 10 mm x 1 mm)
25	11.0
50	24.6

Using a conservative value of 20 scrapes (resulting in 50% removal on calcaneus) and the tool workflow developed, we estimate the time to complete the procedure to be 6-7 minutes (**Test T11**).

Therefore our tool can be implemented into the existing TTC nailing procedure without much extra operating room time. Please see **Appendix M** for the full calculations and estimations for the timing of each step.

G. Blade Scraping Path and Scrape Region

Although not a specific verification test, it is essential to understand how our tool operates within the joint space, especially when considering risks such as damage to major nerves (Risk Analysis, **Section 3J**). Conducting a conclusive analysis of the scraping path of the blade would require a high-fidelity physical prototype with working joints, which we were unable to make within the time constraints of this project. However, as understanding the path of the blade is still a critical aspect of the design, we have undertaken a simplified mathematical estimation based on the tool's degrees of freedom and dimensions, alongside the approximate dimensions of the subtalar joint.

Blade Scraping Path

In **Section 3F**, we estimated the length of the articulating surface to be about 30mm, with the 10mm diameter guide tube placed roughly in the center, meaning there is around 10mm of cartilage on either side. Thus, the blade length should be no longer than 10mm, although it may be further constrained by other geometries.

The combined cross-sectional area of the two rods is 6x3mm. The inner diameter of the guide tube is 10mm, meaning that the cutting tool has room to move in all directions while inside the tube. We expect that during the procedure the tool will be moved both side to side and down out of the reamed hole (**Figure 19**).

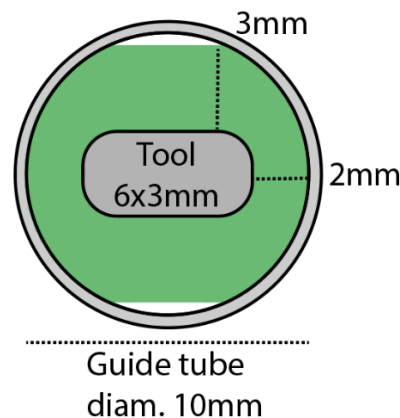


Figure 19: Cross section of tool and guide tube. Based on geometric constraints, the cutting tool can move within the guide tube anywhere in the green area. Relevant distances are marked with dotted lines.

The average inclination angle of the slope of the subtalar joint is 42° [23]. **Figure 20** and **Figure 21** below show the cutting tool in the posterior and anterior portions of the joint, respectively. In both cases, once the tool is expanded in the joint space, it should be pulled/pushed on a 42° diagonal to maintain as even a force as possible on both the talus and calcaneus. Then the tool can be pulled straight down through the reamed hole or reinserted into the joint space.

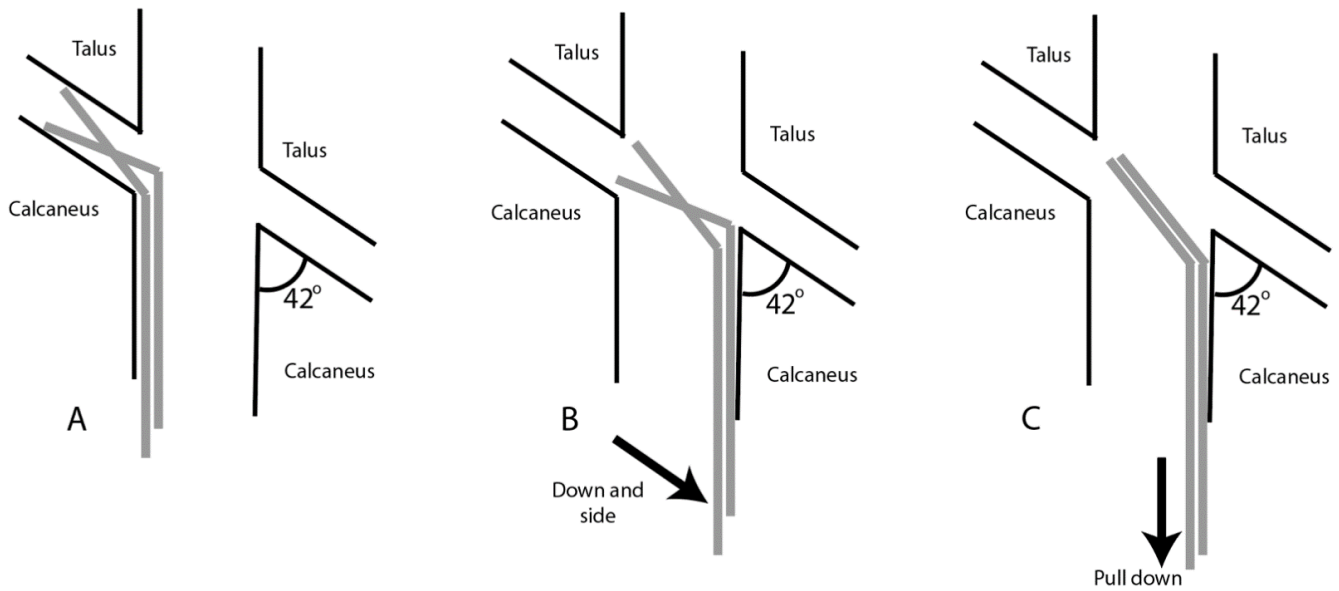


Figure 20: High level diagram of tool use showing posterior scraping. (a) The tool begins in the expanded or “open” configuration, applying cutting force; (b) the tool is pulled on a diagonal down and to the side, following the angle of the joint; (c) the thumbscrew is actuated to close the blades and the tool is pulled straight down out of the hole or reinserted into the joint for further scraping.

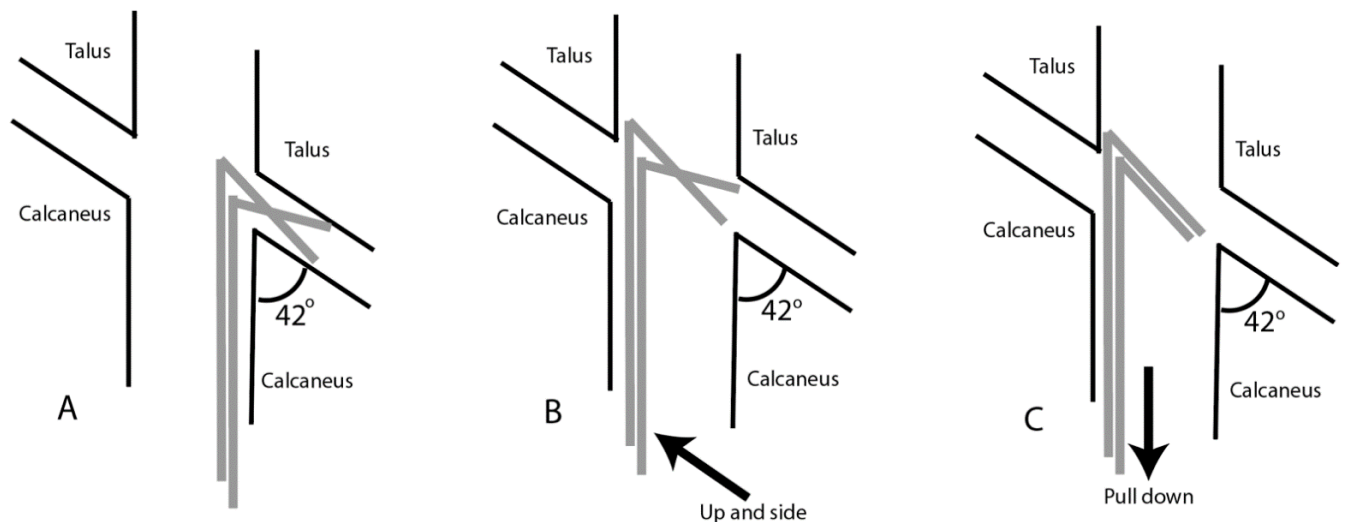


Figure 21: High level diagram of tool use showing anterior scraping. (a) The tool begins in the expanded or “open” configuration, applying cutting force; (b) the tool is pulled on a diagonal up and to the side, following the angle of the joint; (c) the thumbscrew is actuated to close the blades and the tool is pulled straight down out of the hole or reinserted into the joint for further scraping.

In the anterior scraping procedure, there is a potential risk of tool from becoming stuck in the guide tube while bent at the 42° angle. **Figure 22** below shows an approximate calculation for the maximum blade length allowable to mitigate for this risk. With the horizontal side of the triangle set to 6mm based of the maximum freedom of movement calculated in **Figure 19** above, the 42° angle yields a hypotenuse (i.e. blade length) of 9mm.

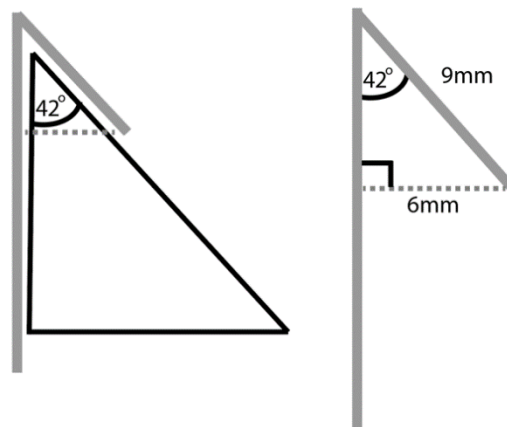


Figure 22: Using average angle of anterior subtalar joint to calculate maximum possible blade length. Grey shape is a simplified representation of the cutting tool.

Given that this result is entirely dependent on the precise relationship between tool, guide tube, and joint geometry, as well as the degrees of freedom at the tool’s joints, further evaluation by physical prototype testing would need to be performed to confirm the optimal blade length. Future work would include tests on cadaver models, ideally with various joint sizes, starting with a high-fidelity prototype with a 10mm blade length (**Test T5**) and making optimizations from there based on the results of hands-on usage.

Scraped Region

In addition to the path of the blade in the foot, we also evaluated the range of the tool with respect to the intended scraping area and the risk of the damage to surrounding structures. **Figure 23** below shows the medial and lateral views of a left foot with the subtalar joint highlighted in green. On the lateral side, the intermediate dorsal cutaneous nerve and the medial sural nerve are the closest nerves to the joint, but

are far enough away from the joint space that our tool could not reach them. On the medial side, however, the tibial nerve runs adjacent to the joint space and warrants further investigation. All blood vessels near the subtalar joint lie right beside the nerves, but are not shown in **Figure 23** below for simplicity.

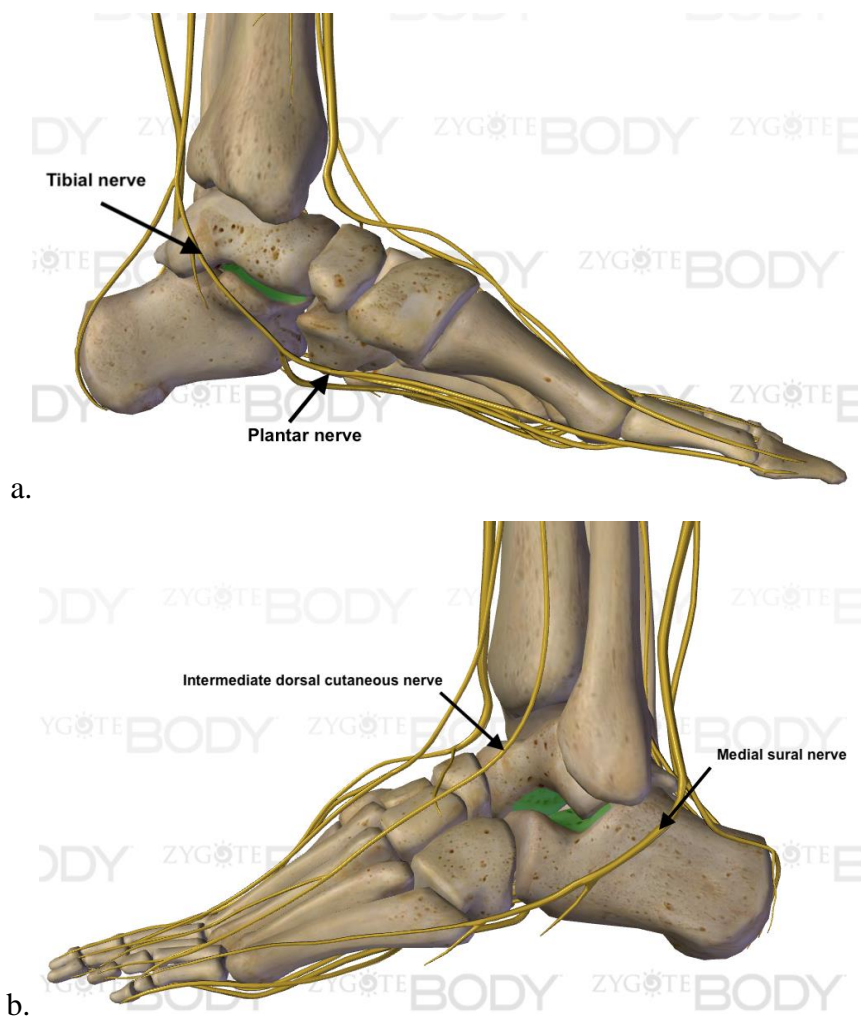


Figure 23: Depiction of left foot ankle anatomy with important nerves labeled and subtalar articulating surface highlighted in green. **(a)** Medial view of left foot. **(b)** Lateral view of left foot. Images obtained using the ZygoteBody online 3D anatomy tool [44].

We performed a simple analysis of the tool’s range with respect to hitting the tibial nerve, taking an image of the calcaneus and marking the approximate positions of the tibial nerve branches as indicated by ZygoteBody [44], an online 3D anatomy tool (see **Figure 24** below). Based on the joint measurements from **Section 3F**, we then overlaid a reamed hole of approximately 11mm diameter on the talar articular surface. Then, taking the maximum blade length of 10mm, a red circle was drawn outside of the reamed hole to indicate the maximum area that would be scrapable by the tool if the guide tube was not used. These estimations suggest that the surgeon is not at risk of damaging nearby nerves with our tool. Additionally, normal use of the guide tube would further constrain the reach of the blade to one circular sector at a time in either the anterior or posterior direction only, rather than a full circle of range.

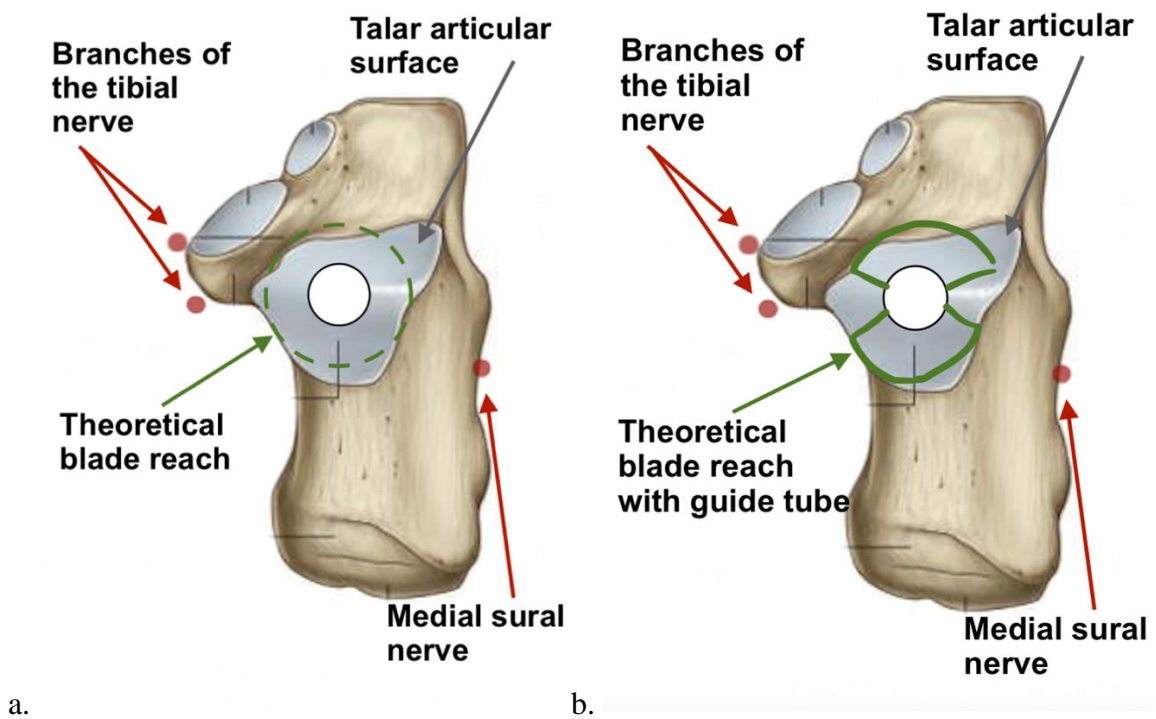


Figure 24: Depiction of right foot articulating subtalar surface with approximate location of important nerves indicated. The reamed hole is the white circle on the joint surface. **(a)** The dotted green circle shows the theoretical scraping range of the tool without use of the guide tube. **(b)** The sketched green sectors represent the area we are intending to scrape in the anterior-posterior (A/P) direction with use of the guide tube.

H. Cost Analysis

For our cost calculations (**Test T10**), we estimated both the cost for the raw materials and the manufacturing costs. These estimates are shown below in **Table 8**.

Briefly, the market price for 1mm-thick 420-series stainless steel was determined by contacting a metal retailer, and was found to be \$0.82 USD per pound (\$1.07 CAD per pound) (**Appendix N**). For tungsten carbide, we used market research to find that costs fluctuate from \$5.00 USD per pound to \$8.25 USD per pound [45]. Taking the higher end of this market price fluctuation, we used a price of \$11 CAD as a conservative cost estimate for our calculations. Finally, and most importantly, we estimated manufacturing costs based on a 2010 article regarding the costs to make surgical instruments [46]. Here, they reported the costs for a completely machined device used in endoscopic surgery for cutting and cauterizing applications, where these manufacturing costs were \$27 USD per tool [46]. Since the article is from 2010, accounting for inflation based on the Bank of Canada’s inflation calculator [47] gave an approximate cost of \$31.62 USD (\$41.11 CAD) per tool for manufacturing. Now, while we understand that manufacturing costs will vary considerably in our tool as compared to this example, it gives an approximate benchmark we can use as an indication of how much raw manufacturing would cost per tool. In addition, even if this price was 2.5 times higher, we would still be within our cost criteria outlined in **Table 1**.

Furthermore, in order to find the cost per tool, the density of tungsten carbide and 420-series martensitic stainless steel [33][34], as well as approximate dimensions of the tool to determine the volume of metal, were needed (**Appendix N**). Overall, we found the cost per tool to be approximately \$42.60 CAD per unit (**Table 8**). This cost estimate will need to be updated once the full manufacturing of the tool is complete and true manufacturing costs for production can be determined.

Table 8: Rough cost estimates for the tool, including the guide tube and the cutting tool.

Item	Market Price (CAD)	Cost per tool (CAD)
420-series martensitic stainless steel (cutting tool body and guide tube)	\$1.07 / lb	\$1. 57 (Appendix N)
Tungsten carbide (blade)	\$11 / lb	\$0.01 (Appendix N)
Manufacturing costs	n/a	\$41.11 [46][47]
Total:		\$42.60 per tool

I. Assessment of Requirements

As a summary, a final assessment of our requirements can be found in **Table 9** below. For the most part, all our requirements have been met or conditionally met upon assessment, with conditional cases requiring re-assessment with a higher-fidelity metal prototype tested in a realistic environment, such as performing the surgery on the lower extremity of a cadaver. Only one requirement (R13) will need to be assessed in the future, as it relies directly on surgeon feedback after using a high-fidelity prototype, and no proxy tests can be done on lower-fidelity models at this time.

Table 9: Final Requirement Assessment Table. For test descriptions, see **Table 3**.

#	Requirement	Test	Assessment
Space			
1	The design must access the ~3mm joint space through an 11 mm reamed hole.	T0	<u>Met.</u> Based on cutting tool and guide tube dimensions (Section 2).
2	The design must be able to traverse up through the reamed hole to access the subtalar joint.	T0	<u>Met.</u> Based on cutting tool and guide tube dimensions (Section 2).
Outcome			
3	The design should achieve cartilage destruction (25-50%).	T1, T2A, T3A, T4A, T5A.	<u>Conditionally Met.</u> Tests T1 (low-fidelity prototype, Section 3B), T2A (surface area calculations, Section 3F), T3A (force calculations, Section 3C & 3D), and T4A (blade simulations, Section 3E), all demonstrate that this requirement can be met for 25-50% cartilage removal; however, it will need to be fully validated through test T5A (test on cadaver) in the future.
4	The design should achieve removal of broken, loose cartilage (50-100% of broken cartilage).	T5B, T6A.	<u>Conditionally Met.</u> The use of the guide tube satisfies T6A, with a “yes” answer to the question of whether the design allows for easy insertion of flexible tubing. Further, the nature of the cutting procedure favours cartilage removal, as the cartilage is pulled into the guide tube rather than pushed away into the joint space. However, it will need to be fully validated by test T5B (test on cadaver for removed cartilage volume) in the future.

5	The design should achieve subchondral bone disruption (50-100% of exposed bone).	T1, T2B, T3B, T4B, T5C.	<u>Conditionally Met.</u> Tests (low-fidelity prototype, Section 3B), T2B (surface area calculations, Section 3F), T3B (force calculations, Section 3C & 3D), and T4B (blade simulations, Section 3E) all demonstrate promise for this requirement. Further, the blade scraping path helps describe how this will occur (Section 3G). However, like R3, it will need to be fully validated through test T5C (test on cadaver) in the future.
6	The design must be able to penetrate into cartilage/subchondral bone on either side of the joint by at least 3.5mm.	T3C, T5D .	<u>Conditionally Met.</u> Test T3C (force calculations, Section 3C) is met through applying a maximum of 27.6N to penetrate and scrape cartilage/subchondral bone at a maximum of 2mm depth increments. However, it will need to be fully validated by test T5D (test on cadaver) in the future.
7	The design's penetration into the cartilage/subchondral bone should be controllable.	T7, T8.	<u>Met.</u> The use of the caliper mechanism satisfies test T7, with a "yes" answer to the question of controllable depth penetration by the tool. In the final prototype design, we want to measure the blade displacement for turns in the caliper thumbscrew by test T8; however, our currently modelled design allows for fine, controllable resolution.
8	The design should be able to act (promote fusion) in the A/P direction (angles $48^\circ \pm 15^\circ$ and $132^\circ \pm 15^\circ$).	T9.	<u>Met.</u> By assessing test T9 on our 3D tool model, the tool can go from $\sim 15^\circ$ to $\sim 345^\circ$ rotation, with restrictions of $\sim 30^\circ$ due to the handle material limiting full rotational motion (and the guide tube providing restrictions). However, regardless, the requirement is satisfied.
9	The design should facilitate deposition of synthetic bone graft into the joint space.	T5E, T6B.	<u>Conditionally Met.</u> By the design's nature, this requirement is met through assessment of test T6B, with a "yes" answer to the question of whether the design allows for easy insertion of flexible tubing. While it will need to be fully validated in the future by test T5E (test on cadaver with x-ray/dissection), it should facilitate deposition into the joint.
Cost			
10	Minimize cost of the device (< \$100 CAD).	T10.	<u>Conditionally Met.</u> Based on the rough cost estimations for our current tool by test T10 (Section 3H), including manufacturing costs, our tool meets the desired cost requirement (estimated cost \sim \$43 CAD). However, manufacturing costs can vary considerably, and thus we will need to re-evaluate the manufacturing costs once we start making a higher-fidelity prototype.
Usability			

11	Minimize surgical time (< 10 minutes).	T11, T12.	<u>Met.</u> Based on a conservative estimate of the time to perform the procedure by test T11 (Section 3F), our design meets this requirement. That said, test T12 (surgeon performs procedure on cadaver) in the future will help verify we did not underestimate the time for certain steps.
12	Minimize changes to technique, such that the device is intuitive to use (avoid time-consuming steps).	T13.	<u>Conditionally Met.</u> Compared to the traditional workflow, our tool adds minimal time-consuming steps to prepare the joint, with the only real differences being the use of the guide tube (Section 2A). Looking to the open procedure (Section 1C), this use of the guide tube can be seen as replacing the opening of the ankle in a typical open procedure, and should be faster due to the time it takes to cut through the soft tissue to reach the bones of the ankle in an open preparation. Otherwise, all other steps in our workflow have analogous steps in the traditional workflow that are expected to be of similar time; however, this should be verified in future surgeon testing sessions.
13	Maximize the intuitiveness and ease of use of the design.	T14.	<u>Future.</u> After making a high fidelity prototype, we can perform test T14 (surgeon survey, Appendix I) following their hands-on use of our prototype in order to assess this requirement.
14	Tool should be able to be used without direct visualization of the joint space.	T15.	<u>Met.</u> By test T15 (is tool visible under X-ray), the answer is “yes” based on the stainless steel materials the tool is made of being visible on x-ray imaging [48].

J. Risk Analysis

We expect our design to fall within a FDA-Class 2 designation, following a 510(k) pathway. In order to assess the risks associated with our tool's design, we developed a comprehensive list that includes the various hazards that may impact the design as well as the risks that have been considered in the design process. These risks were identified through performing a Failure Modes and Effects Analysis (FMEA), by performing task analysis for using our tool and identifying failure modes, causes and effects (**Appendix P**). According to the standard (IEC 60812 [49]), we identified eleven failure modes associated with their failure effects. In terms of analysis, we estimated the severity of failure final effect, likelihood of failure mode and likelihood of detection. We also obtained the risk profile rating by multiplication of rating for each failure cause. The utilization of the FMEA tool enables prioritization of the failure modes for potential treatment. As a result, the identified failure modes are shown below in **Table 10**. We broke them down into the hazard's severity, probability, and tolerability. After identifying the risks, we also detail how we mitigated said risks as well as the tests we have and will conduct for validation. We classified hazard severity and probability using the scale from MIL-STD 882B [50]. For details on this classification, please see **Appendix O**. We defined tolerability by how acceptable a given hazard is for surgeons and our client, taking patient outcomes into account. These were classified as broadly acceptable, conditionally acceptable, or intolerable. The risks from **Table 10** are plotted as a summary in **Figure 25**.

The results from our numerical FMEA can be found in **Appendix P**, with the ranking of the likelihood of occurrence, likelihood of detection, and severity definitions found in **Appendix O**. From FMEA, the highest priority risk was clearly identified as risk #1 (loss of alignment), which was also identified as the most critical risk by our client. Since this is the highest priority risk, we performed a fault tree analysis to identify patient, surgeon, and device factors that could lead to misalignment (**Figure 26**). According to the standard (IEC 61025 [51]), we focus on one of the two approaches – that being a qualitative approach that identifies the potential causes/faults. The risks factors are considered to be OR gated under the risk of misalignment. These are the factors we will continue to be aware of as we refine our tool's design and move towards higher fidelity verification and validation testing on higher-fidelity prototypes.

Table 10: Risk analysis for hazards associated with our final design

#	Hazard + Severity	Estimated Probability	Tolerability	Mitigation Strategies	Appropriate Tests (Section 3A)
1	Loss of alignment across the joint space between the two bones. Critical.	Remote. The guide tool in our design ensures that the joint is only accessed from the top and the bottom, which leaves the sides of the joint intact to preserve alignment.	Intolerable. This was the most critical risk identified by surgeons (Appendix E1 & E3) and thus is a key risk for us to control in our design. It would require an open revision surgery.	Workflow only involves cutting the A/P portion of the joint, thus preserving alignment. In addition, the guide tube accommodates the Kirscher Wire implanted during reaming, reducing the likelihood of misalignment compared to if the wire was taken out.	Test T2A (surface area calculations, Section 3F), Test T5A (cadaver testing). Surface area calculations reveal that enough cartilage is preserved to maintain joint alignment. Further validation to be performed on cadaver model.
2	Additional surgical incisions, which are associated with higher infection rates and poorer outcomes [52]. Marginal.	Improbable. One of the key constraints of our design space is to only address joint preparation through the single plantar incision in the bottom of the foot, as is represented by our proposed design.	Conditionally Acceptable. Dr. LaMothe (Appendix E2) noted that he stopped preparing the subtalar joint due to infectious complications due to incisions from open joint preparation. Thus, this risk would only be tolerated if misalignment occurs (requiring open invasive revision surgery).	Design required no additional incisions, only entering the foot through the hole reamed during the current surgery.	Based on the Detailed Workflow (Section 2D) , since only the reamed hole is used; no additional incisions are required for function
3	Tool does not adequately remove debrided cartilage from the joint, leading to inflammation. Marginal.	Improbable. Our proposed design is fitted such that any cartilage/subchondral bone scraped up is subsequently removed by the tool, limiting the likelihood of this risk occurring.	Broadly Acceptable. For our design to be adopted by surgeons, we want to be confident that our design can not only disrupt cartilage but also remove it, in order to have subtalar union and avoid potential revision surgery [5].	The shape of our blade is designed such that any removed cartilage or subchondral bone will be scraped into the guide tube when the tool is pulled out. The scraped tissue can then be removed from the guide tube either through suction or by the removal of the guide tube.	As discussed above, the guide tube provides suction access and should facilitate removal of broken cartilage. This will need to be tested in the future by Test T5B .

4	<p>User does not scrape away cartilage from the joint, due to poor attempts and/or not enough force. <u>Negligible.</u></p>	<p><u>Remote.</u> X-ray compatibility means the surgeon can confirm tool placement in the joint space. Also, blades on both sides ensure equal pressure on both joint surfaces.</p>	<p><u>Broadly Acceptable.</u> While it may take a few attempts for a novice to learn, practiced surgeons are able to distinguish between cartilage and subchondral bone, noting that you can often feel and hear the difference between the two.</p>	<p>We determined that 27.6N of force is needed to scrape cartilage (Section 3C). With our tool, the surgeon needs ~20 scrapes with ~9N of force to fully prepare the joint (Section 3D, Section 3F). Even with each scrape taking ~10s, the surgeon is still able to remove sufficient cartilage within our time constraints (Section 3F).</p>	<p>Test T1 (low-fidelity prototype, Section 3B), Test T2 (surface area calculations, Section 3F), Test T3 (force calculations, Section 3C & 3D), Test T4 (blade simulations, Section 3E). These tests demonstrate that this requirement can be met for 25-50% cartilage removal.</p>
5	<p>Damage of the nerves, vessels, and/or tendons surrounding the joint through use of the tool. <u>Catastrophic.</u></p>	<p><u>Improbable.</u> The guiding wire ensures that the tool appropriately enters the joint space, and the ability for x-ray visualization provides further confirmation that the surgeon remains in the joint space and does not enter any problem areas.</p>	<p><u>Broadly Acceptable.</u> Causing undue severe and permanent damage to any nerves would severely limit the ability of our product to penetrate the market; however, it is so unlikely to occur that the risk tolerability can be classified as broadly acceptable.</p>	<p>Since blade of our tool will be at most 10mm and only used in the A/P direction, it will not damage surrounding nerves/vessels (as described in Section 3G). Further, x-ray visualization helps with proper alignment of the guide tube. Finally, the bar at the base of the guide tube (Section 2B), while primarily acting to prevent guide tube movement, also acts as a stopper, preventing over-insertion of the guide tube.</p>	<p>Calculations in Section 3G indicate that with the specified blade length, it is impossible for our tool to damage important nerves in the foot.</p>
6	<p>Damaging the joint beyond what is needed for subtalar fusion. <u>Negligible.</u></p>	<p><u>Improbable.</u> Using a guiding tool and allowing the surgeon to confirm tool positioning via x-ray imaging both contribute to making the occurrence of this risk highly improbable.</p>	<p><u>Broadly Acceptable.</u> The goal is to promote fusion, defined by 25-50% of SA when imaged on x-ray and evidenced by clear trabeculation across the site [53] (Appendix E2). There is no understanding of the impact for over-damaging the joint, aside from the potential to cause misalignment.</p>	<p>Similar to above, this risk is mitigated through the use of the guide tube and length of the tool, which restricts the region the tool can act on to avoid over-damaging the joint (Section 3G). Further, the ability to control the penetration depth with the thumb screw (requirement R7) is also important to mitigate this risk.</p>	<p>Calculations in Section 3G indicate that with the specified blade length and guide tube usage, the tool shouldn't over-damage the joint. This will be confirmed through Test T5 in a cadaver model in the future.</p>

7	Tool causes infection of the joint space due to poor sterility. <u>Marginal.</u>	<u>Improbable.</u> The tool uses materials that can be sterilized by appropriate methods (i.e., autoclave) and used in the sterile surgical field, minimizing the likelihood of occurrence.	<u>Broadly Acceptable.</u> In general, infection due not ensuring an appropriate sterile field is adhered to is not acceptable. Our tool's ability to be sterilized means it can be used within a sterile field, and thus the risk is well tolerated by our design.	Tool is composed of martensitic 420-series stainless steel with blade made of tungsten carbide (Section 2E). Since this material is the same as used in current surgical instruments, his can be easily sterilized through autoclave [35][38].	The parameters of our Material Selection (Section 2E) ensure that tool sterilization is applicable to our design [35][38].
8	Issues of biocompatibility between the tool and the patient's tissues. <u>Marginal.</u>	<u>Improbable.</u> The tool will be of similar materials to those used in the current surgical procedures.	<u>Broadly Acceptable.</u> Mitigating for this risk is straight forward, by ensuring that only biocompatible materials are selected in product design.	Tool is composed of martensitic 420-series stainless steel with blade made of tungsten carbide (Section 2E). Both materials are commonly used in surgical instruments, with low biocompatibility issues.	Surgical tools have low biocompatibility issues. In fact, and perhaps disturbingly, surgical instruments have been mistakenly left in patients for years with no serious reactions or complications [48].
9	The tools mechanism of action causes undue thermal damage or corrosive damage. <u>Marginal/Critical.</u>	<u>Improbable.</u> Our design ensures that this does not occur, by using a non-powered mechanical tool.	<u>Broadly Acceptable.</u> Our design does not need to worry about this risk since it does not rely on thermal or chemical means to remove cartilage.	Our tool is purely mechanical, requiring not electricity or chemicals to cut and remove cartilage. Thus, there is no risk of chemical or thermal damage to tissue.	N/A - The tool does not have electrical or chemical components.
10	The tool's cutting blade breaks and remains in the joint space. <u>Critical.</u>	<u>Remote.</u> Our design will undergo regulatory testing to ensure it has a high factor of safety against all expected forces it will experience in the joint space.	<u>Conditionally Acceptable.</u> Due to its unlikely occurrence, the risk is conditionally acceptable. Further manufacturing considerations (i.e., not making the joint between the flexible wire and blade in the cutting tool fragile) will be taken to minimize this risk.	In order to minimize forces on the blade, the rake angle of the blade was set to 45° (Section 2C). This is so that, upon full extension, the rake angle becomes 90°, thus minimizing the force required to cut cartilage (Section 3C).	By Test T3 (force calculations, Section 3C) and Test T4 (blade simulation, Section 3E), the max force exerted on the blade will not cause permanent deformations, nor fracture, our blade, with a factor of safety of ~2. Thus, the chance of breaking during surgery is negligible. Also, since shear is not present during tool use, there is no risk for cutting tool's pin to break (Section 3D).

11	Cutting tool is placed in the wrong area - i.e., guide tube not far enough into the reamed hole, the cutting tool gets stuck in the subchondral bone. <u>Critical</u> .	<u>Improbable</u> . The guide tube positioning will be confirmed prior to inserting the cutting tool. In addition, the surrounding metal shell ensures that the tool does not get stuck upon entrance into the joint space.	<u>Conditionally Acceptable</u> . While current design safeguards help protect against this risk, this risk must be kept in mind during future testing of our proposed design (i.e., Test T5 , cadaver test).	The use of the guide tube in our design (Section 2B) is designed to help mitigate for this risk.	Test T14 (surgeon confidence survey) –If our workflow is followed correctly, it should be highly improbable for the cutting tool to enter the wrong area. The surgeon confidence survey (Appendix I) will be used to determine how initiative the tool is to use, and receive surgeon feedback on such risks.
----	--	--	---	---	---

Risk Likelihood	Risk Severity			
	Negligible	Marginal	Critical	Catastrophic
Frequent				
Probable				
Occasional				
Remote	4		1, 10	
Improbable	6	2, 3, 7, 8	11	5
Incredible		9		

Figure 25: Summary of risks. Figure shows the eleven identified risks in **Table 10** above, plotted as severity versus probability.

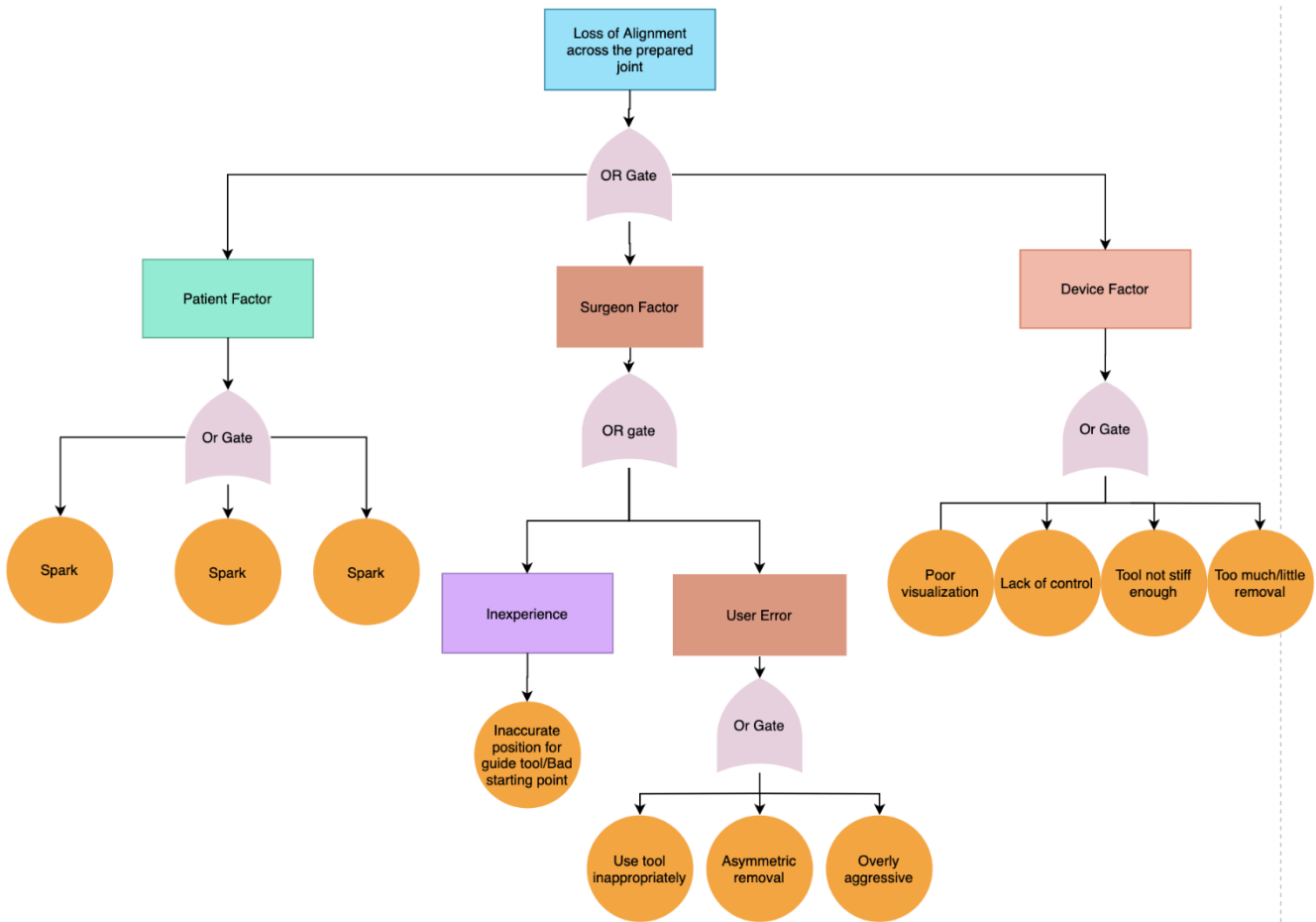


Figure 26: Fault tree analysis (based on standard IEC 61025 [51]) for risk #1, loss of alignment across the joint space between the two bones. Analysis verified by one of our clients (Dr. Montgomery).

4. Summary and Conclusions

A. Summary

In summary, our team has scoped the problem of preparing subtalar joint in a TTC nailing surgery in a trauma setting through a thorough analysis of the project background and requirements (**Section 1**), and has proposed a design. Our proposed design is composed of two modular components: A hinged cutting tool and a stiff hollow, guiding tube, as described above in **Section 2**.

Thus far, we have compiled a number of tests in order to validate and verify our design against the requirements and constraints of our tool (**Section 3**). Our design meets the size constraints of the current surgical workflow and can be used with the aid of static x-ray images. In addition, we have demonstrated through surface area and force calculations that our tool should theoretically meet the cartilage removal and bone disruption requirements. That said, as discussed above, this will need to be confirmed with higher-fidelity prototypes in the future. Our cost is estimated to be around \$43 CAD when accounting for both of material and manufacturing costs, fitting within cost constraints. However, these are very rough estimates, and need to be re-evaluated as additional factors such as reusability and marketability of the design are considered moving forward (discussed in the future steps (**Section 4B**) below). Furthermore, our tool adds minimal time-consuming steps to the surgical procedure and was determined to take less than 10 minutes to operate. Again, these are based on preliminary estimates, and further validation is needed in the future. For measuring surgeon confidence, while we were unable to verify this requirement at this time, our team has proposed a survey (**Appendix I**) for surgeons to use in the future, once we are able to get high-fidelity prototypes into their hands. Finally, our tool is also compatible with bone graft injection, due to the guide tube's ability to guide flexible tubing into the joint space to facilitate graft deposition.

Some ethical concerns for our device are related to the risks associated with our tool. Specifically, surgeon factors and patient factors might incur key ethical conflicts. For instance, since subtalar preparation is currently not performed in the trauma setting, and our tool may add additional risks during the surgery that can impact patient outcomes, introducing it in the surgical workflow poses a potential ethical dilemma. This is especially true when considering that some surgeons are still not convinced of the benefits of subtalar union, as outlined in the Background at the beginning of this report (**Section 1A**). Conflicts such as these will need to be weighed by engineers, surgeons, and patients alike as the device is being considered moving forward.

Overall, our tool is designed to be used in a TTC arthrodesis surgical procedure for the purpose of preparing the subtalar joint in a trauma setting. We anticipate that, if effective, it can be utilized in a variety of contexts that use an intramedullary nail for arthrodesis, not just in the trauma setting. While it is anticipated to help improve patient outcomes, the tool also provides an efficient, effective approach to prepare the subtalar joint, as compared to traditional approaches that require an opening of the ankle joint and use of tools such as curettes and shavers.

B. Next Steps and Future Considerations

Next Steps

The key next steps moving forward will be to make a higher-fidelity prototype. First of all, accurately 3D-printing the tool is a low-cost way for surgeons to test out the tool and give feedback on its overall concept and design. Then, after receiving this feedback, making a higher-fidelity metal prototype to test forces and cartilage scraping ability more accurately, such as in tests on cadavers as outlined in our testing plans above (**Test 5, Section 3A**). These will also allow us to implement and assess surgeon feedback using our developed survey (**Appendix I**). In addition, we would like to continue to gather feedback from surgeons. Thus far, besides our client, we have spoken with two surgeons about our design (Dr. LaMothe and Dr. Halai), but would like to continue to gather other perspectives to help validate the utility of our tool. Lastly, if we are able to bring our tool to market for clinical trials in surgical practice, evaluating subtalar fusion rates in patients when using our tool as compared to not using it will be essential to truly meet the overall objective and goal for this project.

Future Considerations: Ergonomics

While not discussed in this report, as the primary focus of our design process was on making a tool that had the desired functionality for preparing the subtalar joint, the team also understands there are ergonomic considerations to our device that will need to be taken into account as we move towards the production of a higher-fidelity prototype. Referring to guidelines from the Canadian Center for Occupational Health and Safety [54], this includes designing our handle to account for optimal control (recommended handle diameters of 8-16mm) while also allowing for appropriate force and stability (recommended handle diameters of 30-50mm). Recommendations are that handles should be 3cm in diameter and 10cm in length if the whole hand is being used to apply force [55]. Since these two considerations are not synonymous, providing surgeons with high-fidelity prototypes with varying handle sizes can help simplify and make this design consideration, by using a survey like that shown in **Appendix**

I with additional metrics for hand ergonomics [28]. Furthermore, for comfort and reduced effort, we will want to make the handle out of a non-slip, non-conductive material [54], and will need to perform a further consultation of the literature to make such decisions.

Future Considerations: Reusable vs. Disposable Tool

Moving forward, a key consideration for our design is whether to make the tool reusable or disposable. In our current design, we used a high-quality stainless steel for the tool body and even higher quality metal tungsten carbide for the blade, anticipating a reusable tool that could be added into the typical surgical toolset kit used by orthopedic surgeons. That said, our team has also considered the use of a fully-disposable tool, as well as a disposable blade with a reusable tool body.

Looking to a review on the life cycle of surgical scissors [56], where authors focused on the economic and environmental impacts of disposable vs. reusable metal surgical scissors, the authors found that the reusable stainless steel scissors had both a better environmental impact and a better economic advantage as compared to the disposable stainless steel alternative. Moreover, they found that the reusable tool had lower costs of ownership past ~25 use cycles, with estimated sterilization costs included [56]. Considering the life-cycle of scissors exceeds 160 usage counts [57], this should make a reusable tool more cost and environmentally efficient. This points towards making our tool fully reusable. Further, considering the complexity of our tool, it would not make economic sense to be fully disposable (i.e., would be throwing out the guide tube and cutting tool every surgery). That said, the team understands the major convenience that a disposable tool provides, especially in maintaining tool sharpness (reusable tools will require servicing and maintenance). As such, the team has considered a similar approach in our design as taken with the surgical scalpel, which has a reusable handle with disposable blades. A similar implementation is possible in our design and should be considered alongside a fully reusable tool moving forward.

5. Appendices

A. Bibliography

- [1] Brockett CL, Chapman GJ. Biomechanics of the ankle. *Orthopaedics and Trauma* [Internet]. 2016; 30(3): 232-238. Available from: <https://www.ncbi.nlm.nih.gov/pmc/articles/PMC4994968/>.
- [2] Quill GE. Tibiotalocalcaneal Arthrodesis With Medullary Rod Fixation. *Techniques in Foot and Ankle Surgery* [Internet]. 2003; 2(2): 135-143. Available from: https://journals.lww.com/techfootankle/Abstract/2003/06000/Tibiotalocalcaneal_Arthrodesis_With_Medullary_Rod.9.aspx.
- [3] Lee BH, Fang C, Kunnasegaran R, Thevendran G. Tibiotalocalcaneal Arthrodesis With the Hindfoot Arthrodesis Nail: A Prospective Consecutive Series From a Single Institution. *The Journal of Foot & Ankle Surgery* [Internet]. 2018; 57(1): 23-30. Available from: [https://www.jfas.org/article/S1067-2516\(17\)30358-7/fulltext](https://www.jfas.org/article/S1067-2516(17)30358-7/fulltext).
- [4] Bennett GL, Cameron B, Njus G, Saunders M, and Kay D. Tibiotalocalcaneal Arthrodesis: A Biomechanical Assessment of Stability. *Foot & Ankle International* [Internet]. 2005; 26(7): 530-536. Available from: <https://pubmed.ncbi.nlm.nih.gov/16045843/>.
- [5] Yoshimoto K, Fukushi J, Tsushima H, Kamura S, Miyahara H, Mizu-uchi H, Akasaki Y, Nakashima Y. Does Preparation of the Subtalar Joint for Primary Union Affect Clinical Outcome in Patients Undergoing Intramedullary Nail for Rheumatoid Arthritis of the Hindfoot and Ankle? *The Journal of Foot & Ankle Surgery* [Internet]. 2020; 59(5): 984-987. Available from: [https://www.jfas.org/article/S1067-2516\(20\)30165-4/fulltext](https://www.jfas.org/article/S1067-2516(20)30165-4/fulltext).
- [6] Tarkin IS, Fourman MS. Retrograde Hindfoot Nailing for Acute Trauma. *Current Reviews in Musculoskeletal Medicine* [Internet]. 2018; 11: 439-444. Available from: <https://www.ncbi.nlm.nih.gov/pmc/articles/PMC6105487/>.
- [7] Kim JG, Ha DJ, Gwak HC, Kim CW, Kim JH, Lee SJ, Kim SJ, Lee CR, Park JH. Ankle Arthrodesis: A Comparison of Anterior Approach and Transfibular Approach. *Clinics in Orthopedic Surgery* [Internet]. 2018; 10(3): 368-373. Available from: <https://www.ncbi.nlm.nih.gov/pmc/articles/PMC6107825/>.
- [8] Taylor BC, Hansen DC, Harrison R, Lucas DE, Degenova D. Primary Retrograde Tibiotalocalcaneal Nailing For Fragility Ankle Fractures. *Iowa Orthopedic Journal* [Internet]. 2016; 36: 75-78. Available from: <https://www.ncbi.nlm.nih.gov/pmc/articles/PMC4910785/>.
- [9] Amirfeyz R, Bacon A, Ling J, Blom A, Hepple S, Winson I, Harries W. Fixation of ankle fragility

- fractures by tibiototalcalcaneal nail. Archives of Orthopaedic and Trauma Surgery [Internet]. 2008; 128(4): 423-428. Available from: <https://pubmed.ncbi.nlm.nih.gov/18270721/>.
- [10] World Precision Instruments (WPI). Volkman Bone Curette #3, 17cm, Oval, 1cm Cup [Internet]. 2020. Available from: <https://www.wpiinc.com/503689-volkman-bone-curette-3-17cm-oval-1cm-cup>.
- [11] World Precision Instruments (WPI). Osteotomes - Bone Chisel, Lambotte, Straight. [Internet]. 2020. Available from: <https://www.wpiinc.com/var-wp006c-osteotomes-bone-chisel-lambotte-straight>.
- [12] Brasseler Canada. All Port Bone E-Cutter Carbide. [Internet]. 2020. Available from: <https://shop.brasseler.ca/Catalog/Carbides/Surgical-Carbides/Bone-Cutters> (login required).
- [13] Salvin Regenerative. 3mm Ridge Splitting/Expanding Chisel. [Internet]. 2020. Available from: <https://www.salvin.com/3mm-Ridge-Splitting-Expanding-Chisel-pluRIDGE-SPLIT-3MM.html>.
- [14] Fernandez MP, Hoxha D, Chan O, Mordecai S, Blunn GW, Tozzi G, Goldberg A. Centre of Rotation of the Human Subtalar Joint Using Weight-Bearing Clinical Computed Tomography. Scientific Reports [Internet]. 2020; 10(1035). Available from: <https://www.nature.com/articles/s41598-020-57912-z>.
- [15] Akiyama K, Sakai T, Sugimoto N, Yoshikawa H, Sugamoto K. Three-dimensional distribution of articular cartilage thickness in the elderly talus and calcaneus analyzing the subchondral bone plate density. Osteoarthritis and Cartilage [Internet]. 2012; 20:296-304. Available from: [https://www.oarsijournal.com/article/S1063-4584\(12\)00020-9/pdf](https://www.oarsijournal.com/article/S1063-4584(12)00020-9/pdf).
- [16] DiCicco JD, Mückley T, Sorkin AT. T2 Ankle Arthrodesis Nail: Operative Technique. Stryker Osteosynthesis [Internet]. 2009; 1-31. Available from: <https://www.strykermeded.com/media/1602/t2-ankle-arthrodesis-nail.pdf>.
- [17] Qiang M, Chen Y, Li H, Dai H. Measurement of three-dimensional morphological characteristics of the calcaneus using CT image post-processing. Journal of Foot and Ankle Research [Internet]. 2014; 7(19). Available from: <https://jfootankleres.biomedcentral.com/articles/10.1186/1757-1146-7-19>.
- [18] Glazebrook M et al. Establishing the relationship between clinical outcome and extent of osseous bridging between computed tomography assessment in isolated hindfoot and ankle fusions. Foot Ankle Int. [Internet]. 2013; 34(12): 1612–1618. Available from: <https://pubmed.ncbi.nlm.nih.gov/24043351/>.
- [19] Medical News Today. Cartilage damage: Symptoms, causes, diagnosis, and treatment. [Internet]. 2017. Available: <https://www.medicalnewstoday.com/articles/171780#symptoms>.
- [20] Day JS, Ding M, Van Der Linden JC, Hvid I, Sumner DR, Weinans H. A decreased subchondral trabecular bone tissue elastic modulus is associated with pre-arthritis cartilage damage. Journal of Orthopedic Research [Internet]. 2001; 19(5): 914–918. Available from: https://www.sciencedirect.com/science/article/abs/pii/S0736026601000122?casa_token=qR2joWY2dQk

[AAAAA:BYZY2O04Ghxwph3f6RdRNrDFfhTQUThV2DoYUojgqHZrpJiPRQulS4OuuDhgas2ln6lVDjHTqMY.](#)

- [21] Barwick A, Tessier J, Mirow J, de Jonge XJ, Chuter V. Computed tomography derived bone density measurement in the diabetic foot. *Journal of Foot and Ankle Research* [Internet]. 2017; 10(11). Available from: <https://jfootankleres.biomedcentral.com/articles/10.1186/s13047-017-0192-7>.
- [22] Buote NJ, McDonald D, Radasch R. Pancarpal and Partial Carpal Arthrodesis. *Surgery Compendium* [Internet]. 2009; 31(4). Available from: <https://www.vetfolio.com/learn/article/pancarpal-and-partial-carpal-arthrodesis>.
- [23] Krähenbühl N, Horn-Lang T, Hintermann B, Knupp M. The subtalar joint: a complex mechanism. *EFFORT Open Reviews* [Internet]. 2017; 2(7): 309-316. Available from: <https://pubmed.ncbi.nlm.nih.gov/28828179/>.
- [24] Yasui Y, Hannon CP, Seow D, Kennedy JG. Ankle arthrodesis: A systematic approach and review of the literature. *World Journal of Orthopaedics* [Internet]. 2016; 7(11): 700–708. Available from: <https://www.ncbi.nlm.nih.gov/pmc/articles/PMC5112338/>.
- [25] Biomatlante Biologics Solutions. MBCP Syringe: Micro & Macroporous Synthetic Bone Graft Substitute. [Internet]. 2020. Available from: <https://biomatlante.com/en/products/orthopaedics/syringe-mbcp>.
- [26] WhiteCap Dental Solutions. Bone Grafting Syringes. [Internet]. 2020. Available from: <https://shopwhitecap.com/bone-grafting-syringes/>.
- [27] Van Meter MM, Adam RA. Costs associated with instrument sterilization in gynecologic surgery. *Amsterdam Journal of Obstetrics and Gynecology* [Internet]. 2016; 215(5): 652.e1-652.e5. Available from: <https://pubmed.ncbi.nlm.nih.gov/27342044/>.
- [28] Swarup A, Eastwood KW, Francis P, Chayaopas N, Kahrs LA, Leonard CG, Drake J, and James A. Design, prototype development and pre-clinical validation of a novel instrument with a compliant steerable tip to facilitate endoscopic ear surgery. *Journal of Medical Engineering and Technology* [Internet]. 2020; 1-13. Available from: <https://doi.org/10.1080/03091902.2020.1838644>.
- [29] Santos-Carreras L, Hagen M, Gassert R, Bleuler H. Survey on Surgical Instrument Handle Design: Ergonomics and Acceptance. *Surgical Innovation* [Internet]. 2012; 19(1): 50-59. Available from: <https://pubmed.ncbi.nlm.nih.gov/21868419/>.
- [30] Brown S. Likert Scale Examples for Surveys. Iowa State University Extension [Internet]. 2010. Available from: <https://www.extension.iastate.edu/Documents/ANR/LikertScaleExamplesforSurveys.pdf>.

- [31] Metric Coarse Knurled Thumb Screw Steel DIN464. Fastener Data [Internet]. 2020. Available from: <https://www.fastenerdata.co.uk/fasteners/screws/thumb/metric-coarse-knurled-thumb-screw-steel-din464.html>.
- [32] DIN 464 - Knurled thumb screws, high type. Fasteners EU. 2020. Available from: <https://www.fasteners.eu/standards/DIN/464/>.
- [33] Stainless Steel – Grade 420 (UNS S42000). Azo Materials [Internet]. 2001. Available from: <https://www.azom.com/article.aspx?ArticleID=972>.
- [34] Tungsten Carbide – An Overview. Azo Materials [Internet]. 2002. Available from: <https://www.azom.com/properties.aspx?ArticleID=1203&fbclid=IwAR0y0DjdfNMUo91U-cU1YZzq39lgswfEj42t7X84phxLBJFhSy7drzsg0pY>.
- [35] Price, BL. Surgical Instruments: Manufacturing and Care. Veterinary Technician [Internet]. 2012; pp. E1-E6. Available from: http://vetfolio-vetstreet.s3.amazonaws.com/eb/951a30334a11e29e50005056ad4736/file/VT1212_Price_CE.pdf.
- [36] Stainless Steel Grades Chart -- Types of Stainless Steel. McHone Industries [Internet]. 2019. Available from: <https://blog.mchoneind.com/blog/stainless-steel-grades-chart>.
- [37] Baufield, M. What is the difference between surgical steel and stainless steel? Mead Metals Inc. [Internet]. 2019. Available from: <https://www.meadmetals.com/blog/surgical-steel-vs-stainless-steel>.
- [38] Chapter 6: Classical (Open) Surgery. Biomedical Engineering in Gastrointestinal Surgery. 2017; pp. 221-267. Available from: <https://www.sciencedirect.com/book/9780128032305/biomedical-engineering-in-gastrointestinal-surgery>.
- [39] Chen P, Sui J, Wang C. Cutting Force Analysis of Bovine Acetabular Cartilage. Procedia CIRP [Internet]. 2020; 89: 189-193. Available from: <https://www.sciencedirect.com/science/article/pii/S2212827120305163>.
- [40] Ohnishi O, Suzuki H, Uhlmann E, Schröder N, Sammler C, Spur G, Weismiller M. Chapter 4 – Grinding, Handbook of Ceramics Grinding and Polishing. William Andrew Publishing [Internet]. 2015; 133-233. Available from: <http://www.sciencedirect.com/science/article/pii/B9781455778584000042>.
- [41] Mahvash M, Voo LM, Kim D, Jeung K, Wainer J, and Okamura AM. Modeling the forces of cutting with scissors. IEEE transactions on bio-medical engineering [Internet]. 2008; 55(3): 848-56. Available from: <https://www.ncbi.nlm.nih.gov/pmc/articles/PMC2709828/>.
- [42] Nilsen T, Hermanni M, Eriksen CS, Dagfinrud H, Mowinckel P, Kjekken I. Grip force and pinch grip in an adult population: Reference values and factors associated with grip force. Scandinavian Journal of Occupational Therapy [Internet]. 2012;19(3): 288-296. Available from:

<https://pubmed.ncbi.nlm.nih.gov/21355705/>.

[43] SolidWorks Corporation. 2020. Available from: <https://www.solidworks.com>.

[44] ZygoteBody – 3D Anatomy Online Visualizer. Zygote Media Group, Inc. 2020. Available from: <https://www.zygotebody.com>.

[45] Tungsten carbide scrap hits new lows amid headwinds. Argus [Internet]. 2019. Available from: <https://www.argusmedia.com/en/news/1956766-tungsten-carbide-scrap-hits-new-lows-amid-headwinds>.

[46] Bachman K. Stamper cuts costs of making surgical instruments. Stamping Journal [Internet]. 2010. Available from: <https://www.thefabricator.com/stampingjournal/article/shopmanagement/stamper-cuts-costs-of-making-surgical-instruments>.

[47] Inflation Calculator. Bank of Canada [Internet]. 2020. Available from: <https://www.bankofcanada.ca/rates/related/inflation-calculator/>.

[48] Larbi, M. Woman’s horror as X-ray reveals six-inch surgical clamp lodged in her abdomen for 23 years. The Sun [Internet]. 2019. Available from: <https://www.thesun.co.uk/news/9319724/x-ray-reveals-clamp-womans-abdomen/>.

[49] Failure modes and effects analysis (FMEA and FMECA). International Standard IEC 60812, Third Edition. 2018. Available: PDF available from team upon request.

[50] Military Standard 882B (MIL-STD-882B) System Safety Program Requirements. US Department of Defense [Internet]. 1984. Available from: <http://sunnyday.mit.edu/safety-club/882b.htm>.

[51] Fault tree analysis (FTA). International Standard IEC 61025, Second Edition. 2006. Available: PDF available from team upon request.

[52] Shaheen E. Tibiotalocalcaneal Arthrodesis Using a Retrograde Intramedullary Nail for Treatment of a Posttraumatic Ankle Disorders in Elderly. Al-Azhar Medical Journal [Internet]. 2015; 13(3): 218-228. Available from: <http://www.aamj.eg.net/journals/pdf/2766.pdf>.

[53] Zwipp H, Rammelt S, Endres T, Heineck J. High Union Rates and Function Scores at Midterm Followup With Ankle Arthrodesis Using a Four Screw Technique. Clinical Orthopaedics and Related Research [Internet]. 2010; 468(4): 958-968. Available from: <https://www.ncbi.nlm.nih.gov/pmc/articles/PMC2835613/>.

[54] Hand Tool Ergonomics: Tool Design. Canadian Center for Occupational Health and Safety (CCOHS) [Internet]. 2015. Available from: <https://www.ccohs.ca/oshanswers/ergonomics/handtools/tooldesign.html>.

[55] Dul J, Weerdmeester BA. Ergonomics for Beginners: A Quick Guide. CRC Press LLC. 2001. Available from: <https://search.library.utoronto.ca/details?11750051>.

[56] Ibbotson S, Dettmer T, Kara S, Herrmann C. Eco-efficiency of disposable and reusable surgical instruments – a scissors case. *The International Journal of Life Cycle Assessment* [Internet]. 2013; 18: 1137-1148. Available from: <https://link.springer.com/article/10.1007/s11367-013-0547-7>.

[57] Yoshikawa T, Kimura E, Akama E, Nakao H, Yorozuya T, Ishihara K. Prediction of the service life of surgical instruments from the surgical instrument management system log using radio frequency identification. *BMC Health Services Research* [Internet]. 2019; 19(695). Available from: <https://bmchealthservres.biomedcentral.com/articles/10.1186/s12913-019-4540-0>.

B. Work Plan

The biggest challenge the team faced this term with respect to the work plan was adapting to the changing COVID-19 situation. The team decided to work entirely remotely, aside from having a foot model 3D printed in the IBBME Design Studio. The specifics of the work plan are below. An “X” in a cell denotes the leader of the component, while an “A” denotes someone who has contributed significantly to the component. It can be assumed that all members may have participated to some degree in each component.

Table B1: Work distribution among the team

Component	CMC	MDB	KW	YZ
Ideation sessions	A	A	X	A
Client communications		X		
Asana Board	A	A		
CAD and animations	X		A	
Simulation/digital testing	X			
Physical prototyping and at-home testing		X	A	
Materials selection & Cost		X		A
Theoretical testing/calculations	A	A	X	X
Risk analysis		X	A	A
Market Strategy		X		X

Figure B1 shows an updated Gantt chart with our schedule and major milestones. The timeline is divided into four project stages: Stage 1: Define Problem and Basic Design, Stage 2: Detailed Design, Stage 3: Testing and Optimization, and Stage 4: Summarize and Communicate Results. This final

document completes Stage 4. The major change in timeline from the proposal chart is that the final device design was continuously refined after each client meeting, rather than all at once.

Day-to-day tasks, as well as subtasks for deliverables, are tracked in our Asana board. Tasks are split into “To Do/Next Steps,” “General Project Timeline,” “Deliverables,” and “Tasks Done” categories.

Figure B2 shows a screenshot of this Asana board layout.

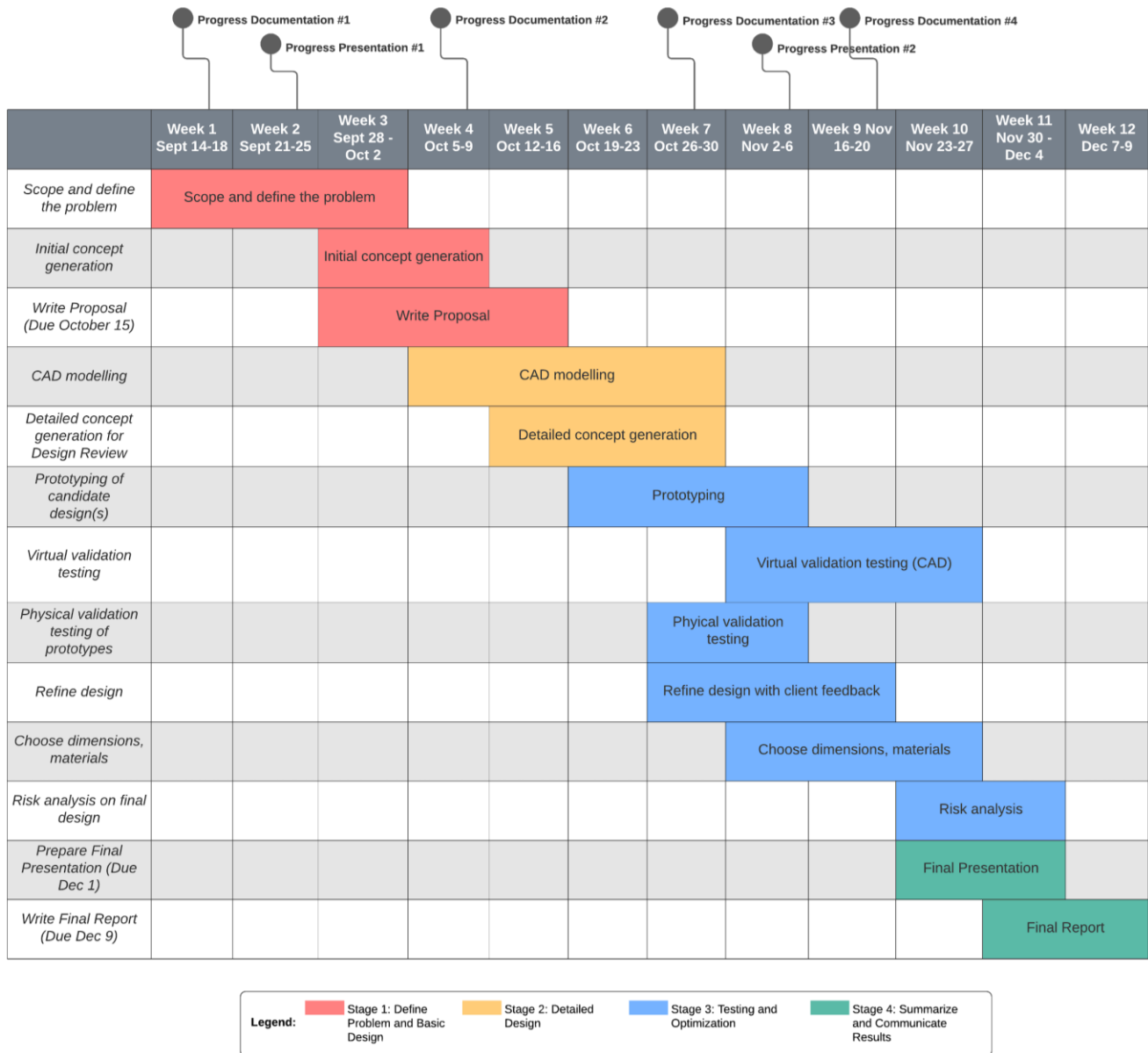


Figure B1: Gantt chart of tasks

Subtalar Joint Fusion Set status

List **Board** Timeline Calendar Dashboard Progress Forms More...

6 tasks completed today Send feedback All tasks Filter

To Do/Next Steps **General Project Timeline** **Deliverables** **Tasks Done**

- Implement feedback for Needs Statement (Thursday)
- Email Dr. Montgomery with updates (Thursday) 3
- Gather and summarize existing solutions (Sep 29) 4
- Pre-meeting concept generation (Sep 29)
- Meeting Tuesday during lab session (Sep 29) 2
- + Add task

- Identify: Defining Problem Statement (Sep 10 - Today) 6
- Identify: Existing Solutions (Sep 16 - Today) 3
- Identify: Design Criteria (Today - Oct 1) 4
- Identify: Verification & Validation Tests (Today - Oct 4) 3
- Invent: Concept Generation and Screening (Sep 23 - Oct 11) 5
- Invent: Concept Preliminary Testing (Sep 29 - Oct 11) 1
- Communicate: Prepare Project Proposal

- Design Progress Meeting #1 (Sep 15) 7
- Progress Presentation #1 (Thursday)
- Design Progress Meeting #2 (Oct 6)
- Project Proposal (Oct 15)
- Design Progress Meeting #3 (Oct 27)
- Design Review with Client (Oct 31)
- Design Progress Meeting #4 (Nov 17)

- First Lecture: 9-11am (Sep 10)
- First Team Meeting 10-11am (Sep 12) 6
- Schedule Client Meeting (Sep 13) 2
- Add questions into Outstanding Question Log (Sep 15) 6
- Client Meeting (Sep 16) 8
- Write 5 needs statements (Sep 20) 4
- Start to think about design criteria for the needs statements within Biodesign framework

Figure B2: Asana board layout

C. Financial Plan

Table C1 below describes costs for project components used thus far. The team has paid for these items and are currently seeking reimbursement from IBBME. If a reimbursement is received, prototypes and 3D models related to the reimbursement will be given to Professor Bouwmeester or Dr. Spencer Montgomery at the conclusion of the project, upon request. The client has not purchased anything directly nor has he paid for the items listed below.

Table C1: Financial Report

Type	Item	Cost (in CAD)	Source
Information Gathering	Surgical information, training videos	\$0	VuMedi.com
	3D ankle bones STL models	\$0	Embodi3d.com (free for non-commercial purposes)
	3D printed ankle bones	\$72.96	IBBME Design Studio (Figure A3)
Prototyping Materials	Prototyping Materials (scissors, rubber bands, ornament hooks, craft sticks/dowels, nail set)	\$11.02	Purchased by Michael from Dollarama (Figure A4)
	Diagtree Vernier Caliper	\$16.68	Purchased by Michael from Amazon (Figure A4)
	Other household materials (Zest soap bars, screws, power drill, clamp)	\$0	Provided by Michael's household
Software	SolidWorks	\$0	U of T ECF license
	AutoDesk Fusion360	\$0	Free university student license
Total		\$100.66	

A key variation from the initial financial plan was not using a Sawbones foot model. This was not necessary given the fidelity of the prototype the team was able to construct within the time and resource constraints of the capstone design course. That said, such a model is very valuable and is suggested to be purchased should the team and client continue with the project. A suitable model, which costs USD \$104.50 + shipping, can be found [here](#). In addition, costs of further 3D printing of prototypes and costs for cartilage/bone were not needed.

Please see below for the receipt from Gary Hoang for our first 3D print job (**Figure C1**) and for the receipts from prototyping materials purchased at Dollarama and Amazon (**Figure C2**).

Receipt Design Studio	
Name	Michael, MacKenzie, Kevin, Irina
Date of Service	Oct 9, 2020
Description	3D printing
Cost	\$6.00/in ³
Quantity used (in ³) (model, support, total)	10.60, 1.56, 12.16
Total cost	\$72.96

Figure C1: Receipt from 3D printed ankle bones in IBBME Design Studio

Order information / Information sur la commande

Order date / Date de commande 19 November 2020

Order # / Commande # 701-3728905-3192235

Shipment date / Date d'expédition 19 November 2020

Shipment # / Expédition # 39265600715301

Invoice details / Détails de la facture

Description	Qty / Quantité	Unit Price / Prix à la pièce
Diagtree 150mm 6inch LCD Digital Electronic Digital Vernier Caliper Carbon Fiber Vernier Caliper Gauge Micrometer Measuring Micrometer - Auto Off Featured Measuring Tool ASIN: B07BC856B5	1	\$16.68

Figure C2: Receipts from Prototyping Materials

D. Report Attribution Table

Table D1: Report Attribution Table

Component	CMC	MDB	KW	YZ
Executive Summary				X
Introduction				
Background		X		
Project Goal		X		
Project Requirements		X		
Final Design				
Overview			X	
Guide Tube			X	
Tool and Blade Design	X			
Detailed Workflow			X	
Materials Selection		X		
Assessment of Final Design				
Verification Overview		X		
Low-Fidelity Prototype		X		
Force to Scrape Cartilage			X	X
Force Calculations on Tool				X
Blade Simulation Testing	X			
SA & Timing Calculations	X			
Blade Scraping Path	X			
Cost Analysis		X		
Assessment of Requirements		X		
Risk Analysis		A	X	X
Summary and Conclusions		A		X
Work Plan	X			

Financial Plan		X		
Signatures	C.M.C.	M.D.B.	K.W.	Y.Z.

E. Transcripts from Surgeon and Client Interviews

All of our team's meeting minutes and client interview notes can be found in our [Master Meeting Documentation Google Doc](https://docs.google.com/document/d/1Dz6YDwE8FGe_5Z7qRUyEk-epCyguM4Rh032ii_I28Inc/edit?usp=sharing) (https://docs.google.com/document/d/1Dz6YDwE8FGe_5Z7qRUyEk-epCyguM4Rh032ii_I28Inc/edit?usp=sharing). You can access all the referenced material in **Appendices E1** and **E3** below by date through linked the table of contents at the beginning of the document. For material in **Appendix E2**, this was an interview performed by our client on September 26th, with the record minutes from the meeting found [here](https://drive.google.com/file/d/1qdY0TBtXk_Z-aGn-Z4eF__lSTQ0qChZw/view?usp=sharing) (https://drive.google.com/file/d/1qdY0TBtXk_Z-aGn-Z4eF__lSTQ0qChZw/view?usp=sharing).

E1: Client Interview - Reference Material

Page 2 of Sept. 16 Meeting Minutes, lines 8-15

- Dr. Montgomery on What we need.
 - Is there a way to prepare the subtalar joint for fusion without requiring a big incision on the side? → in a way in the workflow of how you install one of those retrograde nails.
 - Need to remove a certain % (~ close to 25-50%) to get fusion.
 - Something that fits in the current surgical procedural workflow that surgeons can use and be confident that they can get subtalar union.
 - Designing for an alternative to the open surgery.

Page 3 of Sept. 16 Meeting Minutes, lines 23-24

- Since subtalar is questionable in the literature and some physicians are skeptical on the need to do subtalar union, making it easy enough to do so is important.

Page 1 of Oct. 5 Client Meeting Minutes, lines 19-20

In Canada, no additional billing codes that you can get, as they will be claiming them whether you use it or not... just be a reasonable estimation

Page 1 of Oct. 5 Client Meeting Minutes, lines 38-40; Page 2, lines 1-2

- Models we will print will be based on bone... spaced in between that is cartilage.
 - The model will be closer... would be 3mm of space symmetric along the entire space.
 - Pretty uniform 3mm between... make sure we place something in between the bones.

Page 2 of Oct. 5 Client Meeting Minutes, lines 30-37

Why a camera?

- Need to visualize where you are going... use an X-ray, but the camera can give more precision.
 - To bring a camera means you need to bring in more tools/precisions.
 - Need another person to bring a camera.
 - AVOID direct visualization with a camera... keep it to indirect visualization with an X-ray.
- From a workflow perspective, setting up the perspective will take 5-10 minutes in itself.

Page 3 of Oct. 5 Client Meeting Minutes, lines 1-4

- Don't need to remove the cartilage... inflammatory response is true, but not a killer risk to leave some cartilage behind.
 - Even if you destroyed the cartilage, you could still not remove 100% of it and that won't be a major issue.

Page 3 of Oct. 5 Client Meeting Minutes, lines 13-21

- Maybe all you focus on is the top and bottom and leave the sides as those give you the support and alignment.
 - Maybe you don't need to do radial removal, as it will prevent any loss of alignment.
 - Just removing everything not including lateral should still be able to achieve the union.
 - Most people would include the nail size as a part of the "union" assessment, which will cover 20-25% as is.
 - Just getting the sides should be ok... a reasonable thing to consider.

Page 2 of Oct.9 meeting minutes, Lines 7-10

Overall, likes the idea

Likes that it is 2 components

Likes that it is mechanical

Would be able to see it on X-ray; no camera needed (too expensive)

Page 3 of Oct. 9 meeting minutes, Lines 12-15

It is nice to know what you are feeling → so doing one side at a time.

Feel, can tell the difference between scraping cartilage vs. scraping bone.

Would see via X-ray and so a lot of scraping without X-ray cause you can feel it... can hear if you are scraping bone.

Page 3 of Oct. 9 meeting minutes, Lines 16-21

- Space between joints:
 - Joint can expand.
 - When people put a camera into the joints, use a 2.7mm arthroscope.
 - Use nearly a 3mm arthroscope to put in... expect to be able to open up that joint at least 2mm.
 - 1mm-1.5mm thickness of cartilage.

Page 1 of Nov. 13 meeting minutes, Lines 39-41, 46

- Just going in front and behind; on a lateral X-ray, there is nothing in front and nothing behind... can be much more aggressive
 - If work in a circle, need to be more conscious
- A-P is safe, can reliably say your are in the joint based on the tool.

E2: Dr. LaMothe Interview - Reference Material

Dr. LaMothe is an orthopaedic surgeon, trauma and foot & ankle specialist, in Calgary, AB. He performs TTC nailing for acute trauma ~1 per 4-6 weeks, and has presented internationally on acute TTC arthrodesis for ankle fracture.

Minutes:

- Despite higher complication rates in diabetics, it is probably not the population to pursue as they can have a lot of reasons for non-union. Fragility fractures in the elderly are probably more predictable.
- *Current practice* does not include any formal preparation of the subtalar joint... “although it would probably be beneficial, I know studies say it doesn’t matter but I don’t know if I believe that.”
- *I used to prep the joint surfaces* using an anteromedial incision and a sinus tarsi incision but I had *huge issues with healing* those sites and have since stopped prepping the joints. I have *never had issues with the plantar incision*.
- It can be difficult to get union across the subtalar joint and the *subchondral plate is important for alignment*.

Criteria feedback

- Outcome: 50% union rate on CT at 6 months would be meaningful
 - “Data would suggest between 25-50% of joint surface needs to be bridged by bone for effective fusion”
- Cost: “not cost prohibitive”
- Usability: “no more than 10 minutes, these cases are typically only 35 min long”
 - “if there were a way to add bone graft it could allow for an additional billing code”;
 - “must be intuitive and not finicky”
 - “would be nice if it could also prep tibiotalar joint”
- Risk: “Can’t cause a loss of alignment”
- If you could prep the subtalar joint in less than 10 minutes and achieve 50% union at 6 months, would you use it every case?
 - Yes, provided not cost prohibitive

E3: Dr. Halai Interview - Reference Material

Dr. Halai has been an orthopedic ankle and trauma surgeon since 2001, and has just started working at St. Michael's Hospital in Toronto. He has performed many subtalar joint preparations and fusions (performed one on the day we interviewed him!).

Minutes:

Page 1 of Nov. 20 meeting minutes, Lines 29-30

- Concern: about trying to go anterior and posterior; don't want to go distal-medial.
 - Nerve bundles distal-medial; don't want to go there, just anterior-posterior.

Page 2 of Nov. 20 meeting minutes, Lines 3, 6-8

- Proximal reamer of the nail is 12-14mm.
- Nail diameter 11-14mm
 - Different depending on the nail; some nails you ream a lot more.
 - A lot of people don't have fancy nails,

Page 2 of Nov. 20 meeting minutes, Lines 13-14

- Likes the design.
 - He has interest in foot and ankle; did subtalar prep today.

Page 2 of Nov. 20 meeting minutes, Lines 15-16

- Scraping... depends on how much of a divet... it just scrapes.
 - 1-2mm minimum into the bone, 2-3mm total.

Page 2 of Nov. 20 meeting minutes, Lines 19-20

- Can make golf-balls with the curettes.
 - Want to see that golf ball forming... want to see bone juice coming out... bone marrow as opposed to just hard cartilage.

Page 2 of Nov. 20 meeting minutes, Lines 21-25

- Feeling between cutting cartilage vs. subchondral bone.
 - Hard, as if you are scraping varnished wood with cartilage.
 - With subchondral bone, a lot softer; more of a "catch" feeling, in the suction, you would see more marrow, see bits of fat, see yellow-type honey-comb bone.

Page 2 of Nov. 20 meeting minutes, Lines 28

- 75% of the posterior face to scrape; golf-ball 50% of that is ok.

Page 2 of Nov. 20 meeting minutes, Lines 30-31

- Clinical application to go medial is difficult to convince a surgeon to use; there's tendons there, arteries.. No one would do that blind.

F. Needs Statement Convergence

The team generated a number of needs statements to ultimately converge to our selected statement. The various needs statements generated are shown below.

Table F1: Needs statements considered for design.

Needs Statements
A way to address poor subtalar joint fusion in patients with acute ankle trauma undergoing TTC nailing that allows for better functional outcomes and an avoidance of revision surgery
A way to address poor visualization of the subtalar joint for surgeons performing TTC nailing in order to access the joint without requiring additional incisions
A way to remove cartilage from the subtalar joint for surgeons performing TTC nailing that results in >50% cartilage debridement at the subtalar joint.
A way to address poor subtalar joint fusion for surgeons performing TTC nailing that results in minimal changes to the current surgical procedure, requiring <10 minutes of additional surgical time.
A way to address poor access to the subtalar joint for surgeons performing TTC nailing that results in better subtalar joint fusion outcomes while not requiring additional incisions.
A way to maneuver through the sigmoidal subtalar joint for surgeons performing TTC nailing that allows for easy removal of cartilage without additional surgical incisions.
A way to improve surgical outcomes via ankle arthrodesis in patients with acute ankle trauma and comorbidities undergoing TTC nailing that avoids the need for additional incisions.
A way to address cartilage removal and subchondral bone deposition for surgeons performing TTC nailing in acute ankle trauma that adds minimal/minor changes to the current surgical procedure.
A way to prevent subtalar nonunion in patients undergoing TTC nailing that fits into existing surgical workflow.
A way to access the subtalar joint for surgeons performing TTC (hindfoot) nailing that minimizes additional incisions.
A way to prepare the subtalar joint for fusion for trauma surgeons performing TTC nailing that maximizes chance for bone union and minimizes changes to surgical workflow.
A way to access the subtalar joint for surgeons performing TTC nailing that creates no additional incisions and allows >50% cartilage debridement.

G. QFD Analysis

To perform the QFD analysis (**Figure G1**), we had to carefully consider our 14 requirements and the aspects of our solution, and how those fit within the customer and functional requirements of the design. While the majority of the requirements came directly from our client (customer requirements; what they want), there were 2 requirements that came about due to the nature of the problem space we were working in (functional requirements; how to do this). The other 3 functional requirements came about through the sharp manual cutting tool and the guide tube for accessing the joint space, which are the two primary components of our design. We had converged down to this approach early in our design process, and had come up with numerous designs within this space prior to converging down to our ultimate solution. With these customer and functional requirements listed out, we then assessed at how the functional requirements were impacted by the customer requirements, and assigned an appropriate strong (9), moderate (3), weak (1), or none (0) score to the relationship between them. For example, the removal of cartilage (requirement 3; R3) is strongly dependent on a sharp cutting tool. Similar decisions were made for the remaining customer and functional requirement relationships. It is important to note that, while a customer and functional requirement can have a strong relationship, they can still be orthogonal requirements. For instance, while controllable penetration depth (R7) is orthogonal to deep penetration into cartilage/subchondral bone (R6), since you can have deep penetration that is not controllable, the relationship between these two requirements is strong in the QFD.

After setting these relationships, you can obtain the technical importance score, which is the weight product of the customer importance and the relationship. From this, we see how important the guide tube is to meeting the customer's requirements, as well as the features of the cutting tool (both in complexity and sharpness). Furthermore, a key requirement was working in the range of angles in the A/P direction which was deemed much more important than controllability of depth penetration. This is interesting, as key steps in our design process, iteration, and selection have been based on this requirement to work in a wide range of angles. For example, we switched from a flexible tool body to a hinge mechanism in order to satisfy this requirement (among other reasons). Thus, it illustrates quantitatively the validity of this design decision, and the importance of this requirement in order to meet the other key requirements laid out by our client.

Further, the desired direction of improvement was indicated, which lists whether it is more desirable for this functional requirement to increase or decrease. Here, it is generally more desirable for everything to increase (i.e., sharper, more control in penetration depth, greater angle range, better guide tube) except for the manual cutting tool, where the downward arrow indicates it is preferred to minimize the complexity of this tool. Finally, the correlations between the various functional requirements can be

found, and the correlation is then listed in the intersection of the squares leading from the two design requirements. For example, since a more complex tool will have a broader range of angles to work in, and we want to decrease complexity while increasing the range of angles, these two have a negative correlation (this example is circled red in **Figure G1**). This concluded the QFD analysis, with the correlations helping us understand the relationships between some functional requirements, such as the range of angles, with appropriate tool design (i.e., complexity of the manual cutting tool).

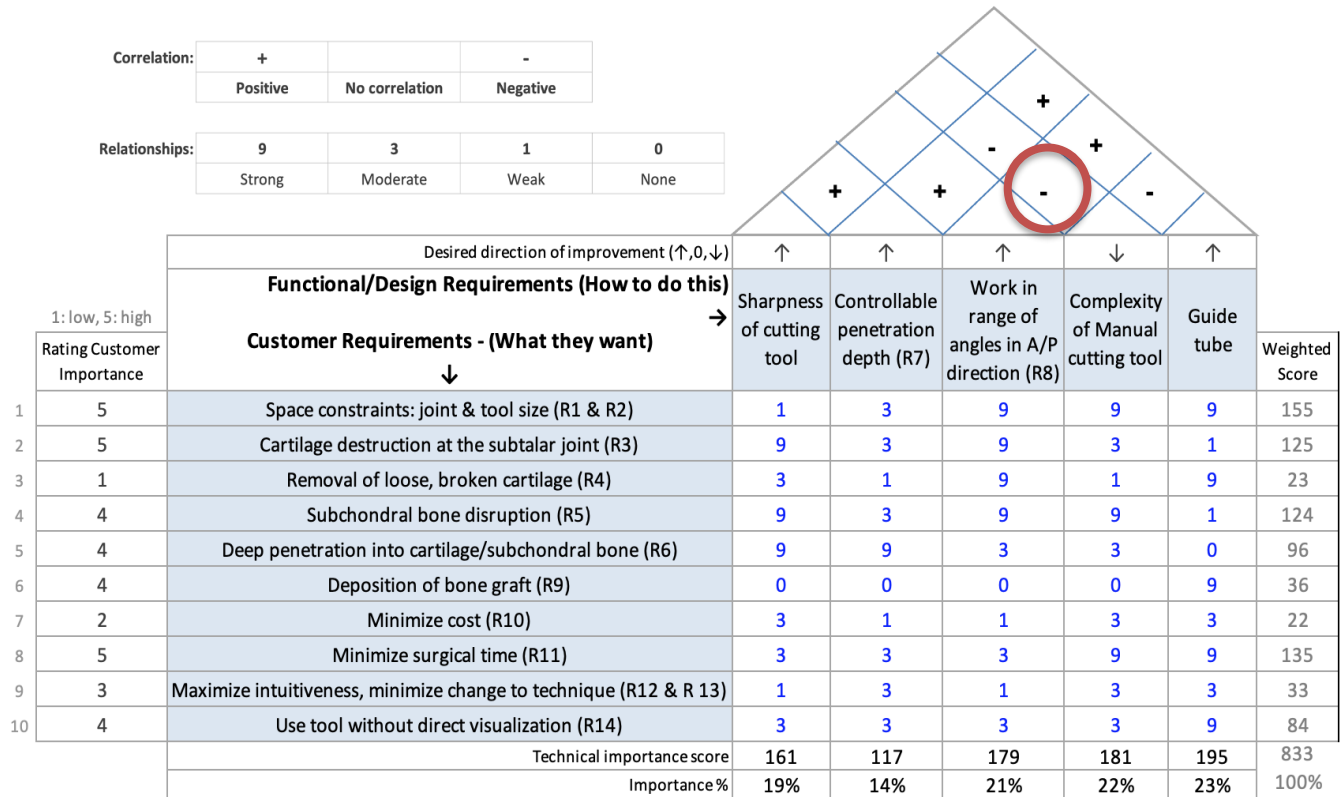


Figure G1: QFD Analysis Chart. Here, “RX” designates requirements, where X is a number between 1-14 corresponding to the appropriate requirement number from **Table 1**.

H. Supplemental Figures for Adult Foot Measurements

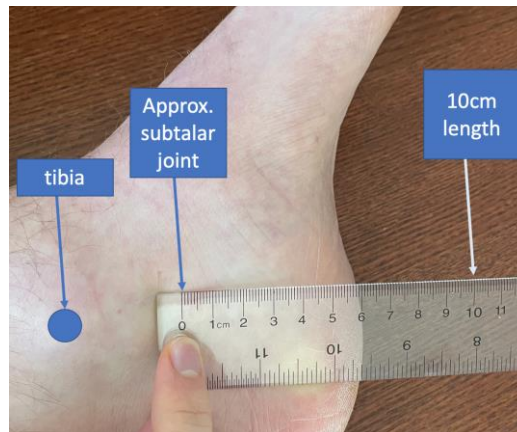


Figure H1: 10cm long tool relative to the subtalar joint on a typical adult foot.

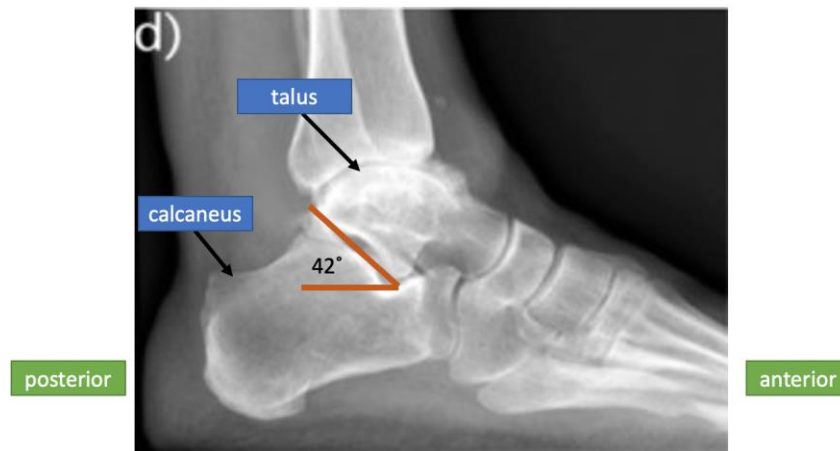


Figure H2: Angle of the subtalar joint in the A/P or sagittal plane on adult foot X-ray. Borrowed from [22], with modifications made to indicate the measured angle.

I. Surgeon Confidence Survey

In order to assess surgeon confidence and ease of use with our tool, we developed a survey based on detailed questionnaires previously provided to surgeons [28][29]. We decided to use a 5-point Likert scale, which has a number of different well-defined terms for the various scoring ranges [30]. These questions are meant to gauge the surgeons experience and ease of use with the tool, and are primarily based on the survey provided in [28] for an endoscopic tool, with modifications to fit our design. The survey relies on surgeons using a high-fidelity metal prototype on a cadaver as an assessment of the tool, and contains questions to get further surgeon feedback on aspects such as intuitiveness, safety, functionality, and usability of the tool, along with overall surgeon confidence with the tool and subtalar joint preparation procedures. While designed to address the requirement for the tool's intuitiveness and ease of use, it can also be used to gauge the surgeon's overall opinion on the procedure, and will be critical to informing future design iterations and changes.

Demographic Information

1. Please indicate your training status (circle one): Resident Fellow Staff
2. Number of years in surgical practice or PGY training level: _____
3. Your age: _____
4. Are you right or left handed (circle one): Left Right
5. What is your surgical glove size: _____
6. Total number of TTC arthrodesis cases performed as primary or assistant surgeon:
0-10 10-50 50-100 >100
7. Total number of open joint preparation cases performed as primary or assistant surgeon:
0-10 10-50 50-100 >100
8. Percentage of TTC arthrodesis cases performed with subtalar joint preparation:
0% up to 50% 50-90% >90%

Instrument Assessment

1. Please rate the following aspects of the instrument operation in terms of its **intuitiveness**. Consider how these features would translate to performing surgery on a live patient in an operating room:

1= Strongly Disagree; 2 = Disagree; 3 = Neutral; 4 = Agree; 5 = Strongly Agree

Instrument Operation – Mental Effort	1	2	3	4	5
Understanding how the instrument works is intuitive					
The effort necessary to perform tasks using the instrument is minimal					
Aligning the guide tube requires minimal effort					
The shape of the tool and guide tube is useful to navigate into the subtalar joint					
Removing cartilage with the tool was not difficult					
Removing subchondral bone with the tool was not difficult					
Opening the tool inside the joint space was not difficult					
The forces applied by the instrument on the tissue were appropriate					

- Comments regarding intuitiveness: (If you disagree with any of the statements, please explain. If you would like to elaborate on anything listed above, please do so).
2. Please rate the following aspects of the instrument in terms of its **range-of-motion, precision, stability, and safety**. Consider how these features would translate to performing surgery on a live patient in an operating room:

1= Strongly Disagree; 2 = Disagree; 3 = Neutral; 4 = Agree; 5 = Strongly Agree

Instrument Operation – Performance and Safety	1	2	3	4	5
The instrument performed as expected					
The instrument tip could be moved and adjusted easily					
The instrument tip could be moved and adjusted accurately					
I was not worried about the tool breaking/bending in the joint space					
I would feel safer using this tool if it were reusable/disposable					

- Comments regarding safety and performance: (Please let us know of any features that would make this instrument safer to use or have better performance).
3. Please rate the following aspects of the instrument in terms of **functionality**:

1= Strongly Disagree; 2 = Disagree; 3 = Neutral; 4 = Agree; 5 = Strongly Agree

Instrument Operation – Functionality	1	2	3	4	5
The instrument can reach all the desired spaces of the subtalar joint.					
The guide tube allows for easy access of suction tubes and bone graft syringes.					
The guide tube can be used to move and position the cutting tool into place.					
The instrument can be used to remove cartilage.					
The instrument can be used to disrupt subchondral bone.					

- Comments regarding instrument functionality: (If you disagree with any of the statements please explain).
- Comments regarding instrument length: (Please indicate whether you think the tool would be more effective at a longer or shorter length, both on the handle and on the scissor-like blade edge).

4. Please rate the following aspects of the instrument in terms of **usability**:

1= Strongly Disagree; 2 = Disagree; 3 = Neutral; 4 = Agree; 5 = Strongly Agree

Instrument Operation – Comfort and Usability	1	2	3	4	5
The instrument is comfortable in my hand.					
The force required to operate the instrument was appropriate.					
Operating the instrument will not likely cause hand fatigue.					

- Comments regarding instrument comfort: (If you disagree with any of the statements please explain).
5. Please rate the following aspects of the instrument in terms of confidence with the tool and with the current preparation of the subtalar joint:

1= Strongly Disagree; 2 = Disagree; 3 = Neutral; 4 = Agree; 5 = Strongly Agree

Instrument Operation – Confidence	1	2	3	4	5
Preparing the subtalar joint is essential to proper subtalar union.					
Preparing the subtalar joint is essential to positive patient outcomes.					
This tool can prepare the subtalar joint in a trauma setting.					
This tool can prepare the subtalar joint in a variety of settings.					
With this tool, I was able to remove cartilage sufficiently to promote union					
With this tool, I was able to activate subchondral bone to a sufficient extent.					

- Comments regarding overall confidence: (If you disagree with any of the statements please explain).
6. If you have any additional comments, please share them here.

J. Supplemental Information for Cartilage Scraping Force Calculations

The Python code for performing the cartilage scraping force calculations is as follows:

```
import numpy as np
import matplotlib.pyplot as plt
from matplotlib.widgets import Slider, Button, RadioButtons

rangle = 45          # rake angle (degrees)
depth = 2           # depth of cut (mm)
position = 0        # initial position of cut (mm)
td = position+depth

if td < 0.6:
    F = (10+(3/0.8)*depth-(10*(position-0.2)))+(10-0.5*rangle)

elif td < 1.4:
    F = (20+(5/0.8)*(td-0.8)-(11*(position-0.2)))+(10-0.5*rangle)

else:
    F = (40+(10/0.2)*(td-1.6)-(13*(position-0.2)))+(10-0.5*rangle)

if depth==0:
    F = 0

print("Rake angle of blade: "+ str(rangle)+'degrees')
print("Depth of cut: " + str(depth) + 'mm')
print("Initial position of cut: " + str(position) + 'mm')
print('Force required for specified cut = '+str(F) + 'N')
```

Sample outputs from this program are shown below in **Figure J1**.

```
[(base) Michaels-MacBook-Pro:BME489 michaeldebiasio$ pythonw Cutting_force.py
  Rake angle of blade: 90degrees
  Depth of cut: 2mm
  Initial position of cut: 0mm
  Force required for specified cut = 27.6N
[(base) Michaels-MacBook-Pro:BME489 michaeldebiasio$ pythonw Cutting_force.py
  Rake angle of blade: 45degrees
  Depth of cut: 1mm
  Initial position of cut: 0mm
  Force required for specified cut = 10.95N
[(base) Michaels-MacBook-Pro:BME489 michaeldebiasio$ pythonw Cutting_force.py
  Rake angle of blade: 45degrees
  Depth of cut: 1.5mm
  Initial position of cut: 0mm
  Force required for specified cut = 25.099999999999994N
(base) Michaels-MacBook-Pro:BME489 michaeldebiasio$ pythonw Cutting_force.py
  Rake angle of blade: 90degrees
  Depth of cut: 1.8mm
  Initial position of cut: 0mm
  Force required for specified cut = 17.6N
```

Figure J1: Sample output for varying rake angle and cutting depth.

K. Supplemental Information for Tool Force Calculations

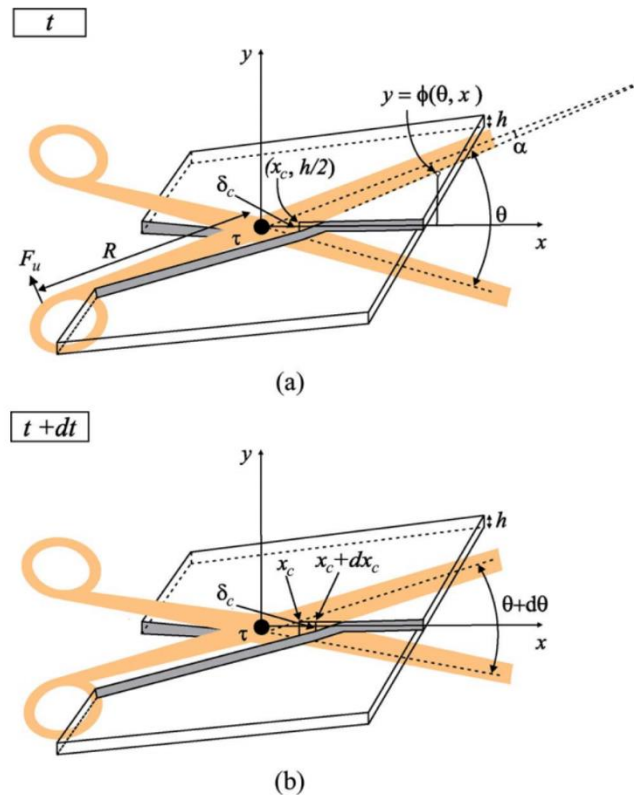


Figure K1: States of scissors and a plate at time t and $t + dt$ of a cutting process. The angle that is relevant in calculating the cutting force is alpha shown above. Borrowed from [41].

The part of MATLAB code that calculates handle force and force on the pin was developed using the relationship set with above diagram (**Figure K1**). In the diagram, alpha is the angle between the blade's edge and the centreline of the blade, as our tool is significant thin, alpha is assumed to be significantly small, with an approximate value of 5° . Theta is determined by the opening angle and pin position, where during the operation, the opening distance between two blades should be varied from 6mm to 8mm to fully scrape cartilage and disrupt subchondral bones. The friction on hinges is determined through balancing the torque caused by the gravity at the scissor's centre of mass (pin) and torque caused by friction on the hinges. Below is the complete MATLAB code used for force calculations, using the appropriate dimensions of our tool. After that is **Table K1**, which gives the calculated force results for varying pin positions, used to determine the optimal pin placement on the scissors.

```
% Force calculations
% joint space dimension: height 4 mm; length 10 mm;
% distance from bottom of foot to join space = 10 mm
```

```

%Define device dimension:
lsis = 10*10^-3;
lsisshort = 3*10^-3; %from hinges to pin 3 is optimal
lsislong = lsis - lsisshort; %from blade edge to pin
D = 2*10^-3; %diameter
alpha = 5*pi/180; %degree, where is the angle between the blade's edge and the
centerline of the blade, refer to diagram above
Xc = 1*10^-3; %m; position of the edge of the crack made by the scissors
widthmin = 6*10^-3; %open blade
widthmax = 8*10^-3;
opendegreemin = 2* asin(1/2*widthmin/lsislong); %in raduis
opendegreemax = 2* asin(1/2*widthmax/lsislong);
L = 30*10^-3; %length of the vertical part
thetamin = opendegreemin/2; %in raduis
thetamax = opendegreemax/2;
%material properties
d = 7800; %kg/m^3 density of surgical stainless steel

%force at blade edge
Fn = 27.6; %from cartilage scraping paper

%1).Handle force
Fu = Xc/lsisshort*Fn*cos(alpha)

%2).Friction on hinges(torque caused by friction of hinge = torque caused by
%gravity of the scissor)
V = pi*(D/2)^2*lsis*2;
w = V*d*9.8;
Tgmin = lsisshort*w*sin(thetamin)
Tgmax = lsisshort*w*sin(thetamax)
%Tf = Tg;
Ff = Tgmin/1*10^-3 %2mm is hinge diameter

%3).Force on pin
Fp = Xc/lsislong*Fn*cos(alpha)

```

Table K1: Calculated force results with varying pin position through MATLAB program

Testing trails	Pin position(mm)	Opening angles(radian)	Cutting force(N)	Handle force(N)	Friction on hinges(N)	Force on the pin(N)
1	1	0.68-0.92	27.6	27.5	1.6e-09	3.06
2	2	0.77-1.05	27.6	13.75	3.6e-09	3.44
3	3	0.89-1.22	27.6	9.17	6.2e-09	3.93
4	4	1.05-1.46	27.6	9.87	9.6e-09	4.58
5	5	1.29-1.85	27.6	10.50	1.4e-08	5.50

L. Force Simulation Results

The results of the force simulations are shown below in **Figures L1-L4**. In all figures, images show, in reading order, the stresses on the blade, strain on the blade, and max deformation of the blade.

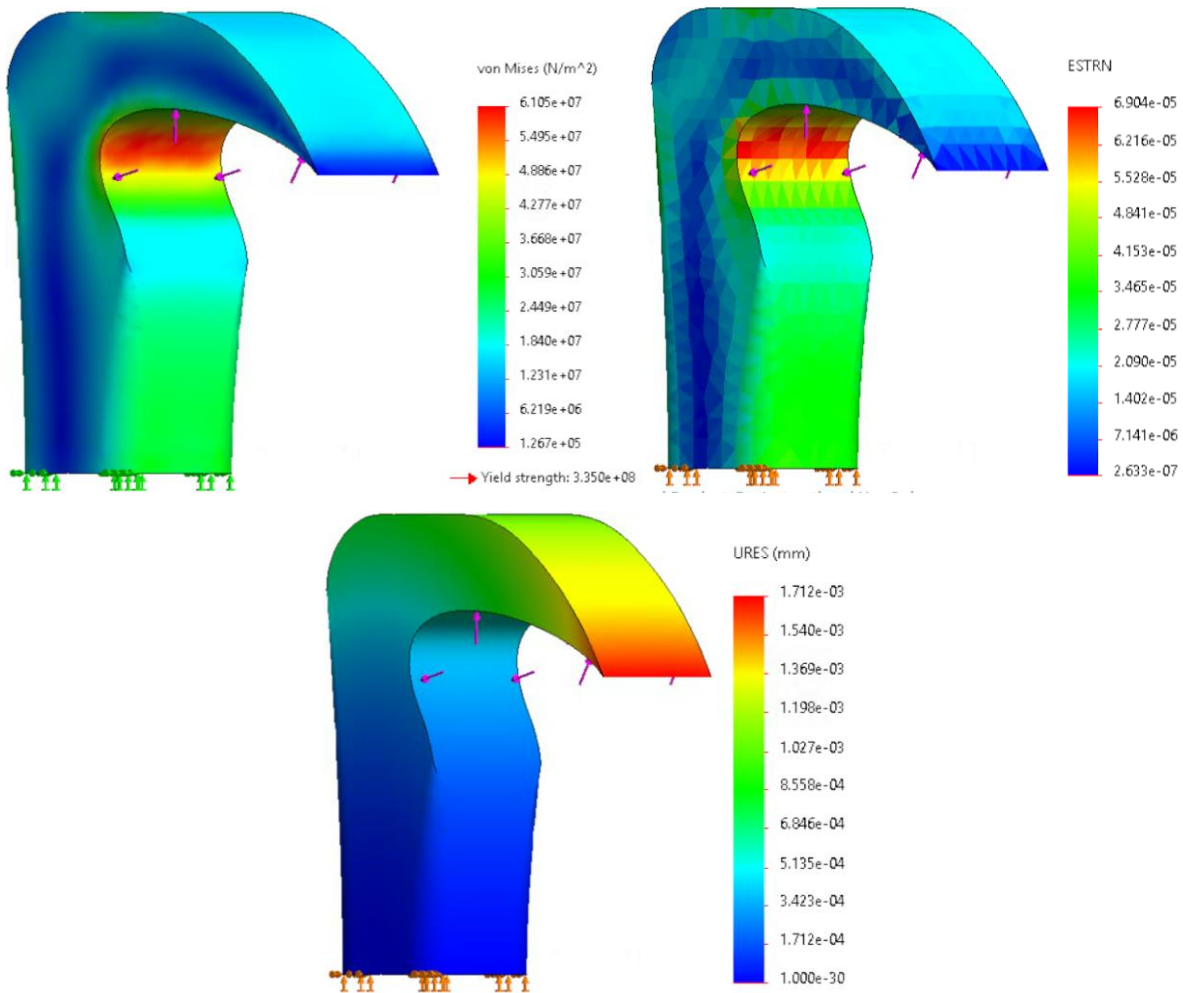


Figure L1: Simulations for 15N force applied to 5mm length of blade.

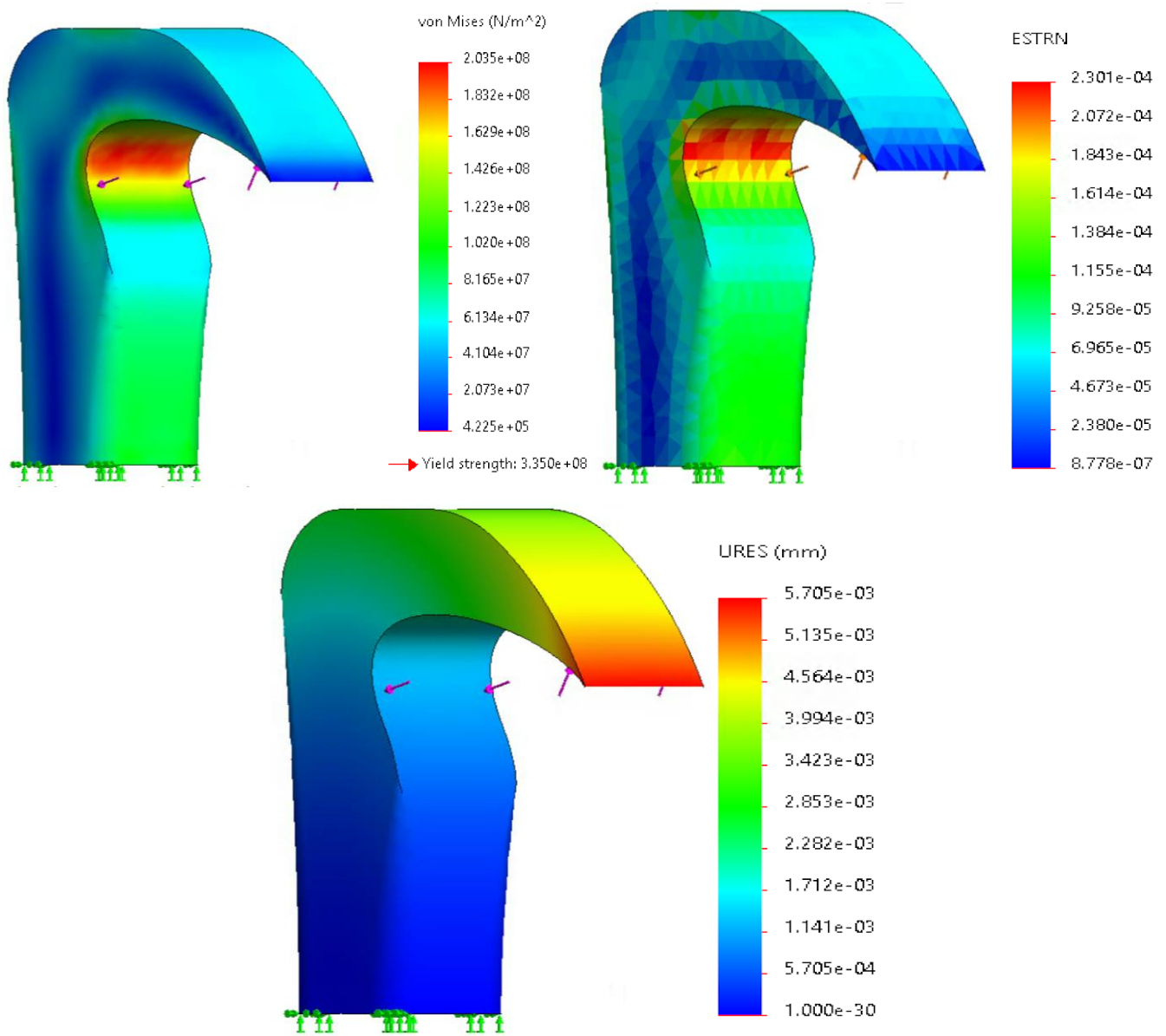


Figure L2: Simulations for 50N force applied to 5mm length of blade.

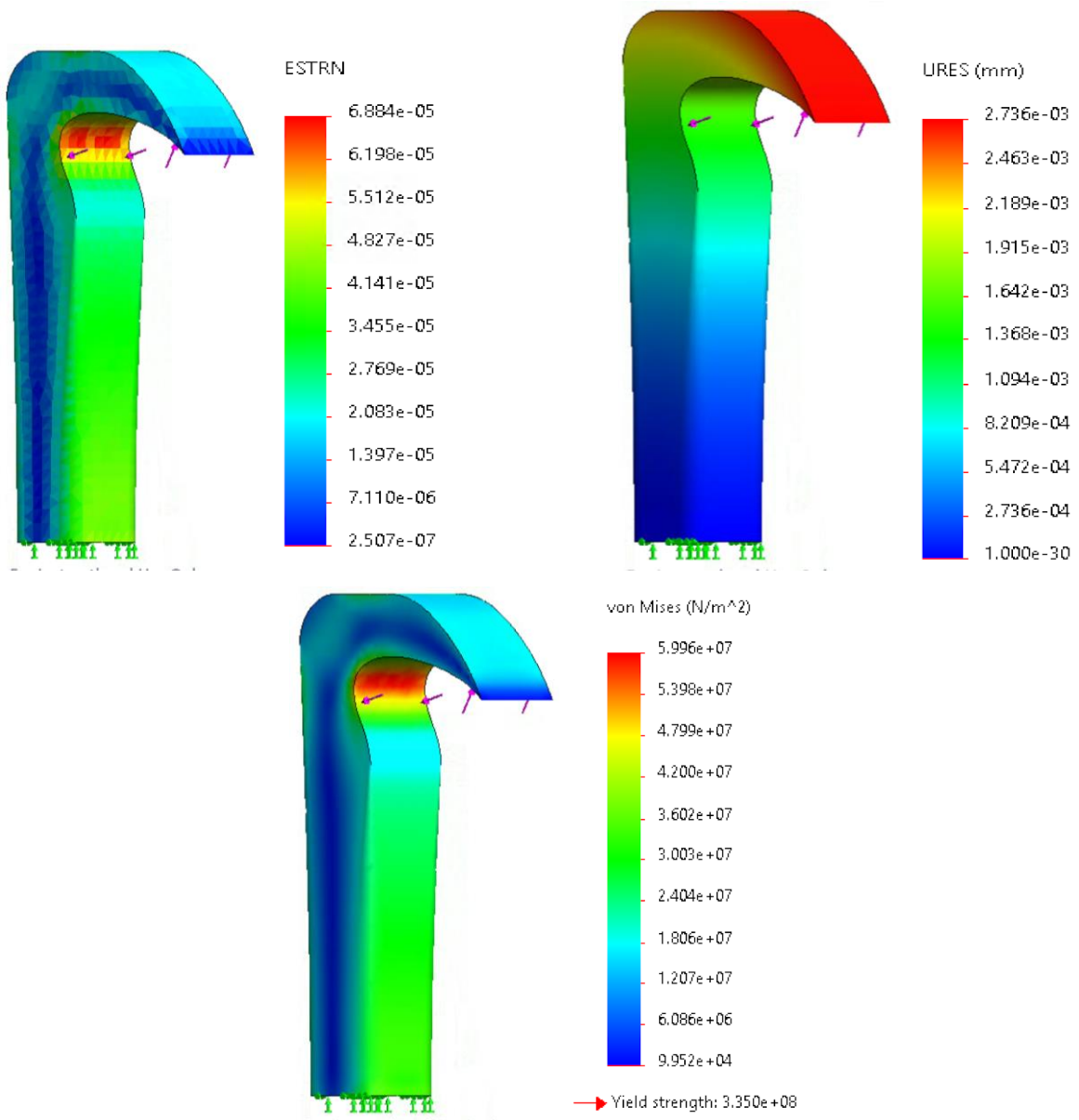


Figure L3: Simulations for 15N force applied to 10mm length of blade.

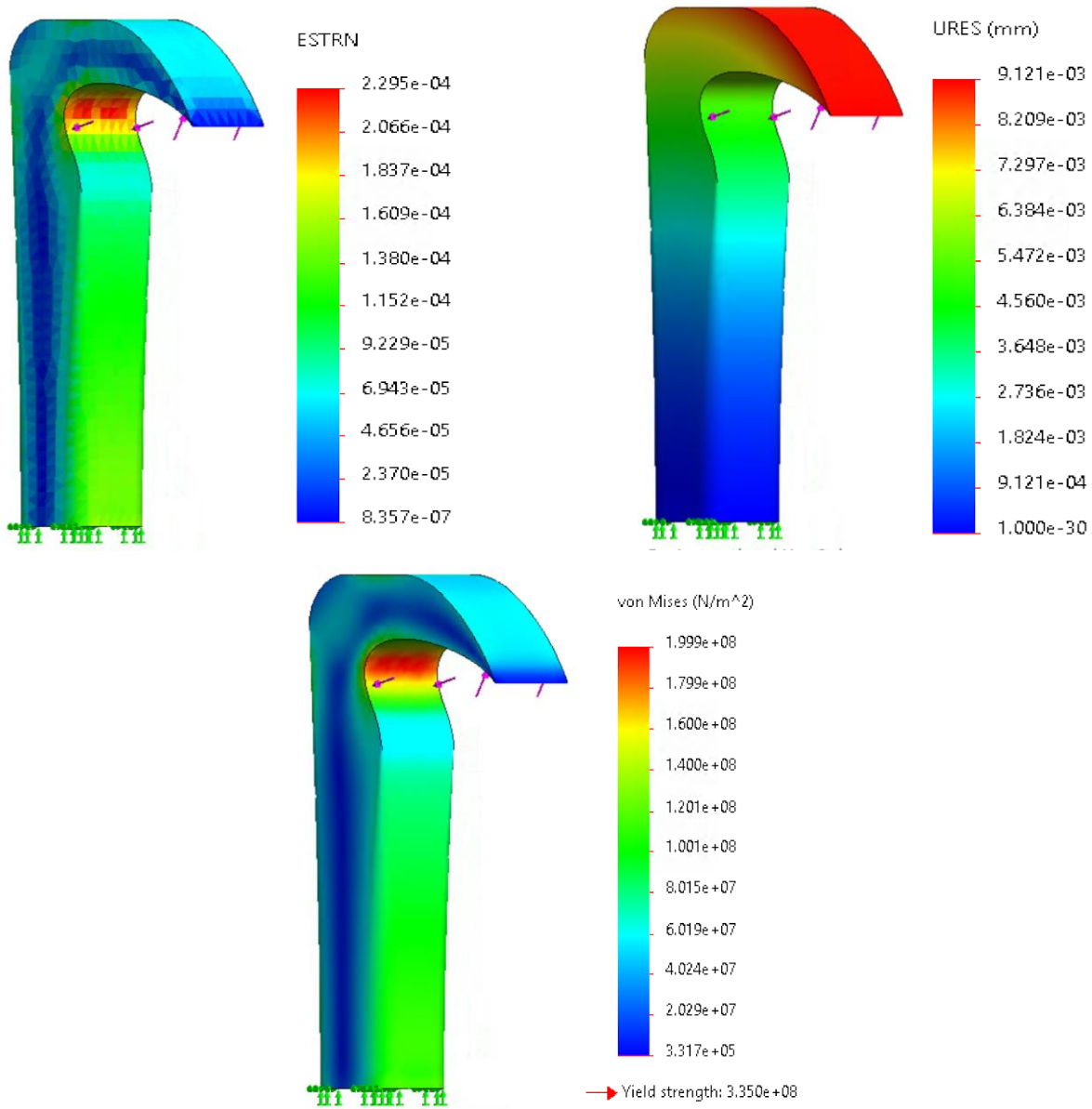


Figure L4: Simulations for 50N force applied to 10mm length of blade.

M. Full Surface Area and Timing Calculations

Below are the surface area calculations, followed by the timing calculations in **Table M1**.

Surface area calculations

Talus:

Approx. Surface area: $20 \times 30 \text{mm} = 600 \text{mm}^2$

25% = 150mm^2

50% = 300mm^2

Subtract reamed hole area: 35mm^2

25% → 115mm^2

50% → 265mm^2

Divide by scrape area: $2 \times 10 \text{mm}$, then multiply by 1.5 to achieve a depth of 1.5mm

25% → 8.7 scrapes

50% → 19.9 scrapes

Calcaneus:

Approx. Surface area: $22 \times 33 \text{mm} = 726 \text{mm}^2$

25% = 181.5mm^2

50% = 363mm^2

Subtract reamed hole area: 35mm^2

25% → 146.5mm^2

50% → 328mm^2

Divide by scrape area: $2 \times 10 \text{mm}$, then multiply by 1.5 to achieve a depth of 1.5mm

25% --> 10.9 scrapes

50% --> 24.6 scrapes

Table M1: Timing calculations

Step	Estimated Time (seconds)
Insert guide tube & adjust position using markers and x-ray images	30s
Insert cutting tool, expand, and cut cartilage	10s x 20 scrapes = 200s
Suction out cartilage	10s x 4 times = 40s
Scrape divots into subchondral bone	5s x 20 divots = 100s
Inject bone graft through guide tube	30s
Total	400s

N. Cost Analysis Supplemental Information

Cost Calculations

As discussed in the body of the report, the prices for the 420-series stainless steel, tungsten carbide, and manufacturing costs were found to be \$1.07/lb, \$11.00/lb, and \$41.11, respectively (all CAD). To calculate cost with these estimates, we first performed conservative estimates for the volumes of the various parts of the tool, outlined in **Table N1** below. In these estimates, cutting tool parts were assumed to be rectangular prisms of metal, to account for any potential metal scraps produced during processing, while the guide tube parts were considered cylindrical blocks of metal.

Table N1: Estimated volume for the parts of the tool.

Material	Part of the Tool	Estimated Dimensions	Estimated Area
Stainless Steel (420-series)	Handle	6mm x 3mm x 100mm	1800 mm ³
	Blade connector + Pin	6mm x 3mm x 10mm	180 mm ³
	Guide tube body	$\pi \times ((10\text{mm})^2 - (9\text{mm})^2) \times 70\text{mm} / 4$	1045 mm ³
	Guide tube washer	$\pi \times ((60\text{mm})^2 - (10\text{mm})^2) \times 30\text{mm} / 4$	82467 mm ³
Tungsten carbide	Blade	5mm x 2mm x 3mm	30 mm ³

With the estimated volumes in **Table N1**, this gave a volume of $8.55 \times 10^{-5} \text{ m}^3$ for stainless steel and $3 \times 10^{-8} \text{ m}^3$ for tungsten carbide. Then, we needed the density of 420-series stainless steel (7800 kg/m^3) [33] and tungsten carbide ($15250\text{-}15880 \text{ kg/m}^3$) [34]. With these numbers, we then calculated the cost with the following formula:

$$\text{cost} = \text{price per pound} \times \text{tool density} \times \text{tool volume}$$

with additional unit conversions embedded. Specifically, the calculation for stainless steel is:

$$\text{cost per tool} = \frac{\$1.07}{\text{lb}} \times 2.2 \frac{\text{lb}}{\text{kg}} \times 7800 \frac{\text{kg}}{\text{m}^3} \times 8.55 \times 10^{-5} \text{ m}^3 = \$1.57$$

and the calculation for tungsten carbide is:

$$\text{cost per tool} = \frac{\$11.00}{\text{lb}} \times 2.2 \frac{\text{lb}}{\text{kg}} \times 15880 \frac{\text{kg}}{\text{m}^3} \times 3 \times 10^{-8} \text{ m}^3 = \$0.01$$

These prices, along with the manufacturing price, were then added together to find the total estimated tool cost.

Market Price for Stainless Steel

Finally, **Figure N1** shows the screenshots from correspondence with the metal company to determine the market price of 1mm-thick 420-grade stainless steel.

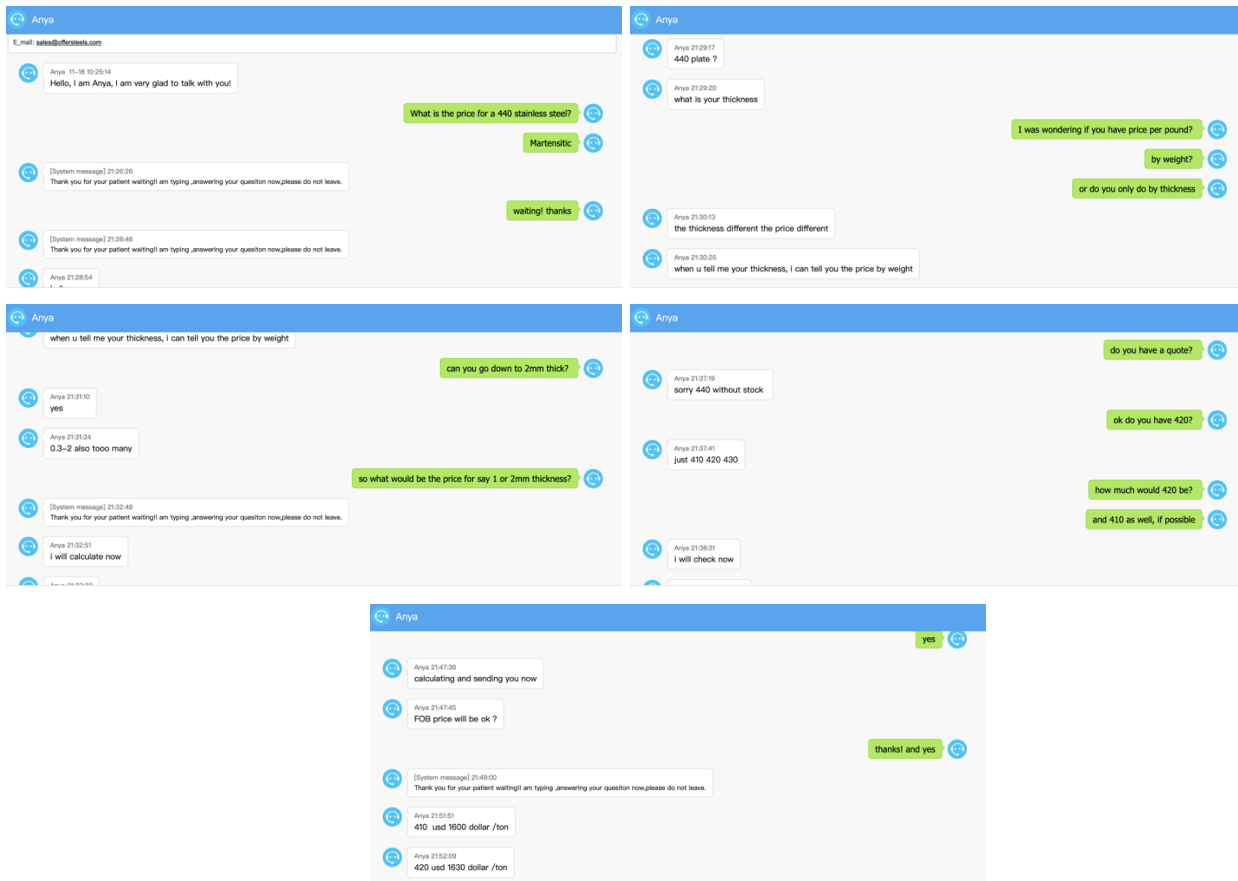


Figure N1: Cost for 420-series stainless steel – record of correspondence with metal company representative. Screenshots in figure move in reading order (left to right, line by line).

O. Risk Analysis Supplemental Info

The following definitions are provided for the risk assessment and analysis found in **Section 3J**, as well as the supplemental FMEA in **Appendix P** below.

Definitions from MIL-STD 882B

Severity:

- catastrophic (death or system loss),
- critical (severe injury, severe occupational illness, or major system damage),
- marginal (minor injury, minor occupational illness, or minor system damage), and
- negligible (less than minor injury, occupational illness or system damage).

Probability:

- frequent (likely to occur frequently; continuously experienced),
- probable (will occur several times in the life of the product; will occur frequently),
- occasional (likely to occur sometime in the life of the product; occurs several times),
- remote (unlikely but possible to occur in the life of an item; unlikely but can reasonably be expected to occur), and
- improbable (so unlikely, it can be assumed occurrence is not possible; unlikely to occur, but may be experienced).

FMEA Definitions

- likelihood of occurrence (how often event happens; scale from 1-10, with 1=improbable),
- likelihood of detection (ability to detect failure before harm or before event becomes catastrophic; scale from 1-10, with lower number = easier to detect),
- severity (how bad is the event; scale from 1-10, with 1=no impact), and
- risk profile number (RPN; the product of the likelihood of occurrence, likelihood of detection, and severity, all on a scale of 1 to 10 as described above).

P. FMEA Risk Analysis

The numerical assessment via a Failure Modes and Effects Analysis (FMEA) approach [49] is shown below in **Table P1**. The highest priority risk was clearly identified as risk #1 (RPN = 243). We will continue to re-assess all risks and re-calculate the RPNs as we update the tool and its usage procedure, especially based on surgeon feedback after testing of our initial high-fidelity prototype concepts. Here, the overall aim is to minimize the RPNs as much as possible.

Table P1: Risk profile number for hazards identified in Table 10, based on a FMEA approach [49].

#	Hazard	A. Likelihood of Occurrence (1-10)	B. Likelihood of Detection (1-10)*	C. Severity (1-10)	Risk Profile # (RPN) = A*B*C
1	Loss of alignment across the joint space between the 2 bones.	3	9	9	243
2	Additional surgical incisions, which are associated with higher infection rates and poorer outcomes [50].	1	1	7	7
3	Tool does not adequately remove debrided cartilage from the joint, leading to inflammation.	2	6	3	36
4	User does not scrape away cartilage from the joint, due to poor attempts and/or not enough force.	1	5	2	10
5	Damage of the nerves, vessels, and/or tendons surrounding the joint through use of the tool.	1	2	10	20
6	Damaging the joint beyond what is needed for subtalar fusion.	2	10	1	20
7	Tool causes infection of the joint space due to poor sterility.	1	7	7	49
8	Issues of biocompatibility between the tool and the patient's tissues.	1	5	4	20
9	The tools mechanism of action causes undue thermal damage or corrosive damage.	1	1	8	8
10	The tool's cutting blade breaks and remains in the joint space.	2	1	9	18
11	Cutting tool is placed in the wrong	3	1	8	24

	area - i.e., guide not far enough into the reamed hole, cutting tool gets stuck in subchondral bone				
--	---	--	--	--	--

* lower number = easier to detect

Q. Blade Angle Determination

To determine the blade angle, we estimated the required angle of the blade when in the “closed position” to ensure that, once fully extended, the blade would be at a 90° angle with the joint surface when at its expected maximal angle. To do this, we use the basics of Pythagorean theorem and our joint anatomy. Given the maximum cartilage thickness is ~1.5mm [15] and we want to extend into subchondral bone by 1-2mm (as discussed in requirement R6), we can calculate the angle of the blade desired on our tool. These estimations are shown in the diagram in **Figure Q1** below. This angle may be modified and adapted based on further testing and validation with a high-fidelity prototype.

Schematic of an infinitesimal portion of the joint space

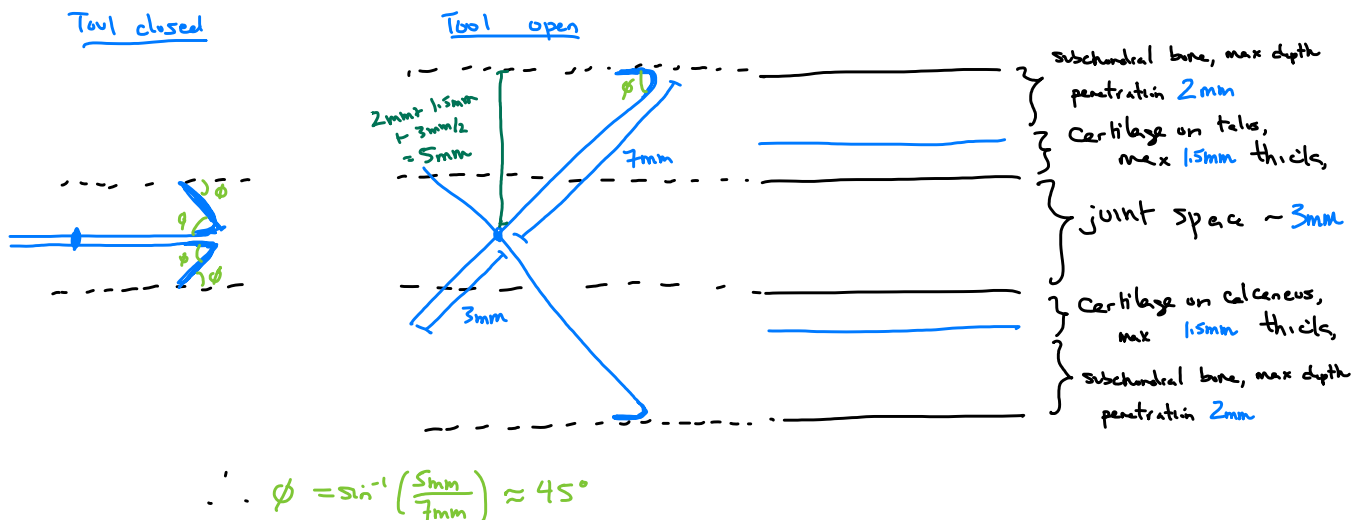


Figure Q1: Blade angle determination based on joint anatomy